CYCLIN-DEPENDENT KINASES AS TUMOR INITIATORS AND THERAPEUTIC TARGETS

By

PATRICK CORSINO

A DISSERTATION PRESENTED TO THE GRADUATE SCHOOL
OF THE UNIVERSITY OF FLORIDA IN PARTIAL FULFILLMENT
OF THE REQUIREMENTS FOR THE DEGREE OF
DOCTOR OF PHILOSOPHY

UNIVERSITY OF FLORIDA

2008

To my Mom

ACKNOWLEDGMENTS

Firstly, I would like to acknowledge my professor Brian Law. For four years he has guided me through my graduate education, and has provided whatever support he could, whenever it was needed. I would like to thank the members of the Law lab (Brad Davis, Mary Law and Nicole Teoh Parker) for their assistance in the lab as well as their friendship. I also thank the members of my committee (Dr. Steven Baker, Dr. David Ostrov and Dr. Thomas Rowe) for helping me with ideas for experiments and in many cases with the experiments themselves. Finally, I would like to thank my family, and in particular my mother, without whom I would not be where I am today, literally and figuratively.

TABLE OF CONTENTS

page

LIST OF FIGURES

LIST OF ABBREVIATIONS

αSMA	alpha-Smooth Muscle Actin
CDK	Cyclin-dependent kinase
D1K2	Cyclin D1/cdk2 Fusion Protein
DAPI	4',6-Diamidino-2-Phenylindole
EGFR	Epidermal Growth Factor
FBS	Fetal Bovine Serum
GFP	Green Fluorescent Protein
H&E	Hematoxylin and Eosin
HGF	Hepatocyte Grwoth Factor
LCS	Leica Confocal Software
MMTV	Mouse Mammary Tumor Virus
mTOR	Mammalian Target of Rapamycin
NCI/DTP	National Cancer Institute/Developmental Therapeutics Program
NLVS	NIP-leu-leu-leu-vinylsulfone
NSC	Nomenclature Standards Committee
PAI1	Plasminogen Activator Inhibitor
PCNA	Proliferating Cell Nuclear Antigen
Rb	Retinoblastoma
RCSB	Research Collaboratory for Structural Bioinformatics
STAT3	Signal Transducer and Activator of Transcription-3
TGFα	Transforming Growth Factor-alpha
TGFβ	Transforming Growth Factor-beta

Abstract of Dissertation Presented to the Graduate School
of the University of Florida in Partial Fulfillment of the
Requirements for the Degree of Doctor of Philosophy

CYCLIN-DEPDENENT KINASES AS TUMOR INITIATORS AND THERAPEUTIC TARGETS

By

Patrick Corsino

December 2008

Chair: Brian K. Law
Major: Medical Sciences—Physiology and Pharmacology

Cyclin D1/cdk2 complexes are present at high frequency in human breast cancer cell lines, but the significance of this observation is not fully understood. This report demonstrates that expression of a cyclin D1-cdk2 fusion protein under the control of the MMTV promoter results in mammary gland hyperplasia and fibrosis, and mammary tumors. These tumors contain regions of spindle-shaped cells expressing both luminal and myoepithelial markers. Cell lines cultured from these tumors exhibit the same luminal/myoepithelial "mixed-lineage" phenotype that is associated with human basal-like breast cancer, and express a number of myoepithelial markers. The MMTV-D1K2 tumor-derived cell lines form highly invasive tumors when injected into mouse mammary glands. Invasion is associated with E-cadherin localization to the cytoplasm, or loss of E-cadherin expression. Cytoplasmic E-cadherin correlates with lack of colony formation *in vitro* and ß-catenin and p120ctn localization to the cytoplasm. Data suggest that the invasiveness of these cell lines results from a combination of factors including mislocalization of E-cadherin, ß-catenin, and p120ctn to the cytoplasm. Similar characteristics were also observed in human basal-like breast cancer cell lines, suggesting that these results are relevant to human tumors. Together these results suggest that abnormal cdk2 activation may contribute to the formation of basal-like breast cancers.

The importance of cdk2 as well as the other cell cycle specific cdks in tumor development indicates their potential usefulness in cancer therapy. For this reason, cdks have been the subject of extensive research, and consequently many inhibitors have been developed to target these proteins. However, the compounds that comprise the current list of cdk inhibitors are largely ATP competitive. This study discusses the identification of a novel structural site on cdk2, which is well conserved between the cell cycle cdks. Small molecules identified by a high throughput *in silico* screen of this pocket exhibit cytostatic effects and act by reducing the apparent protein levels of cell cycle cdks. Drug-induced cell cycle arrest is associated with decreased Rb phosphorylation and decreased expression of E2F-dependent genes. Multiple lines of evidence indicate that the primary mechanism of action of these compounds is the direct induction of cdk aggregation.

CHAPTER 1
BACKGROUND

Introduction

The cellular events of DNA replication and subsequent division from a single cell into two daughter cells are of critical importance to a multicellular organism. When this process is well regulated and functions in a precisely timed manner, an organism grows properly and maintains healthy cell turnover. When the sequence of events leading to cell division become deregulated, cells can develop cancerous traits. Members of the cyclin dependent kinase (cdk) family function at the center of the cell cycle, acting to regulate the progression from the G0/G1 phase to mitosis. The cell cycle specific proteins in this family, namely cdk1, cdk2, cdk4, and cdk6 control cell cycle progression, and in normally dividing cells are subject to multiple levels of regulation. The first part of this study focused on the contribution of cdk2 in the process of tumorigenesis. It examined the characteristics of cancer cells that are driven by a constitutively active version of this protein. The second part of this study was concerned with the identification and characterization of novel cdk inhibitors. As the first step in the drug development pathway, these compounds are characterized in cell culture and *in vitro*, leaving *in vivo* studies yet to be completed.

Cyclin-Dependent Kinases

Cdks are serine/threonine protein kinases that phosphorylate a wide variety of proteins that are involved in cell cycle progression (1, 2). Regulation of these kinases occurs on multiple levels. In order to become enzymatically active, cdks require the binding of an appropriate cyclin, as well as the phosphorylation of the appropriate residue on their activation loop by a cyclin dependant kinase activating kinase (CAK) (3, 4). Mechanisms of inactivation of cdks include phosphorylation on an inhibitory site by wee1 kinase (5) and binding of an inhibitory

protein from one of the two families of cdk inhibitors. The first of these two families consists of $p27^{kip}$ (6), $p21^{cip}$ (7), and $p57^{kip2}$ (8) which primarily inhibits cdks 1 and 2 by binding to the cyclin/cdk complex and preventing access of cdks to substrates for phosphorylation. The second group consists of four proteins encoded by the Ink4a/Arf locus, namely $p15^{ink4b}$, $p16^{ink4a}$, $p17^{ink4c}$, and $p18^{ink4d}$ which inhibit cdks 4 and 6 by preventing cyclin association and subsequent activation (9).

Cdk involvement in a normally regulated cell cycle begins with external stimuli converging to upregulate cyclin D1 (10, 11). Cyclin D1 then binds to and activates cdk4 and cdk6, which translocate to the nucleus and phosphorylate members of the pocket protein family. This family consists of Rb, p107 and p130 (12-14). These proteins bind to members of the E2F family of transcription factors and inhibit their activity by masking their transactivation domains (15, 16). Of the six members of the E2F family, E2F1, E2F2, and E2F3 associate with Rb and are activators of transcription (14). These three transcription factors are essential for cell proliferation, as shown by conditional knockout studies in mice (17). Rb also associates with a histone deacetylase, HDAC1. A complex between Rb, HDAC1 and E2F1 actively represses cis-acting elements and basal promoters, further inhibiting E2F-dependant transcription (18, 19). Once phosphorylated, Rb dissociates from E2F1, thereby leading to its activation, and the transcription of genes involved in triggering the S phase of the cell cycle (14). Transcriptional targets of the E2F family include genes involved in DNA synthesis (Thymidine Kinase, Thymidylate Synthetase, Dihydrofolate Reductase (20, 21)), DNA replication (PCNA and DNA Polymerase-α, (20, 22)), and cell cycle control (cyclin A and cyclin E (23, 24)). Upregulation of cyclins A and E leads to the activation of cdk2, which further phosphorylates Rb, leading to greater E2F dependant transcription (25) and further progression through the cell cycle. At the

end of S-phase, cdk1 is activated by cyclins A and B leading to progression through the G2 phase of the cell cycle and mitosis (26, 27).

Genetic Studies

The generalized view of the cell cycle described above assumes that different cdks can only bind to and become activated by their designated cyclins (cyclin D1 with cdk4 or cdk6, cyclin E with cdk2, etc.). Recently, however, genetic knockout studies in mice have shown that there is a significant degree of promiscuity between the cell cycle specific cdks with regards to their cyclin partners and their cellular substrates (28). Cdk2 was assumed to be an essential protein, because of its requirement for cell cycle progression. It was considered to be the only cdk able to bind to cyclins A and E, and it was known to be involved in critical processes in G1-S phase transitions. One study revealed that a dominant negative mutant of cdk2 induced a block in the cell cycle in the G1 phase (29). However in 2003, it was discovered that mice deficient in cdk2 were not only viable, but were relatively normal with respect to development (30). The fact that these mice were sterile indicated that cdk2 was not essential for mitosis, but only for meiosis in germ cells. Another study revealed that cdk1 was able to compensate for the loss of cdk2 in knockout mice by binding to cyclin E and phosphorylating appropriate substrates (31). This observation was crucial to the understanding of how cdks can substitute for one another. Cdk4 is also nonessential for normal cell proliferation (32). In cdk4 null mice, cdk6 activity increases two-fold in a compensatory mechanism. These mice are more resistant to developing skin and mammary tumors (32). Cdk6 null mice also develop relatively normally, except for a slight impairment in hematopoiesis (33).

Combination knockout studies revealed that although mice could not develop past the late stages of embryogenesis, mouse embryonic fibroblast cells proliferate normally in the absence of both cdk4 and cdk6 (33). Similarly, mice lacking both cdk2 and cdk4 die shortly after

embryonic development, but cell lines derived from those embryos become immortalized and exhibit regular cell cycle kinetics (34). Finally, triple knockout mice, deficient in cdk2, cdk4, and cdk6 develop to embryonic day 12.5 (35). Mouse embryonic fibroblast cells derived from these embryos undergo proliferation *in vitro*, although with altered cell cycle kinetics. In these cells, cdk1 was able to bind to all cyclins and phosphorylate Rb, leading to successful completion of the cell cycle. In light of these studies, it is clear that there is a significant degree of functional redundancy between cdks. This issue becomes important when developing a strategy for halting the growth of cancer cells with the use of cdk inhibitors. If an inhibitor has a high degree of specificity and targets only one cdk, the remaining, unaffected cdks will likely compensate for the loss in activity, and the cells will continue to divide. According to the results from the genetic knockout studies, an effective inhibitor must be able to act on multiple cdks in order to have a significant effect on the rate of cancer cell proliferation.

Cdk Aberrance in Cancer

Uncontrolled cell division is a defining feature of cancer. As cdk activity is intimately linked with cell cycle control, it would stand to reason that an overabundance of cdk activity would lead to unrestrained cell growth. There are many examples in which defects in the components of cdk regulatory machinery are linked to specific cancers.

In normally dividing cells, cdk levels do not fluctuate dramatically. Cyclins however, are subject to many fold changes in levels depending on the phase on the cell cycle. As cyclins are the regulatory partners of cdks, their presence or absence determines the activation state of cdks. Therefore, an upregulation of cyclins can lead to overactivated cdks. Cyclin E upregulation for instance has been linked to neuroendocrine lung tumors (36), as well as basal-like breast tumors (37). High levels of cyclin E also correlate with a poor outcome in breast cancer patients (38). Moreover, a truncated, lower molecular weight form of cyclin E induces a higher level of cdk2

activity than the full length protein. This truncated version of cyclin E has been linked to breast tumorigenesis (39, 40).

Similarly, cyclin D1 upregulation, caused by overexpression (by gene amplification, for example) has been observed in 40-50% of human breast cancers (41, 42). Increases in cyclin D1 levels can affect cell cycle regulation dynamics through multiple mechanisms. Firstly, as cyclin D1 is a regulator of cdk4 and cdk6, higher cyclin D1 levels could result in increased cdk4 and cdk6 dependent kinase activity. Secondly, increased cyclin D1/cdk4 and cyclin D1/cdk6 complexes act as molecular sinks for the cdk inhibitory proteins p21 and p27. By decreasing the availability of these proteins, cyclin D1 upregulation would indirectly increase cdk1 and cdk2 activity by preventing their inhibition by p21 and p27. Thirdly, overexpression of cyclin D1 results in higher levels of cdk4 due to increased transcription (43). Other links between cyclin D1 and cancer include a chromosomal translocation event in the cyclin D1 gene occurring in 90% of Mantle Cell lymphoma cases (44, 45). Also, a G870A polymorphism in the cyclin D1 gene has been associated with several cancers, including a squamous cell carcinoma of the head and neck, and cervical cancer (46, 47).

Perturbations in the proper functioning of cdk inhibitory proteins can also lead to hyperproliferation of cells via overactivated cdks. Mislocalization and proteolysis of p27 have been implicated in breast and other cancers (48, 49). Similarly, p21is mislocalized in cancers, as cellular staining in human primary breast cancer samples show a predominantly cytoplasmic rather than nuclear localization pattern (50, 51). Cdks exert their function primarily in the nucleus. By localizing to the cytoplasm, p21 and p27 can no longer interact with cdks, and inhibit their activity. Therefore, with respect to cdk activity, improper localization of p21 and p27 has the equivalent effect of reducing their total levels.

The loss of function of the cyclin D1/cdk4 and cyclin D1/cdk6 regulator p16 is also linked to cancer. Whether due to point mutations, homozygous deletion, or promoter methylation, reduced p16 activity has is an important factor in carcinogenesis in many cases (52).

An alternative mechanism by which increased cdk activity could potentially lead to cancer is an activating mutation in the cdk itself. Transgenic mice engineered to express cdk4 with an R24C mutation, which renders the kinase unable to bind to the inhibitory protein p16, develop tumors with varied etiology (53). Taken together these studies reveal the potential consequences of unregulated cdk activity and highlight the need for effective inhibitors in cancer therapy and prevention.

Cyclin D1/Cdk2 Complexes

Although the standard view of the cell cycle involves specific pairing of cyclins and cdks (cyclin D1 with cdk4 and cyclin A with cdk2 for example), genetic knockout studies reveal that cdks can replace one another by binding to alternative cyclins. It has been known for many years that cyclin D1/cdk2 complexes can form in cells, including human breast cancer cells (54-56). However, for some time, the functions of these complexes were unclear, and it was unknown if cdk2 in complex with cyclin D1 was catalytically active. Our laboratory has previously published a study examining the characteristics of such complexes (57). A fusion protein in which a His_6-tagged cdk2 was attached to a Flag-tagged cyclin D1 by a flexible poly-Glycine linker was generated. This fusion protein allowed cyclin D1/cdk2 complexes to be isolated and studied. In this study, it was shown that these complexes are properly phosphorylated on the appropriate activating residue (Threonine 160) by CAK and phosphorylate the appropriate substrates (pRB and Histone H1) *in vitro*. Cell lines constructed to overexpress the fusion protein display anchorage independent growth, and their proliferation is resistant to the inhibitory effects of the cell signaling protein TGF-β. The potential importance of these

complexes is underscored by the fact that cyclin D1 is overexpressed in approximately 50% of human breast cancers (41, 42). That cyclin D1 can bind to and activate cdk2 indicates that these complexes may have important roles in mammary carcinogenesis. The following two chapters will discuss the use of the cyclin D1/cdk2 fusion protein as a basis for tumor studies in transgenic mice.

Cdk Inhibitors, Classic and Novel

Unregulated cdk activity can lead to tumorigenesis. This indicates that cdks may be ideal targets for anti-cancer therapeutics. As kinases, cdks must bind to ATP for enzyme catalysis. An obvious method of inhibiting cdk activity would be to prevent ATP binding. This premise explains the rationale behind the mechanism of action of the majority of cdk inhibitors in existence today. There are several different classes of these inhibitors, such as adenine derivatives, flavones, and oxindole derivatives (58). These cdk inhibitors reversibly occupy the ATP binding site on cdks, preventing catalysis. Flavopiridol is one of the furthest developed cdk inhibitors of the ATP-competitive sort. This synthetic flavone is derived from a natural product found in the Indian plant, Dysoxylum binectariferum (59). As a pan-cdk inhibitor, Flavopiridol affects the activity of cdks 1, 2, 4, 6, and 7, and has an IC_{50} for inhibiting cell proliferation in the nanomolar range (60). It has also been used clinically for a number of years, in both phase I and phase II clinical trials in the treatment of cancer (61-63). While promising, this drug has displayed side effects, with the dose-limiting toxicity being severe diarrhea (64). Flavopiridol also affects multiple cellular processes that may not be related to cdk inhibition. Flavopiridol increases apoptosis, induces differentiation, displays antiangeogenic properties, and decreases the levels of cyclin D1 through transcription inhibition (65).

Other ATP-competitive cdk inhibitors in clinical trials include Roscovitine and UCN-01. Roscovitine is relatively specific to cdk1 and cdk2 *in vitro*, and has shown moderate success in

phase I trials (66-68). UCN-01 is a non-specific cdk inhibitor and also acts on multiple pathways unrelated to cdks (65). In clinical trials it has mostly been used in combinations with other drugs, including topoisomerase inhibitors such as irinotecan and topotecan (69, 70), and DNA damaging agents such as cisplatin (71).

These drugs have had reasonable success, and demonstrate the potential of ATP-competitive agents to be of clinical importance in the treatment of cancer. However, their mechanism of action is coupled with an inherent limit in target specificity; all kinases possess an ATP-binding site. This introduces the possibility that some of these molecules may inhibit kinases unrelated to cdks and perhaps lead to unwanted side effects in the clinic. If, on the other hand, drugs were developed to bind to sites unique to cdks, and were distinct from the ATP-binding cleft, they would have an advantage in terms of target specificity. In recent years this is the approach many researchers have taken in developing new cdk inhibitors.

A number of crystal structures of cdk2 have been solved, including in complex with cyclin A (72), cyclin E1(73), cyclin A and p27 (74), bound to ATP-competitive inhibitors (75, 76), as well as in apo form (77). Crystal structures of cdk6 have also been solved, including one with a bound viral cyclin (78), and one in a ternary complex with cyclin K and the inhibitory protein p18 (79). Unfortunately, no structures of cdk1 or cdk4 have been solved as of yet. Nevertheless, the wealth of structural information obtained from the structures of cdk2 and 6 have helped to provide the basis for rational drug design.

One example of this effort is the identification of a D-amino acid hexapeptide molecule, NBI1 that inhibits the kinase activity of cdk2 by binding to cyclin A (80). This molecule does not interfere with ATP or substrate binding. NBI1 effectively inhibits proliferation and induces

apoptosis in several cancer cell lines, and was found to inhibit cdks 1 and 2 to a significant extent.

A similar approach to cdk-directed drug design was taken in identifying a series of cyclic peptides that bind to the substrate recognition site of cdk complexes (81). In this study, peptides were designed based on the sequence of p27 in an attempt to mimic the inhibitory properties of the protein. These molecules inhibit cdk2 kinase activity, block cyclin A from binding to cdk2 *in vitro*, and are relatively potent, with IC_{50} values in the low micromolar range. No other kinases were tested in this study, so it is unknown whether these molecules have any effect on other cdks.

One other example of novel approaches to cdk inhibition is the use of a small, 39 amino acid peptide based on a pRb2/p130 pocket protein amino acid sequence, which is a spacer domain that inhibits the kinase activity of cdk2 (82). The molecules designed based on this spacer domain not only inhibit cdk2 activity, but induce cell cycle arrest, and exhibit effects on tumor sizes in mice *in vivo*.

Finally, the natural product Silibinin inhibits cdks through an unusual mechanism. Isolated from the milk thistle plant Silybum marianum, this compound effectively inhibits prostate cancer in mouse model systems (83, 84). Silibinin is surprisingly non-toxic, with no dose limiting toxicity observed in mice. It appears to affect multiple cellular processes, including decreasing total levels of cdks 1, 2, 4, and 6 in cells, as well as several cyclins. The mechanism by which Silibinin reduces levels of these cell cycle regulators is as yet undetermined, however it presents a novel means by which to control aberrant cdk activity in cancer. The fact that it is tolerated as well as it is also allows for the possibility of its use as a cancer chemopreventive agent.

These novel cdk inhibitors are promising, but have several limitations. Firstly, in general, they do not act as pan-cdk inhibitors. In some tumor types, this may not be problematic, as in some cell lines, inhibition of a single cdk is sufficient to result in decreased cell proliferation and/or apoptosis. However, the redundancy of cdks discussed previously could reduce the clinical potential of these drugs, as in some cases, unaffected cdks would simply substitute for the inhibition of other cdks. Secondly, the novel cdk inhibitors developed are largely peptide-based. These molecules may be subject to drug delivery problems. Based on the examples of currently used inhibitors, and the problems they present, an ideal cdk inhibitor would be one that would 1) bind to a site that is unique and specific to cdks, 2) affect multiple cell-cycle specific cdks, and 3) have characteristics which would allow for proper drug delivery, including being cell permeable and resistant to degradation in the human digestive/circulatory system.

CHAPTER 2
TUMORS INITIATED BY CONSTITUIVE CDK2 ACTIVATION EXHIBIT TRANSFORMING GROWTH FACTOR-BETA RESISTANCE

Introduction

Cdk2 becomes activated during mammary tumorigenesis through a number of mechanisms including cyclin E overexpression and proteolytic processing (39), p21 and p27 downregulation and mislocalization (49-51, 85-87), and cyclin A1 re-expression (88). Recent studies indicate that cdk2 is likely to be an important target for anti-cancer agents (60, 89, 90). Therefore it is important to understand how cdk2 activation through various mechanisms leads to tumor formation, and the biochemical and cellular mechanisms involved. Complexes between cyclin D1 and cdk2 were shown to be present in mammary carcinoma cells some time ago (56), but the function of these complexes is unclear. Cyclin D1 overexpression occurs in approximately 50% of human breast cancers (42), thus cyclin D1/cdk2 complexes might contribute to the oncogenic effects of cyclin D1 overexpression. Different cyclins and cyclin-dependent kinases interact with each other rather promiscuously making it difficult to ascribe specific functions to particular cyclin/cdk complexes. To circumvent this problem we designed a cyclin D1-cdk2 fusion protein in which the cyclin D1 domain stimulates the phosphorylation and kinase activity of the cdk2 domain through an intramolecular mechanism (57). We constructed a transgenic mouse model in which mammary expression of the cyclin D1-cdk2 fusion protein is driven by the mouse mammary tumor virus (MMTV) promoter (MMTV-D1K2) (Fig. 2-1A). MMTV-D1K2 transgenic mice exhibit mammary fibrosis and hyperplasia and develop mammary tumors associated with significant desmoplasia. The MMTV-D1K2 transgenic mouse model may prove useful for testing cdk2 inhibitors and for the development and testing of novel therapeutic agents targeting tumor cells.

Materials and Methods

Construction of MMTV-Cyclin D1-Cdk2 (MMTV-D1K2) Transgenic Mice

The cDNA encoding the cyclin D1-cdk2 fusion protein was excised from the pAdTrack vector described previously (57) with EcoRI and EcoRV and subcloned into the EcoRI and BstXI sites of MMTV-TGFα (91). This resulted in the replacement of the TGFα transgene with the cDNA encoding the cyclin D1-cdk2 fusion, creating the MMTV-cyclin D1-cdk2 (MMTV-D1K2) vector. The MMTV-D1K2 vector was verified by DNA sequencing. The transgene and MMTV promoter were excised from the MMTV-D1K2 vector using AatII and NruI. The purified AatII/NruI fragment was submitted to the Vanderbilt University Transgenic Mouse/Embryonic Stem Cell Shared Resource and transgenic mice were created in the inbred FVB strain. Transgenic animals were initially identified by Southern blotting of genomic tail DNA and routinely screened by polymerase chain reaction (PCR) using primers complementary to the region encoding the FLAG epitope tag (5'- GACTATAAGGACGATGATGAC-3') and the flexible linker joining the cyclin D1 and cdk2 domains (5'-CCTCCAGAACCTCCACCACC-3'). Multiple lines of transgenic mice were obtained. Lines designated #34 and #44 were selected for further study.

Whole-Mount Staining and Histological Analyses

Whole mount preparation and staining with hematoxylin was performed as described (92). Tissue samples were fixed with 4% paraformaldehyde in phosphate-buffered saline (PBS) for 14 hours at 4°C and switched to 70% ethanol for 24 hours, followed by an additional 24 hour incubation in 70% ethanol at 4°C. The University of Florida Molecular Pathology Core embedded the tissue samples in paraffin, prepared 5 μm sections, and stained the sections with hematoxylin and eosin (H&E) or Trichrome.

Isolation and Culture of Cancer and Tumor-Associated Fibroblast Cell Lines

Cancer cells were cultured from the tumors as described previously (92). Fibroblasts were removed from colonies of tumor cells by differential trypsinization and retained and cultured separately. Established cell lines were propagated in Dulbecco's Modified Eagle's Medium (DMEM) supplemented with 10% fetal bovine serum (FBS). Recombinant adenoviruses and retroviruses and the procedures used for infection and selection were described previously (57, 93). Roscovitine, a TGFß Receptor I kinase inhibitor (Cat. # 616452), and rapamycin were obtained from EMD Biosciences Inc. (La Jolla, CA). Recombinant human TGFß1 and recombinant human HGF were obtained from Chemicon International (Temecula, CA).

Immunoblot Analysis of Tumor Samples and Tumor-Derived Dell lines and Rb Kinase Assays

Preparation of tumor and cell lysates and subsequent immunoblot analysis were performed as described previously (57, 93). Antibodies to the FLAG epitope (F-3165) and α-Smooth Muscle Actin (A-2547) were obtained from Sigma-Aldrich, Inc. (St. Louis, MO). Her2/c-*neu* antibody (MS-730) was obtained from Neomarkers (Fremont, CA). E-Cadherin antibody was obtained from BD Biosciences (San Jose, CA). P-Cadherin antibody (sc-7893) was obtained from Santa Cruz Biotechnology, Inc. (Santa Cruz, CA). Antibodies to c-Met (#3127), c-Met phosphorylated on tyrosine residues 1234/1235 (#3126), Akt (#9272), Akt phosphorylated on threonine 308 (#9275), STAT3 (#9132), and STAT3 phosphorylated on tyrosine 705 (#9145P) were purchased from Cell Signaling Technologies (Beverly, MA). The anti-HIRA antibody (94) was generously provided by Dr. Peter Adams (Fox Chase Cancer Center Philadelphia, PA). The sources of the other antibodies were listed previously (57, 93, 95, 96). Rb kinase assays of anti-Flag and anti-cdk4 immunoprecipitates were performed as described previously (57, 93).

Transcriptional Reporter Assays and Cell Proliferation Analyses

The Mv1Lu cell line with the plasminogen activator inhibitor-1 (PAI-1) promoter driving a luciferase reporter gene (PAI-Luc cells) was provided by Dr. D. Rifkin (New York University, New York, NY) and has been described previously (97). Conditioned cell culture medium was prepared by incubating equal numbers of cells with the same volume of medium over a period of five days. The medium was collected and debris was removed by centrifugation, followed by passage through a 0.2 μm filter. PAI-Luc cells were incubated with conditioned medium samples for twenty-four hours, luciferase assays were performed, and the results normalized to protein concentration as described (57).

^{3}H-thymidine incorporation assays were performed as described previously (93). Flow cytometry analysis of propidium iodide stained nuclei and data analysis were performed by the University of Florida Flow Cytometry Core Laboratory.

Results

Characterization of MMTV-D1K2 Mammary Glands

Two transgenic mouse MMTV-D1K2 lines termed #34 and #44 engineered to express the cyclin D1-cdk2 fusion protein in the mammary gland (Fig. 2-1A) were characterized. Mammary glands from 56 week old virgin females were examined as hematoxylin stained whole mounts and by hematoxylin and eosin (H&E) staining of tissue sections (Fig. 2-1B). Mammary glands from wild type FvB females exhibit a fully developed ductal tree, but little side branching. Mammary glands from transgenic lines #34 and #44 exhibit a significant degree of side branching. H&E stained mammary sections indicate that epithelial structures are sparse in wild type glands, but dense assemblies of epithelial structures are present in the transgenic animals. Mammary glands from aged transgenic females exhibit a progressively more abnormal phenotype. Glands from 102 week old line #44 MMTV-D1K2 animals exhibit hyperplastic

lesions. Examination of H&E stained sections of these mammary glands indicate that these lesions consist of ductal structures surrounded by fibroblasts (Fig. 2-1C). The strong blue staining by trichrome overlaps with the fibroblasts and is consistent with collagen deposition associated with the fibrosis. The hyperplastic lesions observed frequently progressed into tumors and by two years of age about 70% of the animals in the MMTV-D1K2 #44 line had developed mammary tumors (Fig. 2-1D). Salivary gland tumors occurred less frequently and were not included in the data used to plot Fig. 2-1D. Several mammary and salivary tumors were also observed in the MMTV-D1K2 #34 line indicating that tumor formation in the MMTV-D1K2 animals is not an artifact of the transgene insertion site. No tumors of any kind were observed in wild type virgin female littermates. Mammary tumors were not observed in male transgenic mice.

Characterization of MMTV-D1K2 Tumors

MMTV-D1K2 mammary tumors exhibit a prominent stromal reaction (Fig. 2-2A) and in many cases a large fraction of the tumor bulk was made up of cells of mesenchymal morphology (arrows) distributed throughout the tumors. In one mouse, L44-7f, a mammary gland lesion was observed that resembled human mammary sclerosing adenosis. These lesions are considered benign yet premalignant in humans and consist of atypical glandular structures that proliferate to various extents in a fibrotic stroma with proliferating myoepithelial cells. Tumors from MMTV-*neu* transgenic animals were examined in parallel because the human homolog of the rat *neu* gene, Her2 is overexpressed in approximately 30% of breast cancers (98, 99), cyclin D1 is thought to play an important role in *neu*-induced tumorigenesis (100, 101), and because we had previously isolated and characterized cancer cell lines derived from MMTV-*neu* tumors. The phenotype of MMTV-D1K2 mammary tumors differed from the MMTV-*neu* tumors, which exhibited a relatively homogenous center surrounded by a thin layer of stroma (arrow).

Examination of H&E stained tissue sections from several representative tumors indicated that the majority of the MMTV-D1K2 tumors were mammary gland adenocarcinomas ranging from low to high grade (Fig. 2-2B). Adenosquamous differentiation was observed in one tumor. Two tumors were observed in salivary glands and one of these (L34-57f) appeared to be of salivary origin.

Immunoblot analysis of tumor lysates (Fig. 2-2C) demonstrated that the FLAG-tagged cyclin D1-cdk2 fusion protein is expressed in the MMTV-D1K2 tumors. MMTV-D1K2 tumors contained similar levels of E-Cadherin and Actin as MMTV-*neu* tumors, but on average expressed higher levels of α-Smooth muscle actin. Higher levels of α-Smooth muscle actin could result from either a greater proportion of myofibroblasts or myoepithelial cells in the MMTV-D1K2 tumors than in the MMTV-*neu* tumors. Immunoblot analyses examining a MMTV-D1K2 tumor extract with a MMTV-*neu* tumor extract serving as the control (Fig. 2-2D) demonstrated that Rb is hyperphosphorylated in the MMTV-D1K2 tumor, and that the protein products of the E2F-dependent genes BRCA1, p107, and E2F1 are upregulated relative to the level observed in the MMTV-*neu* tumor lysate. Immunoprecipitation of these tumor lysates with anti-FLAG-agarose resin demonstrated that the Flag-tagged cyclin D1-cdk2 fusion protein present in the MMTV-D1K2 tumor lysate was present in complexes with p21, p27, and PCNA (Fig. 2-2E). It is likely that the fusion protein drives tumor formation by directly phosphorylating substrates, and by sequestering p21 and p27.

Derivation and Characterization of Cancer Cell Lines from MMTV-D1K2 Tumors

The large proportion of fibroblasts in the MMTV-D1K2 tumors made it difficult to study the biochemical properties of the cancer cells. We isolated a series of cancer cell lines and tumor-derived fibroblast cell lines to allow a detailed analysis of the properties of each cell type

in isolation and to study how these two cell types might functionally interact in tumors. The *neu*T cell line was derived from an MMTV-*neu* tumor and serves as a reference for comparison with results obtained with cell lines derived from MMTV-D1K2 tumors. Five cancer cell lines were derived from five different MMTV-D1K2 tumors and termed D1K2-T1, D1K2-T2, D1K2-T3, D1K2-T4, and D1K2-T5. D1K2-T1 was isolated from a mammary tumor arising in the L44-25f MMTV-D1K2 transgenic mouse. D1K2-T3 was isolated from a salivary tumor arising in the L34-57f MMTV-D1K2 transgenic mouse. The D1K2-T1 and D1K2-T3 cell lines exhibit the cuboidal morphology typical of luminal epithelial cells and are similar in appearance to the *neu*T cells (Fig. 2-3A). The D1K2-T2, -T4, and T5 cell lines exhibit myoepithelial morphology and express markers of both the luminal and myoepithelial lineages. These cell lines are the subject of ongoing investigation and will not be described further here.

We performed propidium iodide staining followed by flow cytometry analysis to determine whether expression of the cyclin D1-cdk2 fusion protein significantly altered the cell cycle profile (Fig. 2-3B). Rapidly growing *neu*T cells exhibit a typical cell cycle profile. In contrast, the D1K2-T1 cells and to a lesser extent the D1K2-T3 cells, exhibited multiple peaks suggesting that these cell lines are aneuploid. Similar observations were made with the D1K2-T4 and D1K2-T5 cell lines (data not shown). In all cases, each of the observed peaks of fluorescence intensity was shifted to exactly twice the fluorescence intensity by a 24 h treatment of the cells with the M-phase arresting agent nocodazole (data not shown). The results suggest that the peaks represent different populations of cancer cells with different states of ploidy. Overall, four of the five cell lines derived from MMTV-D1K2 tumors exhibited evidence of aneuploidy by flow cytometry. This observation is consistent with the observations that cyclin D1 overexpression induces aneuploidy (102), and that hyperactivation of cdk2 induces aneuploidy

(103). Thus the induction of aneuploidy may be an additional mechanism by which the cyclin D1-cdk2 fusion protein, and by extension cyclin D1/cdk2 complexes, drive tumorigenesis.

Cell lines were derived from the *neu*T cells by transduction with a control retroviral vector (*neu*T/Hyg) or the same vector encoding the cyclin D1-cdk2 fusion protein (*neu*T/D1K2). Immunoblot analysis of lysates from these cells demonstrated that expression of the cyclin D1-cdk2 fusion protein was higher in the D1K2-T1 cells than in the D1K2-T3 cells (Fig. 2-3C). The *neu*T/D1K2 cells express the cyclin D1-cdk2 fusion protein at levels similar to those observed in the D1K2-T3 cells. Interestingly, Rb phosphorylation levels are similar in the *neu*T/Hyg, *neu*T/D1K2, and D1K2-T3 cell lines but higher in the D1K2-T1 cells. D1K2-T1 cells also exhibit altered p130 electrophoretic mobility consistent with p130 hyperphosphorylation. Together, the results indicate that high-level expression of the cyclin D1-cdk2 fusion protein can occur in tumors and is associated with Rb hyperphosphorylation and cell cycle deregulation. However, lower levels of cyclin D1-cdk2 expression that do not cause obvious biochemical perturbations as observed in the D1K2-T3 cells are apparently sufficient to initiate tumor formation. Immunoblot analysis of lysates from the *neu*T, D1K2-T1, and D1K2-T3 cell lines demonstrated that expression of the HGF receptor c-Met is elevated in the D1K2-T1 and D1K2-T3 cell lines relative to the *neu*T cell line (Fig. 2-D). Cdk2 immunoblots indicated that expression of the cyclin D1-cdk2 fusion protein (*) in the D1K2-T1 cells is about twice that of endogenous cdk2 (-), while the fusion protein was barely detectable in the D1K2-T3 cells using the cdk2 antibody. Analysis of the phosphorylation status of the cdk2 domain of the fusion protein on the regulatory sites Tyr15 and Thr160 using phospho-specific antibodies indicated that the level of phosphorylation of the fusion protein on both sites is higher than that of endogenous cdks. This is consistent with our previous observations indicating that the cyclin D1

domain of the fusion protein stimulates the phosphorylation of the cdk2 domain through an intramolecular mechanism (57). The observation that inhibitory phosphorylation of Tyr15 of the fusion protein is enhanced suggested that the cyclin D1-cdk2 fusion protein might not be catalytically active. We addressed this issue by performing kinase assays of the cyclin D1-cdk2 fusion protein immunoprecipitated using the FLAG antibody (Fig.2-3E). We also examined whether expression of the cyclin D1-cdk2 fusion protein altered the activity of endogenous cdk4. Although the fusion protein was heavily phosphorylated on both Tyr15 and Thr160, it phosphorylated Rb *in vitro*. This result suggests that a population of the fusion protein molecules exists in which the activating site, Thr160, is phosphorylated, but the inhibitory site, Tyr15, is not phosphorylated. The levels of cdk4 kinase activity toward Rb were similar in the *neu*T, D1K2-T1, or D1K2-T3 cell lines, indicating that expression of the cyclin D1-cdk2 fusion has minimal effects on endogenous cdk4 activity. These results demonstrate that the cyclin D1-cdk2 fusion protein expressed in the MMTV-D1K2 cancer cell lines is enzymatically active, is overexpressed only marginally relative to endogenous cdk2 levels, and that the fusion protein displays enhanced regulatory phosphorylation relative to endogenous cdks.

Derivation and Characterization of Fibroblast Cell Lines from MMTV-D1K2 Tumors

Given the large proportion of fibroblasts in the MMTV-D1K2 tumors and the close proximity between the epithelial cells and fibroblasts in hyperplastic lesions (Fig. 2-1C) all the way to fully developed tumors (Fig. 2-2A), it is likely that tumor-associated fibroblasts have a significant influence on the progression and growth of MMTV-D1K2 tumors. We isolated fibroblast cell lines from the MMTV-D1K2 tumors to examine the properties of these cells. The tumor-derived fibroblast lines 1 and 2 (D1K2-TDF1 and D1K2-TDF2) exhibit the elongated morphology typical of fibroblasts and lack the extensive cell-cell contacts characteristic of colonies of epithelial cells (Fig. 2-4A). Immunoblot analysis demonstrated that D1K2-TDF1 and

D1K2-TDF2 cells did not express proteins typically present in cancer cells of epithelial origin such as c-Met, E-Cadherin, and P-Cadherin (Fig. 2-4B). The tumor derived fibroblast cell lines also did not express the cyclin D1-cdk2 fusion protein, but expressed very high levels of α-Smooth muscle actin (α-SMA). α-SMA is expressed in fibroblasts that have differentiated into myofibroblasts. Such differentiation might arise as a result of cell culture *in vitro*. However the presence of myofibroblasts in the MMTV-D1K2 tumors could explain the relatively high levels of α-SMA present in the tumors and could also explain the high levels of collagen detected by trichrome staining (Figs. 2-1 and 2-2) since myofibroblasts are thought to be the major cell type responsible for collagen deposition during fibrosis (104-106). The differentiation of stromal fibroblasts in the vicinity of tumors is thought to be caused by TGFß secreted by tumor cells since TGFß1 is capable of inducing the differentiation of mammary stromal fibroblasts to myofibroblasts *in vitro* (107, 108), fibroblast differentiation to myofibroblasts occurs in the vicinity of tumors in a graded manner (109), and tumors are known to secrete significant amounts of TGFß (110).

Discussion

Cyclin D1/cdk2 complexes are present in human breast cancer cell lines (56), and the levels of these complexes correlate well with the degree of cyclin D1 overexpression. It is unknown whether these complexes participate in the transforming effects of cyclin D1 overexpression. We constructed a gene encoding a cyclin D1-cdk2 fusion protein to explore in a selective fashion the potential functions of cyclin D1/cdk2 complexes in cell transformation and mammary tumorigenesis (57). The results presented here demonstrate that expression of this cyclin D1-cdk2 fusion protein (D1K2) in the mammary gland under the control of the MMTV promoter causes precocious lobuloalveolar differentiation of mammary glands in virgin mice.

The extent of the phenotype increases with age and results in the formation of hyperplastic lesions and eventually breast tumors. MMTV-D1K2 tumors induce a strong desmoplastic reaction as compared with MMTV-*neu* tumors. Biochemical analyses demonstrated cell cycle deregulation in the tumors, including Rb and p130 hyperphosphorylation and upregulation of E2F-dependent gene products.

The MMTV-D1K2 mice and cell lines derived from their tumors will be valuable tools for further delineating the mechanisms involved. A more thorough understanding of the mechanisms at work in this cycle is critical because of the high frequency with which similar desmoplastic reactions are observed in a wide variety of human tumors, the connection between tumor-induced stromal desmoplasia and tumor invasiveness and metastatic potential, and because several key elements of the cycle including c-Met (111, 112), TGFß receptors (113-115), and cdk2 (60, 89, 90) are targets for agents under development as anti-cancer therapeutics.

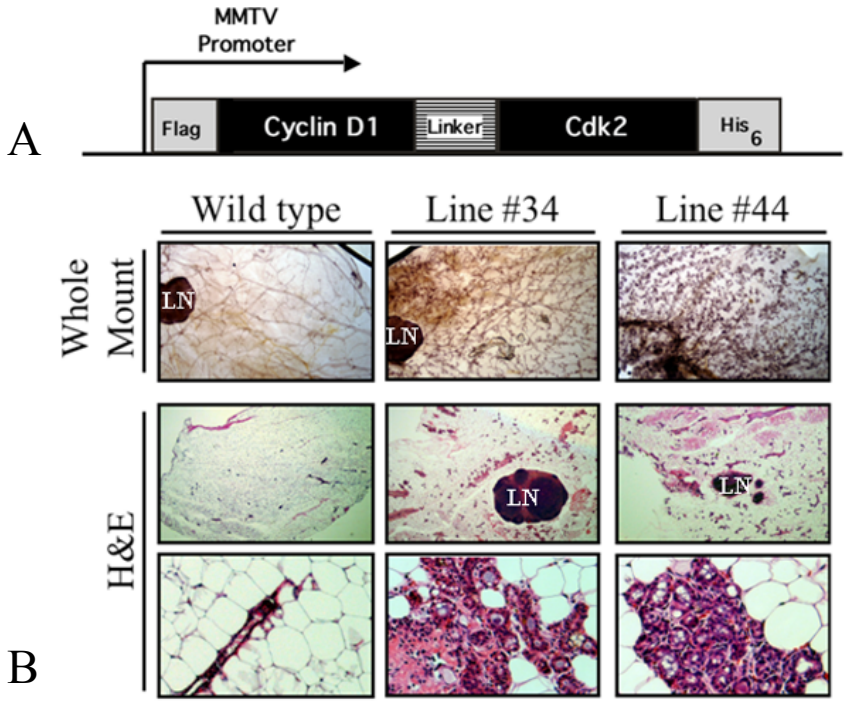

Figure 2-1.MMTV-cyclin D1-cdk2 (MMTV-D1K2) transgenic model and mammary phenotype. A) Model depicting the MMTV promoter driving the expression of the transgene encoding the N-terminal FLAG epitope tag, the cyclin D1 domain, a flexible linker, the cdk2 domain, and the C-terminal His_6 affinity tag. B) Representative mammary whole mounts from 56 week old wild type female mice and the #34 and #44 lines of the MMTV-D1K2 transgenic mice stained with hematoxylin (top panel). Inset panels show branching morphology at higher magnification. The bottom panels are hematoxylin and eosin (H&E) stained histological sections at low and high magnification. Mammary lymph nodes are marked LN. C) H&E and trichrome stained mammary gland sections from 102 week old MMTV-D1K2 transgenic mice of the #44 line displaying regions of epithelial hyperplasia associated with fibrosis. Lymph nodes are marked LN. D) Kaplan-Meier curve showing tumor incidence in wild type and line #44 mice as a function of age in months. The number of virgin female animals in each group is shown in the inset legend.

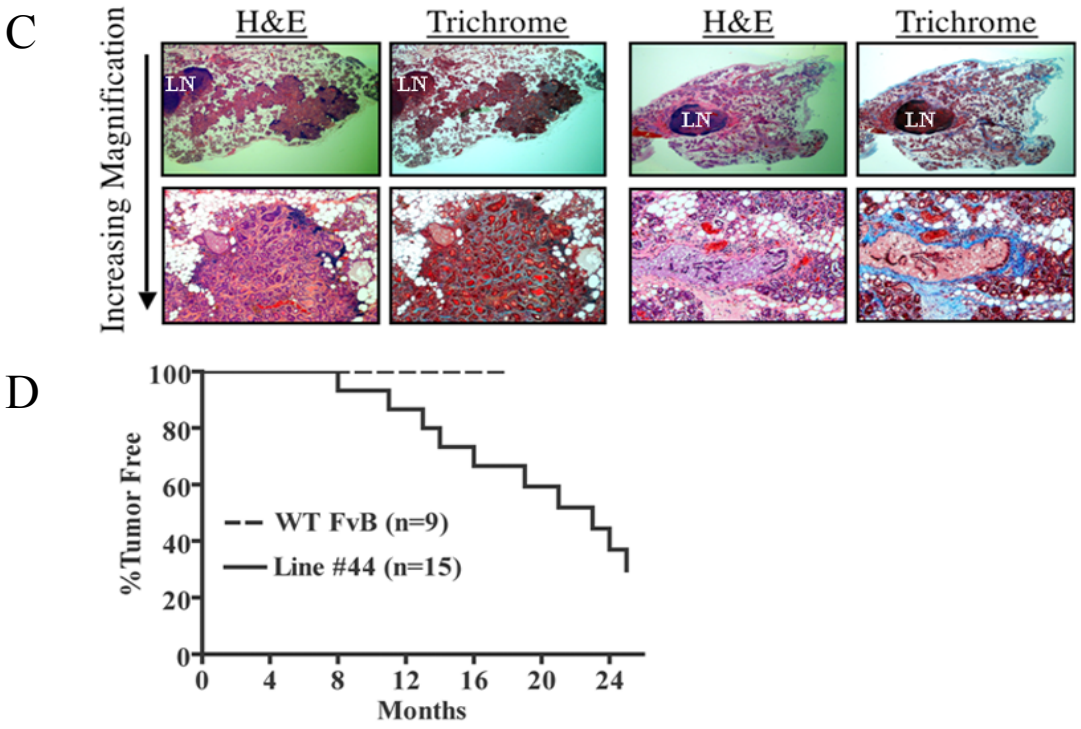

Figure 2-1.Continued.

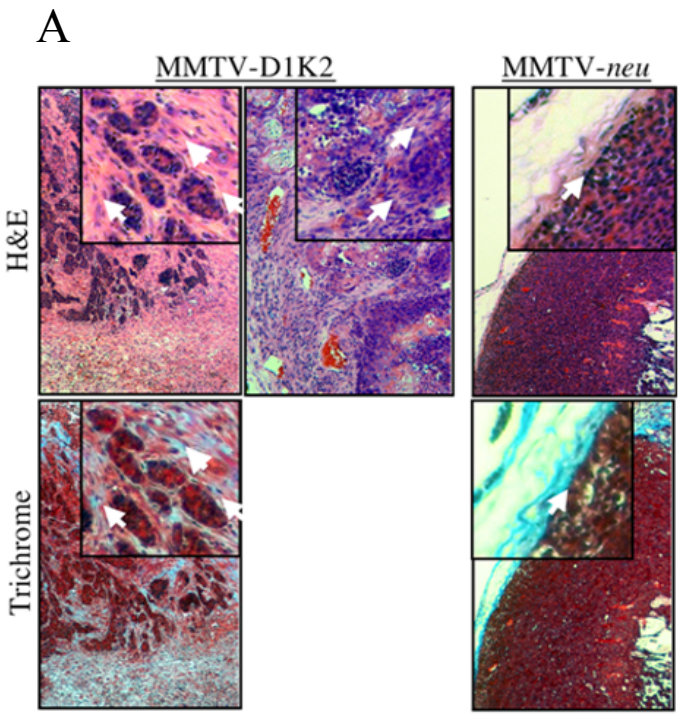

B

Mouse ID	Sample	Diagnosis
L34-57f	Tumor	Salivary gland with adenocarcinoma
L44-7f	Tumor 1	Salivary gland with adenocarcinoma
	Tumor 2	Mammary gland adenocarcinoma
L44-18f	Tumor	Mammary gland adenocarcinoma
L44-25f	Tumor	Mammary gland adenocarcinoma
L44-29f	Tumor	Mammary gland adenocarcinoma
L44-31f	Tumor	Mammary gland adenosquamous carcinoma
L44-79f	Tumor	Mammary gland adenocarcinoma

Figure 2-2.MMTV-D1K2 mammary and salivary tumors.
A) H&E and trichrome stained histological sections of MMTV-D1K2 and MMTV-*neu* mammary tumors. B) Morphological characterization of several representative tumors arising in the #34 (L34-) and #44 (L44-) transgenic lines. C) Immunoblot analysis of extracts from four different MMTV-D1K2 and four different MMTV-*neu* mammary tumors demonstrating expression of the flag-tagged cyclin D1-cdk2 transgene product (Flag (D1K2)) and c-*neu*. Tumor lysates were also analyzed for the levels of E-Cadherin, alpha-Smooth Muscle Actin (α-SMA), and Actin as a loading control. D) Immunoblot analysis demonstrating the hyperphosphorylation of Rb on multiple residues in a MMTV-D1K2 tumor extract relative to a MMTV-*neu* tumor extract. P-Rb and P-p130 represent the phospho-forms of Rb and p130, and Rb and p130 represent the corresponding unphosphorylated forms. Multiple products of E2F-dependent genes are upregulated in the MMTV-D1K2 tumor relative to the MMTV-*neu* tumor including, BRCA1, p107, and E2F1. Hira serves as a loading control. E) Lysates from MMTV-*neu* and MMTV-D1K2 tumors were subjected to immunoprecipitation with Anti-Flag-agarose to isolate complexes containing the cyclin D1-cdk2 fusion protein. Immunoblot analysis indicated that these complexes contain the cyclin D1-cdk2 fusion protein (Flag), p21, p27, and PCNA.

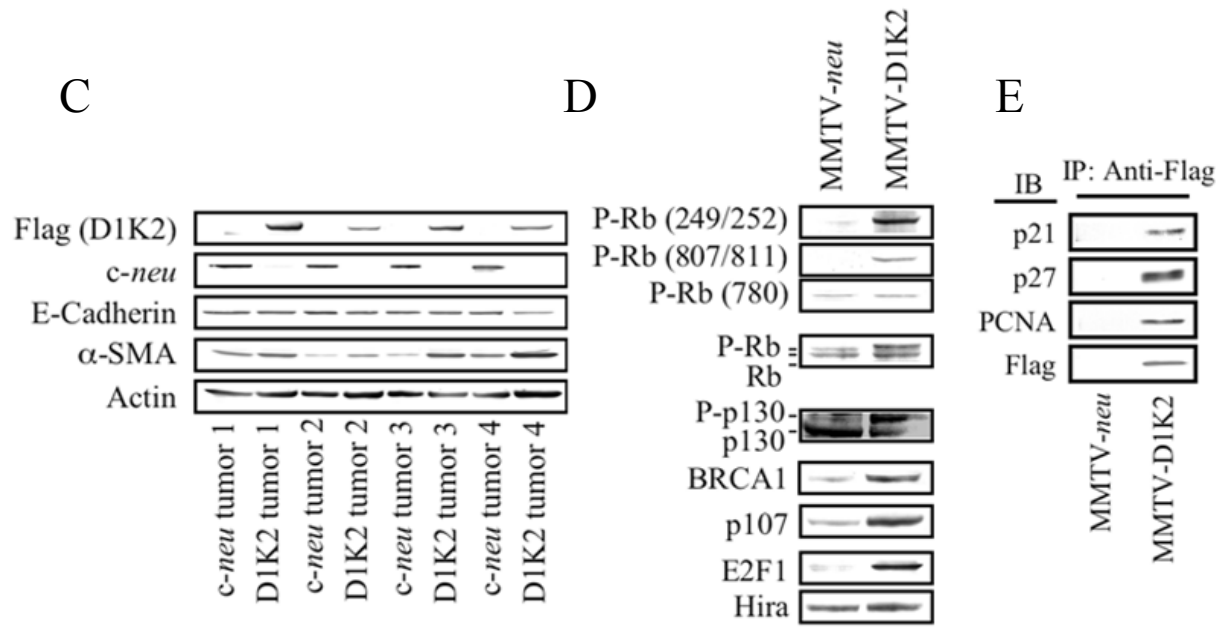

Figure 2-2.Continued.

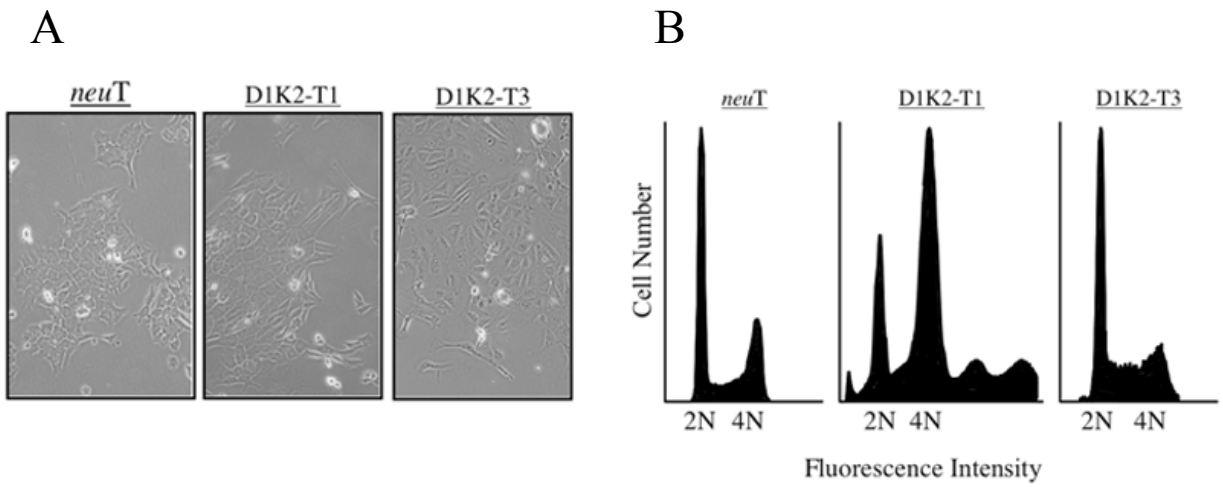

Figure 2-3. Isolation and characterization of MMTV-D1K2 cancer cell lines
A) Phase contrast micrographs of cell lines derived from an MMTV-*neu* tumor (*neu*T) and two different MMTV-D1K2 tumors (D1K2-T1 and D1K2-T3). B) Flow cytometry analysis of rapidly growing *neu*T, D1K2-T1, and D1K2-T3 cells stained with propidium iodide. C) Immunoblot analysis of the *neu*T/Hyg and *neu*T/D1K2 cell lines prepared by retroviral transduction of the *neu*T cells with an empty retroviral vector or a vector encoding the cyclin D1-cdk2 fusion protein, respectively, and the D1K2-T1 and D1K2-T3 cell lines. The results indicate expression of the cyclin D1-cdk2 fusion protein (Flag (D1K2)) in the appropriate samples and demonstrate Rb and p130 hyperphosphorylation in the D1K2-T1 cell line. E-Cadherin is expressed at similar levels in the four cell lines. Actin serves as a loading control. D) Immunoblot analysis demonstrating the levels of expression of the cyclin D1-cdk2 fusion protein (*) relative to the levels of endogenous cdk2 (-), and phosphorylation of the cyclin D1-cdk2 transgene product on the activating Thr^{160} (P-cdk2(T160)) and inhibitory Tyr^{15} (P-cdk2(Y15)) phosphorylation sites of the cdk2 domain. C-Met is expressed at higher levels in the D1K2-T3 and D1K2-T1 cell lines than in the *neu*T cell line. E) Assay of the kinase activity of the cyclin D1-cdk2 fusion protein and endogenous cdk4. Extracts of the indicated cell lines were immunoprecipitated using the FLAG antibody to isolate the cyclin D1-cdk2 fusion protein, or a cdk4 antibody to isolate endogenous cdk4. Immunoprecipitates were assayed for kinase activity using GST-Rb as the substrate, and site-specific Rb phosphorylation was detected by immunoblotting with phospho-specific antibodies. Controls included the use of *neu*T cell extracts in FLAG immunoprecipitations, and omission of the cdk4 antibody (No 1º).

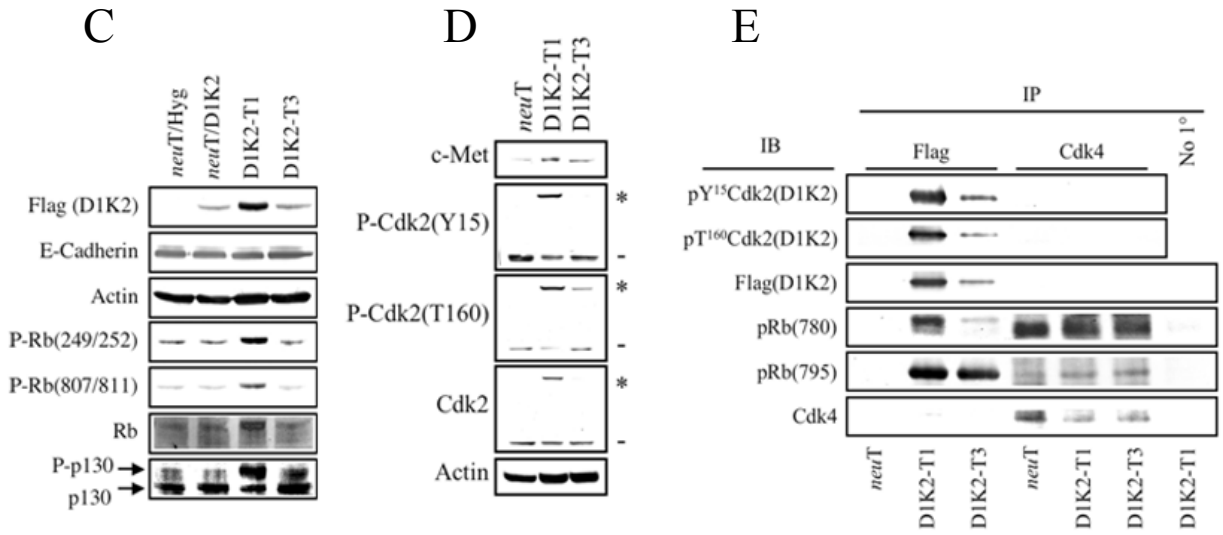

Figure 2-3.Continued.

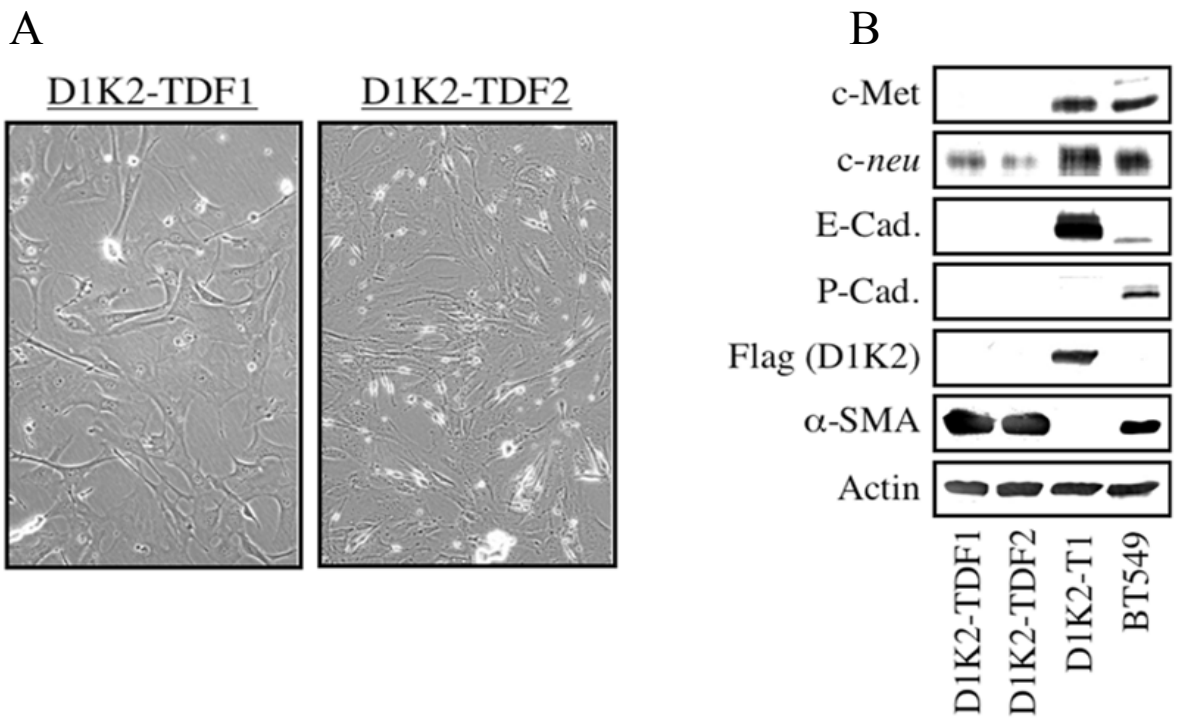

Figure 2-4. Isolation and characterization of tumor-derived fibroblast cell lines. A) Phase contrast micrographs of fibroblast cell lines derived from two different MMTV-D1K2 tumors (D1K2-TDF1 and D1K2-TDF2). B) Immunoblot analysis of extracts from the tumor derived fibroblast cell lines D1K2-TDF1 and D1K2-TDF2, the MMTV-D1K2 tumor cell line D1K2-T1, and the BT549 human mammary carcinoma cell line. The results demonstrate a lack of E-Cadherin, P-Cadherin, c-Met, or the cyclin D1-cdk2 transgene (Flag (D1K2)) in the tumor derived fibroblasts. The D1K2-TDF1 and D1K2-TDF2 cells express high levels of alpha-Smooth Muscle Actin (α-SMA). D1K2-T1 and BT549 lysates served as positive controls for the immunoblot analysis and Actin serves as a loading control.

CHAPTER 3
MAMMARY TUMORS INITIATED BY CONSTITUTIVE CDK ACTIVATION CONTAIN AN INVASIVE BASAL-LIKE COMPONENT

Introduction

Microarray analyses have recently allowed breast tumors to be categorized as luminal, basal-like, normal-like, or Her2 positive, based on distinct gene expression profiles, morphological characteristics, prognostic outcomes, and responsiveness to currently available therapeutic approaches (116, 117). The basal-like subtype represents approximately 20% of human breast cancers overall, but 39% of breast tumors in premenopausal African American women (118). These tumors are associated with a high rate of recurrence and poor outcome (117). The basal-like subtype of cancers is also termed "triple negative" because these tumors typically lack Estrogen Receptor (ER), Progesterone Receptor, and Her2 overexpression, but generally express a subset of myoepithelial markers, including Cytokeratin 14 (CK14), Cytokeratin 5 (CK5), α-Smooth Muscle Actin (αSMA), Nestin, or p63 (119-121). Basal-like tumors lack responsiveness to Tamoxifen and Aromatase inhibitors that target ER positive luminal tumors, and Herceptin that targets Her2 positive tumors.

The mouse basal-like breast cancer models described to date involve genetic deletion of the BRCA1 and p53 tumor suppressor genes (122, 123). Tumors initiated by BRCA1 inactivation in mice express the Progesterone Receptor (124) and overexpress Her2 (125) and thus do not fit the "triple negative" clinical definition of basal breast cancer. Therefore it is likely that additional genetic lesions contribute to the formation of sporadic human basal-like breast cancers. Microarray studies have suggested several candidate "drivers" of basal breast cancer including Epidermal Growth Factor Receptor (EGFR), c-Kit, c-Met, and cyclin E. However, none of these genes have yet been demonstrated to specifically induce basal-like breast cancer when overexpressed. Interestingly, human basal-like breast tumors frequently exhibit p16

overexpression, low levels of Rb and cyclin D1 expression, and high levels of cyclin E expression (126). Based on these observations it was proposed that Rb inactivation is mechanistically linked to the basal-like subtype (126). Together these results suggest that basal-like tumors may have low levels of cdk4/cdk6 activity, but perhaps high levels of cdk2 activity.

In the previous chapter, a novel mouse transgenic model of breast cancer was described, in which expression of a cyclin D1-cdk2 (D1K2) fusion protein (57) under the control of the MMTV promoter/enhancer induces mammary tumorigenesis (MMTV-D1K2 animals) (127). Mammary tumors from these animals exhibit Rb hyperphosphorylation, high levels of cdk2 activity, and upregulation of E2F-dependent transcription (127). Thus, MMTV-D1K2 tumors exhibit functional inactivation of Rb tumor suppressor activity.

MMTV-D1K2 tumors are heterogeneous and induce a desmoplastic reaction associated with TGFß secretion by the cancer cells. As mentioned previously (127), some of the cancer cell lines derived from the MMTV-D1K2 tumors exhibit the morphological features of myoepithelial cells. This chapter is focused on a more extensive characterization of MMTV-D1K2 cell lines and demonstrates that these cells express protein markers associated with the basal/myoepithelial lineage.

E-cadherin is a potent invasion suppressor expressed in nontransformed mammary epithelial cells (128). The MMTV-D1K2 cell lines exhibit decreased or mislocalized E-cadherin expression in culture. Introduction of cell lines derived from MMTV-D1K2 tumors into the mammary glands of wild type syngeneic mice results in the formation of invasive tumors composed of spindle-shaped cells that exhibit E-cadherin mislocalization to the cytoplasm and the expression of basal/myoepithelial markers. Morphological and immunohistochemical analyses of the primary tumors demonstrate a biphasic morphology characteristic of adeno-

myoepithelial-type carcinoma with populations of spindle-shaped cells. These spindle-shaped cells exhibit E-cadherin downregulation and localization to the cytoplasm and expression of the myoepithelial marker αSMA. These studies indicate the presence of a subpopulation of invasive basal-like breast cancer cells in the primary MMTV-D1K2 tumors.

In vitro analysis of multiple clonal cell lines derived from MMTV-D1K2 tumors demonstrate the expression of various subsets of myoepithelial and luminal epithelial markers, a finding consistent with the "mixed-lineage" properties of human basal breast cancers (129-131). In all of the cell lines isolated, E-cadherin expression is either low and/or mislocalized to the cytoplasm. E-cadherin mislocalization is associated with the inability of the cells to form colonies with normal cell-cell contacts in culture and correlates with the lack of ß-catenin and p120ctn staining at cell-cell junctions. In some cell lines, decreased E-cadherin expression is associated with an increase in N- or P-cadherin expression. This "cadherin switch" from E- to N-cadherin expression is associated with increased invasiveness and part of the epithelial to mesenchymal transition (EMT) that occurs during the progression of some tumor types (132). EMT has been shown to occur in the basal-like category of breast cancers (133).

Materials and Methods

Isolation of Tumor Cell Lines

MMTV-D1K2 cancer cell lines were isolated essentially as described (127). When differential trypsinization was performed, the cells remaining adherent to the flasks as well as the detached cells were retained. This is critical because several of the basal breast cancer cell lines adhere very loosely to tissue culture flasks or flasks coated with rat tail collagen. The loosely adherent myoepithelial-like cancer cells were separated from myofibroblasts by taking advantage of their differential rates of adhesion. The cancer cells were cloned by limiting dilution. All

cells were maintained in Dulbecco's Modified Eagles Medium (DMEM) supplemented with 10% heat inactivated fetal bovine serum (Mediatech, Inc., 35-011-CV, Manassas, VA, USA).

Preparation and Analysis of Tumor and Cell Extracts by Immunoblot

Cell extracts were prepared as described (127) and immunoblot analysis was performed using antibodies from the following sources: Santa Cruz Biotechnology, Inc., Santa Cruz, CA, USA (N-cadherin (sc-7939), P-cadherin (sc-7893), Vimentin (sc-32322), Nestin (sc-23927), ß-Catenin (sc-7199), Zyxin (sc-6437), p130 (sc-317), cdk2 (sc-163), Actin (1616), and p53 (sc-100)); Sigma-Aldrich (St. Louis, MO, USA) (Flag, M2 (F-3165), α-Smooth Muscle Actin (A-2547)). Antibodies specific for EGFR (#2232) were obtained from Cell Signaling Technology, Inc., Danvers, MA, USA. P53 antibodies were also obtained from Oncogene Science (Cambridge, MA, USA). Antibodies specific for Cytokeratin 14 (MS-115) and Her2/*neu* (MS-730) were obtained from LabVision/Neomarkers, Inc., Fremont, CA, USA. P120 catenin (610133) antibody was obtained from BD Transduction Laboratories, San Diego, CA, USA.

Tumor samples contain large amounts of immunoglobulin, which interferes with subsequent immunoblot and immunoprecipitation assays. Tumor-associated immunoglobulin was removed by preclearing aliquots of tumor lysate containing 1 mg of protein with 100 µl/tube packed Protein G-Sepharose (Invitrogen, 10-1242, Carlsbad, CA, USA). The supernatants were retained for subsequent analyses.

Immunofluorescence Microscopy

Cells were plated onto glass coverslips in six-well plates. After a 24 hr incubation, cells were fixed with 1% Paraformaldehyde in phosphate-buffered saline (PBS) for 20 minutes, followed by a 10 minute incubation with quench solution (50 mM Ammonium Chloride + 0.5% TritonX-100 in PBS). The cells were then blocked for one hour with antibody buffer (10% Goat Serum + 0.5% Triton X-100 in PBS). Primary staining was performed using the following

antibodies at a 1:100 dilution in antibody buffer for two hours: Cytokeratin 14 (Neomarkers, Inc., MS-115); E-cadherin (610181) and p120 Catenin (610133) from BD Biosciences Pharmingen; E-cadherin (24E10) from Cell Signaling Technology, Inc.; and Zyxin (sc-6437), ß-Catenin (sc-7199), N-cadherin (sc-7939) from Santa Cruz Biotechnology, Inc. Following four washes with PBS, cells were incubated with secondary antibody for one hour using either goat anti-Rabbit Fluor 488 (Invitrogen Molecular Probes (Carlsbad, CA, USA), A11008), goat anti-Mouse Fluor 488 (Invitrogen Molecular Probes, A11001), rabbit anti-Goat Fluor 488 (Invitrogen Molecular Probes, A11078), or Goat anti-Mouse Cy3 (Zymed (Carlsbad, CA, USA), 81-6515), at either a 1:200 dilution in antibody buffer for single staining, or 1:300 dilution for double staining. Following four washes with PBS, coverslips were mounted onto slides with Vectashield + DAPI (Vector Laboratories, H-1200, Burlingame, CA, USA). Actin was visualized using Texas-Red-X Phalloidin (Invitrogen Molecular Probes-T7471), added during the secondary staining step at a dilution of five units per slide. Images were captured using a Zeiss (Thornwood, NY, USA) Axioplan2 upright microscope and visualized using Openlab 5.3.0 Improvision software.

Orthotopic Tumor Growth Studies

Cells in log growth phase were collected by trypsin digestion, suspended in 10% FBS-DMEM, and washed three times with Hepes balanced salt solution (HBSS) (Mediatech, Inc., 21-020-CV). The cells were counted and diluted to a concentration of 107 cells/ml in HBSS. The cell suspension (100 µl) was injected into the #4 mammary glands of adult wild type female FvB mice just beneath the surface of the nipple. Three mice were injected with each polyclonal cell line and tumor formation occurred from two to six weeks in all of the injected animals. Tumors were excised at a small size (2-6 mm in diameter) so that tumor invasion into the surrounding stroma could be observed.

Immunohistochemical Analysis of Tumor Tissue Sections

Two micrometer serial sections of paraformaldehyde-fixed, paraffin-embedded tumor tissue were dewaxed in Tissue-Clear (Sakura Finetek Europe, Zouterwoude, The Netherlands) and hydrated through a series of diluted ethanol followed by antigen retrieval in 10 mM Tris, pH 9.0, 0.5 mM EGTA solution using microwave oven treatment (15 min.). Immunostaining was performed with a commercially available kit; Animal Research Kit – ARK (DakoCytomation, Glostrup, Denmark) in accordance with the manufacturer's instructions. Additional blocking of endogenous biotin was performed with the DAKO Biotin Blocking System (DakoCytomation) in accordance with the manufacturer's instructions. The following antibodies were employed: Monoclonal Mouse Anti-Human Smooth Muscle Actin, Clone 1A4, dilution 1:200, Monoclonal Mouse Anti-Human E-cadherin, Clone NCH-38, dilution 1:25 (both DakoCytomation); Monoclonal Mouse Anti-Human Keratin 14 Ab-1, clone LL002, dilution 1:400 (LabVision/NeoMarkers Inc.). Images were captured using an Olympus BX51 microscope equipped with a Color View camera using AnalySIS getIT version 5.0 (Soft Imaging System, Munster, Germany).

The tumor analyzed by immunohistochemistry in Figure 3-5A is from a 58 year-old caucasian woman diagnosed with invasive ductal carcinoma, grade III. Morphologically the tumor is described as a "ring carcinoma" because of its necrotic center.

Results

Mouse Mammary Tumor Virus-D1K2 Hypercellular Lesions Exhibit an Invasive Phenotype

In the previous chapter it was shown that tumors arise in transgenic mice in which a cyclin D1-cdk2 fusion protein (57) is driven by the MMTV promoter/enhancer (127). Tumors arising in these animals are heterogeneous and contain ductal structures surrounded by spindle-shaped

cells. The identity of these spindle-shaped cells is unclear. However these cells are of interest because they appear to invade into the surrounding mammary fat pad (Fig. 3-1A). This is in contrast to MMTV-*neu* tumors or tumors derived from MMTV-*neu* tumor cells that show well-demarcated boundaries (Fig. 3-1B). We isolated cell lines from different MMTV-D1K2 tumors to more fully characterize the cell types composing them. Several of the cell lines, including D1K2-T2 and D1K2-T4, display features in culture similar to that of primary myoepithelial cells (134-137) including an elongated morphology, multiple cellular extensions or processes, and a relative lack of cell-cell adhesion (Fig. 3-1C). The BT549 human basal-like breast cancer cell line (138) exhibits a similar morphology. In contrast, nontransformed mouse mammary epithelial NMuMG cells have a cuboidal shape and form distinct colonies that exhibit a "cobble-stone" morphology.

Mouse Mammary Tumor Virus-D1K2 Tumor Cells Display Characteristics Consistent with Basal-Like Breast Cancer

Because the MMTV-D1K2 tumor-derived cell lines exhibit a myoepithelial morphology, we examined whether they expressed myoepithelial markers. Immunoblot analysis indicates that the cell lines derived from MMTV-D1K2 tumors express varying amounts of several basal/myoepithelial markers including P-cadherin, Epidermal Growth Factor Receptor (EGFR), CK14, αSMA, and Nestin (Fig. 3-2A). In contrast, the *neu*T cell line derived from an MMTV-*neu* tumor (127) expresses low or undetectable levels of these basal markers. Several of the D1K2 cell lines also express the luminal epithelial marker E-cadherin. Because the polyclonal D1K2 cell lines exhibit a wide variety of cell morphologies, clonal cell lines were isolated. Specifically, the D1K2-T2,CL1 and D1K2-T2,CL6 clonal lines exhibit different morphologies in culture and different expression profiles in immunoblot analyses. This observation indicates that the cancer cell lines isolated are heterogeneous and is consistent with the heterogeneous nature of

the primary tumors (127). The D1K2-T4 cell line does not exhibit detectable transgene expression (Fig. 3-2A), although the DNA from this cell line tests positive for the presence of the transgene by PCR analysis (not shown). Thus, expression of the cyclin D1-cdk2 fusion protein may not be required for maintenance of the basal-like/myoepithelial phenotype. The D1K2 tumor cell lines express high levels of the intermediate filament protein Nestin (see Fig. 3-2A) which was shown to be a basal breast cancer/myoepithelial marker (119). Quantitative proteomic analyses of protein extracts from the invasive D1K2 tumor cell lines and the BT549 cell line indicate that these cells express higher levels of the structural protein Zyxin than the *neu*T and mouse mammary gland NMuMG cell lines (proteomic analyses will be described in detail elsewhere). This was verified by immunoblot (Fig. 3-2A).

The cell lines isolated from the MMTV-D1K2 tumors might represent a small fraction of the cells present in the primary tumors and therefore may not be typical of the overall tumor composition. Immunoblot analyses of the primary tumors (Fig. 3-2B) demonstrated that the tumor from which the D1K2-T1 cell line was derived expressed relatively high levels of the D1K2 fusion protein as measured by staining with Flag antibody (Flag (D1K2)). The tumor of origin of the D1K2-T1 cells also displayed low Her2 expression, high levels of E-cadherin expression, and low levels of αSMA staining. The tumor from which the D1K2-T4 cell line was derived did not express the cyclin D1-cdk2 fusion protein, expressed low levels of E-cadherin, low levels of Her2, and high levels of αSMA. MMTV-*neu* tumors exhibit high Her2 expression that correlates with high E-cadherin expression. In contrast, αSMA expression is inversely related to Her2/*neu* transgene expression and E-cadherin expression. Collectively these results suggest that the cell lines isolated for analysis have protein expression patterns similar to the primary tumors.

The lack of expression of the cyclin D1-cdk2 transgene product in the D1K2-T4 cell line and in the primary tumor from which it was derived was unexpected because these cells resemble the other MMTV-D1K2 cell lines in their morphology and expression pattern of luminal and basal markers. Immunoblot analyses were performed to examine the possibility that other molecular changes occurred that might substitute for D1K2 expression. The results showed that the D1K2-T4 cell line exhibited several features that could render D1K2 expression dispensable including cyclin A overexpression, (presumably mutant) p53 overexpression, and low levels of Rb and p21 expression (Fig. 3-2C).

Mouse Mammary Tumor Virus-D1K2 Tumor Lines Display Mixed Luminal/Myoepithelial Character

In the normal mammary gland E-cadherin is expressed in luminal epithelial cells while αSMA and CK14 are expressed in myoepithelial cells. The observation that luminal proteins such as E-cadherin and myoepithelial markers such as αSMA and CK14 are expressed in the same polyclonal cell population could be explained by the presence of cell subpopulations that each express different subsets of markers. Clonal cell lines were derived from the MMTV-D1K2 tumor cell lines to determine whether these luminal and myoepithelial markers are expressed in the same cells. Immunoblot analysis indicates that in multiple cases the clonal cell lines express luminal markers such as E-cadherin and Cytokeratin 19 (CK19) and also express basal/myoepithelial markers such as P-cadherin, EGFR, CK14, αSMA, and Nestin (Fig. 3-3A). Interestingly, two of the four D1K2-T4 subclones exhibit p53 overexpression.

Immunofluorescence microscopy experiments demonstrated that the D1K2-T1,CL1 cell line expresses both CK14 and E-cadherin uniformly in all of the cells (Fig. 3-3B). Together the results in Fig. 3-3A and 3-3B indicate that the cell lines derived from the MMTV-D1K2 tumors exhibit a mixed luminal/myoepithelial protein expression pattern at the single cell level.

A number of human mammary carcinoma cell lines have been analyzed in microarray experiments and classified into luminal or basal-like subgroups (138). Interestingly, analysis of some of these mammary carcinoma cell lines by immunoblot suggests that human breast carcinomas may also frequently exhibit a luminal/myoepithelial mixed lineage phenotype (Fig. 3-3C). The T47D, MCF7, and MDA-MB-361 cell lines, classified as luminal by microarray analysis, express the myoepithelial marker P-cadherin. Likewise, the MDA-MB-468 and BT549 cell lines, classified as basal by microarray analysis, express the luminal marker E-cadherin (Fig. 3-3C). In contrast, the nontransformed mouse mammary gland NMuMG cell line does not express P-cadherin, and the nontransformed human basal-like cell lines MCF10A and HBL100 do not express E-cadherin. P53 overexpression in the T47D, MDA-MB-468, BT549, MDA-MB-231, and MDA-MB-435s carcinoma cell lines is expected because these cells harbor mutant p53 alleles (76, 139-141).

Mouse Mammary Tumor Virus-D1K2 Tumor-Derived Cell Lines Form Invasive Tumors *In Vivo*

Basal-like tumors are often invasive, therefore we examined whether the MMTV-D1K2 tumor-derived cell lines would form invasive tumors *in vivo*. The polyclonal D1K2-T1, D1K2-T2, D1K2-T4, and D1K2-T5 cell lines were injected into the mammary glands of three wild type female FVB mice. All of the mice formed tumors from two to six weeks after injection. The tumors exhibited invasion into the surrounding mammary fat pad and muscle (Fig. 3-4A). Invasion of individual cancer cells between adipocytes and muscle fibers was observed at the tumor/stroma interface. The infiltrative tumors exhibited inclusions of adipocytes. The disorganized and poorly differentiated appearance of the tumors is similar to that of the cells in hypercellular lesions in the MMTV-D1K2 transgenic mammary glands that exhibit invasion into the fat pad (see Fig. 3-1A). The blue Trichrome staining at the invading edge of the tumors (Fig.

3-4A, D1K2-T1 and D1K2-T2) coincides with cells of fibroblastic morphology and is indicative of desmoplasia and fibroblast infiltration into the tumors. The MMTV-D1K2 cell line-derived tumors were negative for Estrogen Receptor and Progesterone Receptor expression and Her2 overexpression by immunohistochemistry (data not shown), consistent with the expression pattern of the cell lines *in vitro* (Figs. 3-2A, 3-2C). The finding that some of the D1K2 cell lines express high levels of E-cadherin in cell culture (see Figs. 3-2B and 3-3A) seems inconsistent with the poor ability of the cells to form distinct colonies *in vitro* (Fig. 3-2A), and the invasiveness of the cell lines observed *in vivo* (Fig. 3-4A).

Immunohistochemistry experiments examining the localization of E-cadherin within the tumors demonstrated that the noninvasive tumors derived from neuT cells exhibit strong E-cadherin staining at cell-cell junctions (Fig. 3-4B), and lack expression of αSMA and CK14 (not shown). In contrast, tumors derived from the D1K2-T1, D1K2-T4, and D1K2-T5 cell lines exhibit weak, diffuse cytoplasmic E-cadherin staining, suggesting that E-cadherin localization to the cytoplasm contributes to the invasiveness of these cell lines. The D1K2-T1, D1K2-T2, and D1K2-T4 cell line-derived tumors also express variable levels of CK14 (Fig. 3-4C). The positive staining of the tumors for both E-cadherin and CK14 suggests that the tumors, like the initiating cell lines, exhibit a mixed luminal/myoepithelial phenotype.

We next examined whether populations of cancer cells with a mixed lineage phenotype were present in the primary MMTV-D1K2 tumors. The primary tumor from which the D1K2-T1 cell line was derived has a biphasic morphology characteristic of adeno-myoepithelial-type carcinoma, with both glandular structures and clusters of less differentiated spindle-shaped cells (Fig. 3-4D). Immunohistochemical staining of serial tumor sections showed that these spindle-shaped cells stain positively for E-cadherin diffusely localized to the cytoplasm, and also show

positive staining for αSMA. In contrast, the surrounding glandular structures are composed of cells that express E-cadherin at their cell-cell junctions and lack αSMA expression. This observation suggests that the primary MMTV-D1K2 tumors contain both luminal/myoepithelial mixed-lineage cell populations and cells that exhibit a luminal-like staining pattern. Thus, it seems likely that the basal-like cancer cell lines isolated from the MMTV-D1K2 tumors represent the spindle-shaped subpopulation of cells present in the primary tumors.

Mouse Mammary Tumor Virus-D1K2 Tumors Resemble Human Basal-Like Breast Cancers

MMTV-D1K2 cancer cells resemble human basal-like breast cancer cell lines in terms of their morphology, protein expression patterns, and invasiveness *in vivo*. Therefore we examined how the morphology of the MMTV-D1K2 tumors compares with that of human basal-like (triple-negative) breast tumors. The representative triple-negative breast tumor shown is from a 58 year-old caucasian female with grade III invasive ductal carcinoma. This tumor was verified to lack Estrogen Receptor, Progesterone Receptor, and Her2 overexpression in two separate immunohistochemical analyses (data not shown). The tumor contains a necrotic core and an expanding boundary that invades into the surrounding mammary fat pad and contains inclusions of adipocytes (Fig. 3-5A).

Immunohistochemical staining shows that the tumor cells express αSMA, E-cadherin, and CK14. Red Van Gieson's staining indicates that the tumor contains extensive collagen deposits (fibrosis) interspersed between clusters of cancer cells. This fibrosis colocalizes with tumor-associated fibroblasts. In many areas of the tumor, the tumor-associated fibroblasts make up a larger fraction of the tumor volume than the cancer cells. We also examined whether the MDA-MB-231 and MDA-MB-436 cell lines, which exhibit basal-like expression profiles (138), form tumors that display features similar to human basal-like breast cancers and similar to tumors

formed from MMTV-D1K2 cancer cell lines. Ten million cells of each line were injected orthotopically into three adult female athymic nude mice. The animals developed tumors from three to six weeks after injection. Tumors were excised when they reached two to six millimeters in diameter so that invasion into the surrounding stroma could be visualized. Fig. 3-5B shows that MDA-MB-231 and MDA-MB-436 tumors grown as xenografts in athymic nude mice form invasive tumors that contain inclusions of adipocytes, exhibit fibroblast accumulation and fibrosis at the tumor/stroma boundary, and develop a fibrotic necrotic core when tumors grow larger than approximately three millimeters in diameter. The invasive growth pattern of the MDA-MB-231 cells *in vivo* is similar to that observed with the MMTV-D1K2 tumor-derived cell lines.

Mouse Mammary Tumor Virus-D1K2 Tumor-Derived Cell Lines Exhibit Extensive Stress Fiber Formation and Cytoplasmic E-Cadherin, p120ctn, and ß-Catenin Localization

Primary myoepithelial cells exhibit constitutive stress fibers in culture (135, 136). Zyxin is a component of focal adhesions and associates with Actin stress fibers (142). Immunoblot experiments (Fig. 3-2B) indicate that the D1K2 tumor cell lines express higher levels of Zyxin and Nestin than the *neu*T cell line. Therefore we examined Zyxin localization and colocalization with Actin in immunofluorescence microscopy studies (Fig. 3-6A). The *neu*T cells grow as colonies and exhibit cortical actin staining but no detectable stress fibers. Zyxin is present primarily at the outer border of the *neu*T colonies. In contrast, the D1K2 cancer cell lines exhibit constitutive stress fiber formation. Zyxin colocalizes with the ends of actin stress fibers and is present around the periphery of each of the cells that is not part of a colony.

It is unclear from the studies in Figs. 3-1 to 3-4 whether the cytoplasmic E-cadherin localization observed in the tumors formed from the MMTV-D1K2 cancer cell lines results from environmental influences in the tumor milieu or is due to intrinsic properties of the cancer cells

themselves. Immunofluorescence microscopy studies indicate that the noninvasive *neu*T cancer cells form colonies in culture and that E-cadherin and the E-cadherin-associated protein p120ctn localize to cell-cell contacts in these colonies (Fig. 3-6B). In contrast, in several of the D1K2 tumor cell lines E-cadherin and p120ctn are largely localized to the cytoplasm. This is not specific to the D1K2 cancer cell lines because the BT549 and MDA-MB-435s (Fig. 3-6B) and MDA-MB-231 and MDA-MB-436 (data not shown) human basal-like breast cancer cell lines also exhibit punctate cytoplasmic E-cadherin localization and diffuse cytoplasmic p120ctn localization. E-cadherin also functions to sequester ß-Catenin by localizing it to adherens junctions and preventing it from translocating to the nucleus and functioning as a transcriptional coactivator. E-cadherin localization to the cytoplasm (or loss of E-cadherin expression as observed in the D1K2-T5, CL1 cell line) correlates with decreased junctional ß-Catenin staining in the D1K2 and BT549 cell lines (Fig. 3-6C). These observations are significant because E-cadherin is thought to function as a tumor suppressor by mediating cell-cell adhesion, and by restraining the proinvasive, oncogenic effects of ß-Catenin (143-145) and p120ctn (128, 146, 147).

Discussion

Mouse Mammary Tumor Virus-D1K2 Tumors

Cyclin D1 is overexpressed in approximately 40-50% of human breast cancers (41, 42), but cyclin D1 overexpression typically occurs in luminal tumors rather than basal-like breast cancers (126). Cyclin E overexpression has been noted in basal-like breast cancers (37). Cyclin E overexpression in breast cancers correlates with Estrogen Receptor (ER) negativity and poor prognosis, while cyclin D1 overexpression correlates with ER expression and a favorable outcome (148). Cyclin E potently activates cdk2 and the cyclin D1-cdk2 fusion protein functions as a constitutively active form of cdk2 (57, 127).

Whether any type of constitutive cdk2 activation is sufficient to induce basal breast cancer formation requires further study. The animal models of basal-like breast cancer constructed to date involve genetic inactivation of BRCA1 and p53 (122, 149). It is unknown whether the cyclin D1-cdk2 fusion protein induces the formation of basal-like cancer cells through a mechanism distinct from BRCA1 and p53 deletion, or whether expression of the cyclin D1-cdk2 fusion protein is functionally equivalent to BRCA1 and p53 deletion. Interestingly, cdk2 has recently been shown to inhibit the ubiquitin ligase activity of the BARD1/BRCA1 complex (150), and the BARD1/BRCA1 ubiquitin ligase complex appears to mediate the tumor suppressive functions of the BRCA1 gene (151). P53 function is frequently lost in breast cancers, and p53 inactivation is thought to contribute to cell invasiveness (152). P53 also suppresses tumorigenesis in part by inducing expression of the cdk inhibitor p21. P21-mediated inhibition of proliferation plays a critical role in suppressing tumorigenesis in some contexts (153). We have shown previously that D1K2 can function to sequester p21 and p27 (57, 127), therefore D1K2 may partially override p53 function, with respect to p21.

"Mixed Lineage" Characteristics of MMTV-D1K2 Tumor Cell Lines

Previously studies of transgenic mouse breast cancer models (154)) showed that expression of cyclin D1 in the mammary gland under the control of the MMTV promoter resulted in adenocarcinomas in 75% of the mice, although some squamous differentiation was observed (155). MMTV-cyclin D2 transgenic mice also develop adenocarcinomas albeit at a lower frequency (19%) (156). In contrast, MMTV-cyclin D3 mice form primarily squamous cell carcinomas (157). These studies indicate that the type of cell cycle deregulation that drives tumor formation can influence the differentiation status of the resulting tumors. The MMTV-cyclin D1-cdk2 transgenic mouse tumors described here are morphologically heterogeneous, including metaplastic, adenosquamous as well as adeno-myoepithelial-type carcinomas (127).

The spindle cell myoepithelial-like component of these tumors stains positively for E-cadherin and αSMA and exhibits E-cadherin mislocalization to the cytoplasm. Cell lines isolated from these tumors exhibit several similarities with human basal-like breast cancers including: (a) the expression of myoepithelial markers such as αSMA, Nestin, Cytokeratin 14, and EGFR, (b) lack of Her2 overexpression and lack of Estrogen Receptor-α expression, (c) the expression of subsets of luminal markers including E-cadherin, Cytokeratin 18 (not shown), and Cytokeratin 19, consistent with the luminal/myoepithelial "mixed lineage" nature of human basal-like breast cancers (129-131), (d) the cells exhibit myoepithelial-like morphology and cytoskeletal features *in vitro*, (e) the cell lines form invasive tumors with spindle morphology in wild type mouse mammary fat pads *in vivo*, and (f) the cells appear to have undergone EMT which has recently been shown to occur in the basal-like subtype of breast tumors (133). MMTV-cyclin D1-cdk2 transgene expression in a mammary stem-like cell might explain the observed heterogeneity in tumor morphology. Alternatively, cyclin D1-cdk2 expression may inhibit lineage specification or block differentiation. Both of these hypotheses are consistent with the observation that the markers Cytokeratin 14 and Nestin expressed in the MMTV-cyclin D1-cdk2 tumor cell lines are associated with relatively undifferentiated cell populations (158-163).

Mouse Mammary Tumor Virus-D1K2 Invasiveness

Several non-mutually exclusive mechanisms could contribute to the invasiveness of MMTV-D1K2 tumors including E-cadherin mislocalization/downregulation and expression of proteins previously correlated with invasiveness such as Nestin (164) and Zyxin (165). The role of cdk2 activation in these processes is unclear. Chronic treatment with the cdk2 inhibitor Roscovitine did not revert the MMTV-D1K2 cell lines to a luminal-like morphology or increase the formation of adherens junctions in culture (data not shown). It is possible that cdk2

activation directly influences cell invasiveness, perhaps by functionally inactivating Rb. Recently it has been shown that knock-down of Rb expression by short-interfering RNAs decreases E-cadherin expression and induces EMT (166). However it is also possible that cdk2 activation induces irreversible changes to the cells that result in increased invasiveness. The mixed-lineage nature of the MMTV-D1K2 cells may result from an alteration in the normal differentiation program that causes increased invasiveness. The observation that invasive human basal-like breast cancer cell lines exhibit the same E-cadherin downregulation/mislocalization and mixed-lineage expression pattern is consistent with this hypothesis.

We have shown previously that MMTV-D1K2 cell lines exhibit aneuploidy (127). Cdk2 activation may induce genetic instability that results in subpopulations of tumor cells with increased invasive properties. The observation that the D1K2-T4 cells do not express D1K2, but exhibit E-cadherin mislocalization, a mixed lineage phenotype, and invasiveness *in vivo* raises the possibility that D1K2 initiates the formation of a subpopulation of invasive cells, but is not required for its maintenance. Intriguingly, the D1K2-T4 cells exhibit alterations that might mimic D1K2 function and mediate invasiveness in its absence, including p53 mutation (152) and decreased Rb expression (166).

Another potential explanation for the E-cadherin downregulation and cytoplasmic localization is the production of TGFß by the MMTV-D1K2 cancer cells. We have previously shown that the MMTV-D1K2 cells secrete TGFß (127). TGFß is capable of inducing EMT associated with E-cadherin downregulation/cytoplasmic localization (167). TGFß signaling has been associated with basal-like breast cancers (168-170), and EMT has been specifically associated with basal-like tumors (133). Chronic treatment with a TGFß type I receptor kinase inhibitor did not convert the MMTV-D1K2 cell lines to a luminal morphology in culture (data

not shown). However, autocrine TGFß might function to induce an aberrant luminal/myoepithelial mixed lineage differentiation status that cannot be reversed by blocking TGFß signaling. The previously observed tumor-associated fibrosis (desmoplasia) in the MMTV-D1K2 tumors (127) is recapitulated in the tumors generated from the MMTV-D1K2 tumor-derived cell lines (Fig. 3-4A). This suggests that the desmoplasia is due to the cancer cells themselves, and rules out possible effects caused by transgene expression in the stroma. Desmoplasia initiated by the MMTV-D1K2 cancer cells could result from TGFß production because TGFß is well known to induce fibrosis and desmoplasia (171, 172).

In summary, the evidence presented here suggests that constitutively active cdk2 in the form of a cyclin D1-cdk2 fusion protein induces tumors that contain an invasive component that exhibits multiple features in common with human basal-like tumors and tumor-derived cell lines. Current efforts are focused on understanding the respective roles of cdk2 hyperactivation, genetic instability, and TGFß production in the formation of the invasive basal-like cancer cells in the MMTV-D1K2 tumors. It is hoped that these studies will yield insights into the mechanisms responsible for the invasiveness of human breast tumors.

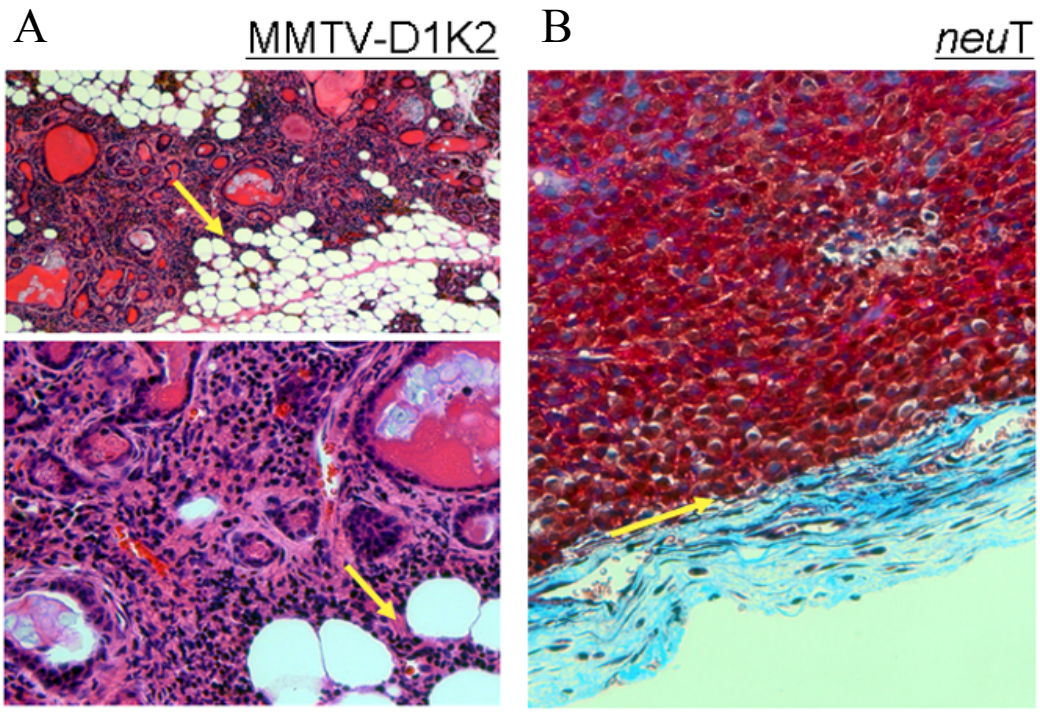

Figure 3-1.MMTV-D1K2 hypercellular lesions invade into the mammary stroma. A) Representative mammary MMTV-D1K2 tumor section stained with H&E at low and high magnification displays areas of poorly differentiated cells invading into the surrounding mammary fat pad. B) Tumors derived from MMTV-*neu* tumor cells stained with Masson's Trichrome exhibit distinct tumor cell compartmentalization from the surrounding stroma. C) Phase contrast micrographs of nontransformed mouse mammary NMuMG cells, MMTV-D1K2 tumor-derived cell lines D1K2-T2 and D1K2-T4, and the BT549 human basal-like breast cancer cell line.

C

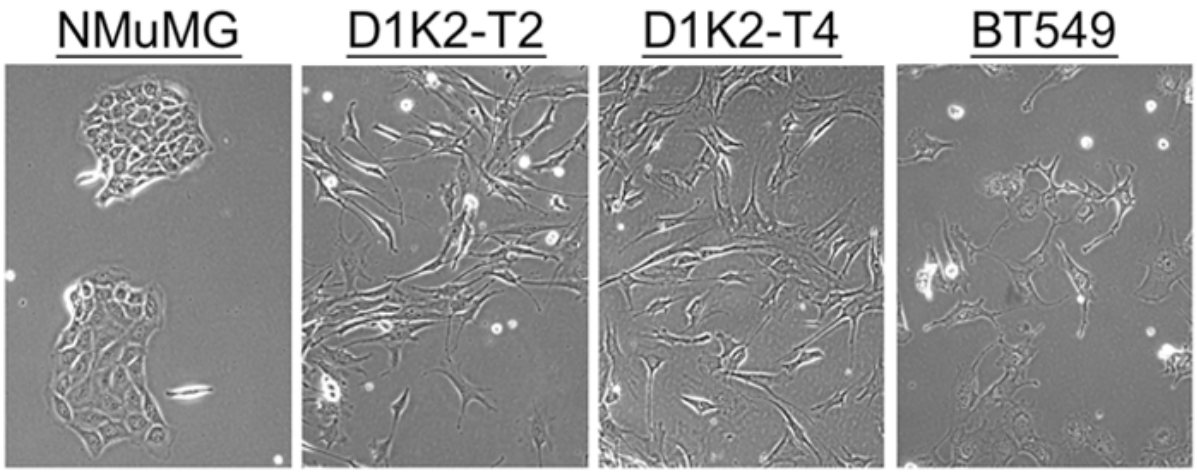

Figure 3-1.Continued.

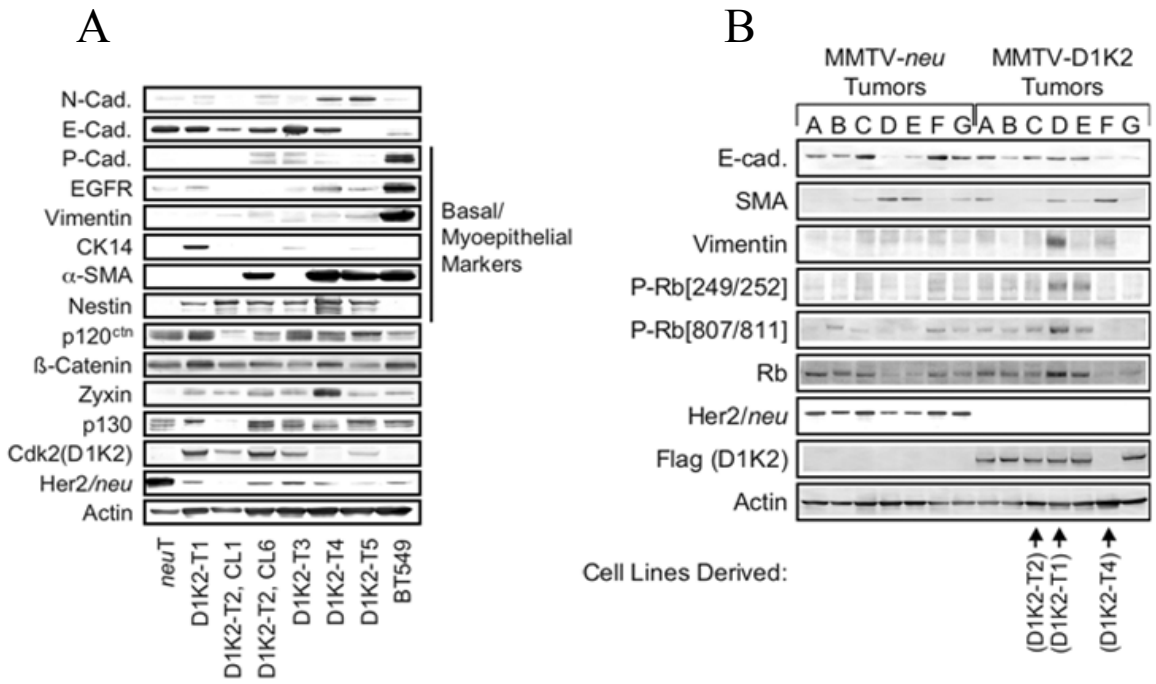

Figure 3-2.Cell lines derived from MMTV-D1K2 tumors exhibit protein expression profiles consistent with basal-like breast cancer.
A) Immunoblot analysis of cells derived from MMTV-D1K2 tumors, an MMTV-*neu* tumor (*neu*T), and the BT549 basal-like human mammary carcinoma cell line, using antibodies specific for N-cadherin (N-Cad.), E-cadherin (E-Cad.), P-cadherin (P-Cad.), Epidermal Growth Factor Receptor (EGFR), Vimentin, Cytokeratin 14 (CK14), α–Smooth muscle Actin (αSMA), Nestin, p120 Catenin ($p120^{ctn}$), ß-Catenin, Zyxin, p53, p130, the cyclin D1-cdk2 fusion protein (detected with a cdk2 antibody (cdk2(D1K2)), Her2/*neu* (*neu*), and Actin as a loading control. D1K2-T2, CL1 and D1K2-T2, CL6 are clonal cell lines derived from the D1K2-T2 cancer cell line. B) Immunoblot analysis of primary MMTV-*neu* and MMTV-D1K2 tumors (arbitrarily labeled A-G) using antibodies specific for Flag (detecting the cyclin D1-cdk2 fusion protein (Flag(D1K2)), Her2/*neu*, E-cadherin (E-Cad.), α-Smooth Muscle Actin (α-SMA), Vimentin, Rb, Rb phosphorylated on residues 249/252 (P-Rb[249/252]), Rb phosphorylated on residues 807/811 (P-Rb[807/811]), and Actin as a loading control C) Immunoblot analysis of the indicated cell lines with the indicated antibodies. "-D1K2" represents expression of the cyclin D1-cdk2 fusion protein detected with either cyclin D1 or cdk2 antibodies. "End. cyclin D1" and "End. cdk2" represents levels of endogenous cyclin D1 and cdk2.

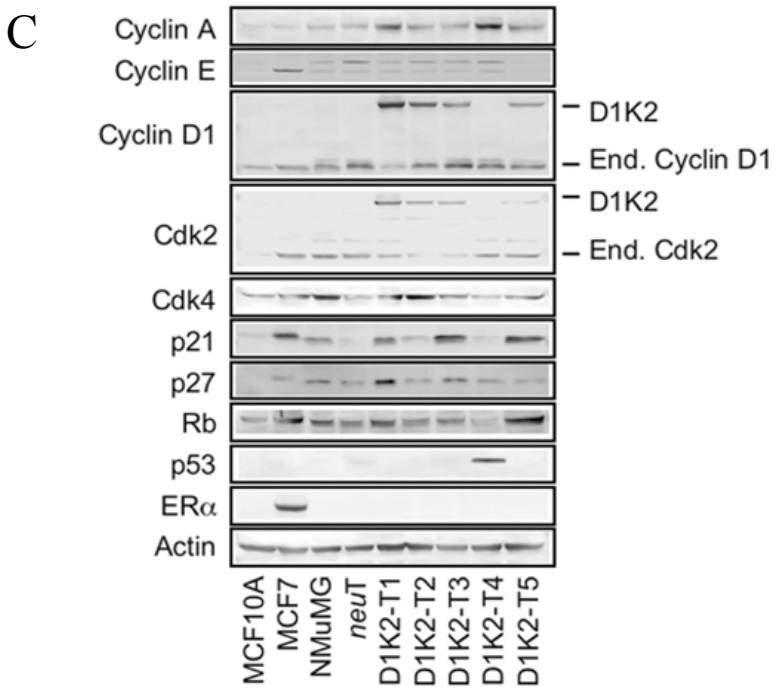

Figure 3-2.Continued.

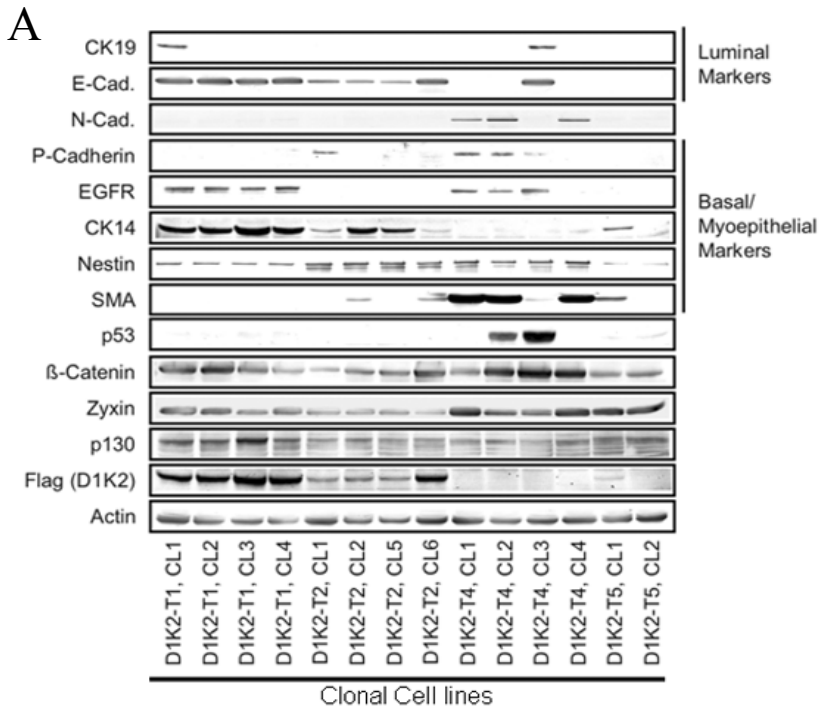

Figure 3-3.MMTV-D1K2 tumor cell lines exhibit mixed luminal/myoepithelial lineage
A) Immunoblot analysis of clonal MMTV-D1K2 cancer cell lines using the antibodies listed in Fig. 3-2, and a Cytokeratin 19 antibody (CK19). Clonal lines are designated by the name of the original cell line followed by the clone number. B) Immunofluorescence micrographs showing nuclear DAPI staining (blue) in the no primary antibody control (No 1º), Cytokeratin 14 staining (CK14, orange), E-cadherin staining (E-Cad., green), and a merged image showing coexpression of E-cadherin and Cytokeratin 14 at the single cell level (CK14 + E-Cad. + DAPI). C) Immunoblot analysis of human mammary carcinoma cell lines (T47D, MCF7, MDA-MB-361, MDA-MB-468, BT549, MDA-MB-231, MDA-MB-435S, and MDA-MB-436) and nontumorigenic mammary epithelial cell lines (NMuMG, MCF10A, and HBL100) was performed using the indicated antibodies.

B

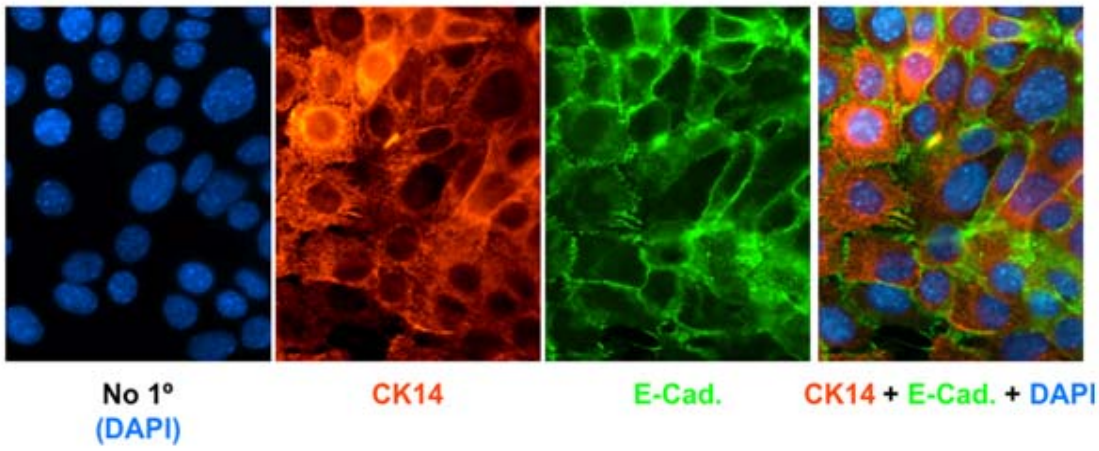

Figure 3-3.Continued.

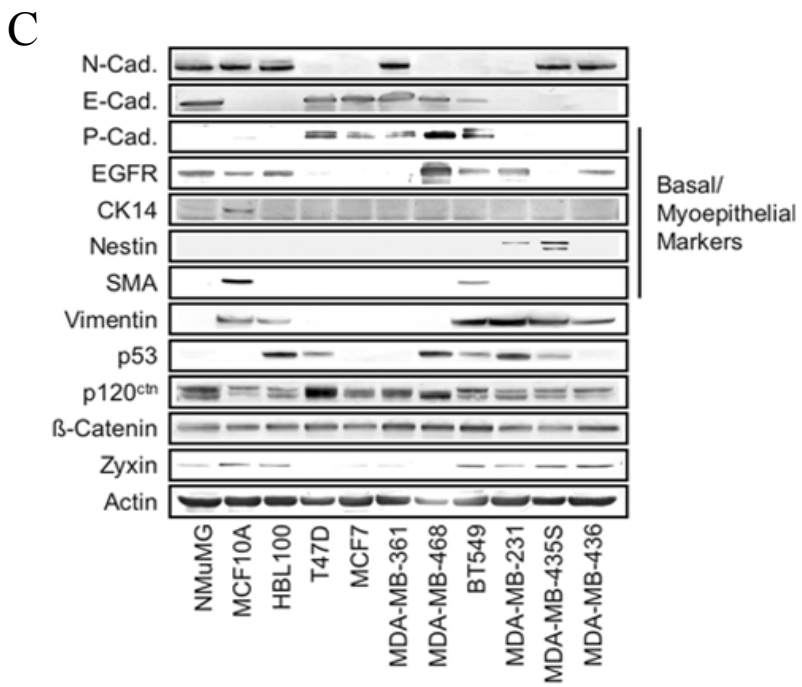

Figure 3-3.Continued.

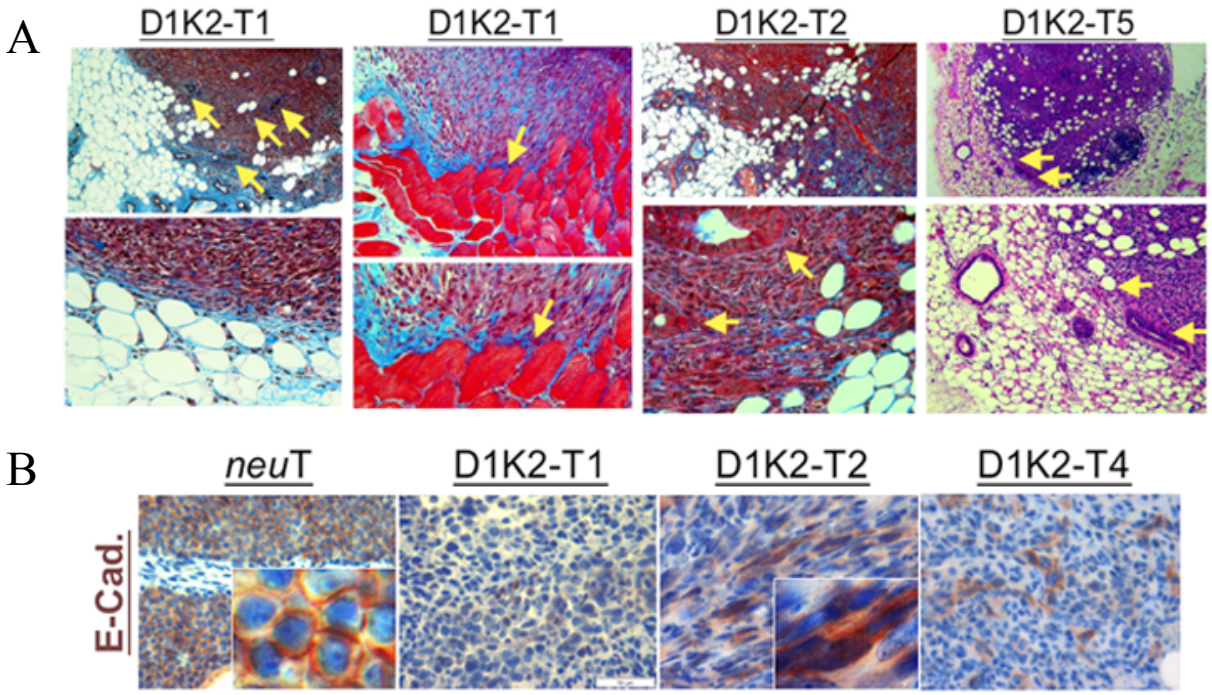

Figure 3-4.Tumors formed from MMTV-D1K2 cancer cell lines exhibit stromal invasion and E-cadherin mislocalization/downregulation upon orthotopic implantation. A) Masson's Trichome staining of histological sections from tumors derived from D1K2-T1 cells invading into the mammary fat pad (first panel), muscle (second panel), and a tumor derived from D1K2-T2 cells invading into the mammary fat pad (third panel). H&E stained section of a tumor derived from D1K2-T5 cells invading into the mammary fat pad (fourth panel). B) Immunohistochemical E-cadherin detection (brown staining) in histological sections of tumors generated from the indicated polyclonal cell lines. E-cadherin is localized to sites of cell-cell contact in *neu*T tumors (inset). In contrast, tumors formed from the D1K2-T1, D1K2-T2, and D1K2-T4 cell lines exhibit weak, mosaic E-cadherin expression. E-cadherin is localized diffusely throughout the cytoplasm (*e.g.* D1K2-T2, inset) in cells that express it. C) Cytokeratin 14 (CK14) immunohistochemical analysis of tumors generated from the indicated polyclonal cell lines (red staining). D) Hematoxylin and Eosin (H&E) histochemical staining of an MMTV-D1K2 primary tumor (left panels) showing poorly differentiated spindle-shaped cell populations with abundant cytoplasm surrounded by more densely packed cells. Immunohistochemical staining (brown) of serial sections of the same tumor for E-cadherin (E-Cad., center panel) and α-Smooth Muscle Actin (SMA, right panel). Sections were counterstained with hematoxylin. Note the diffuse cytoplasmic E-cadherin staining (inset) and positive staining for α-Smooth Muscle Actin in the compartments containing the spindle-shaped cells.

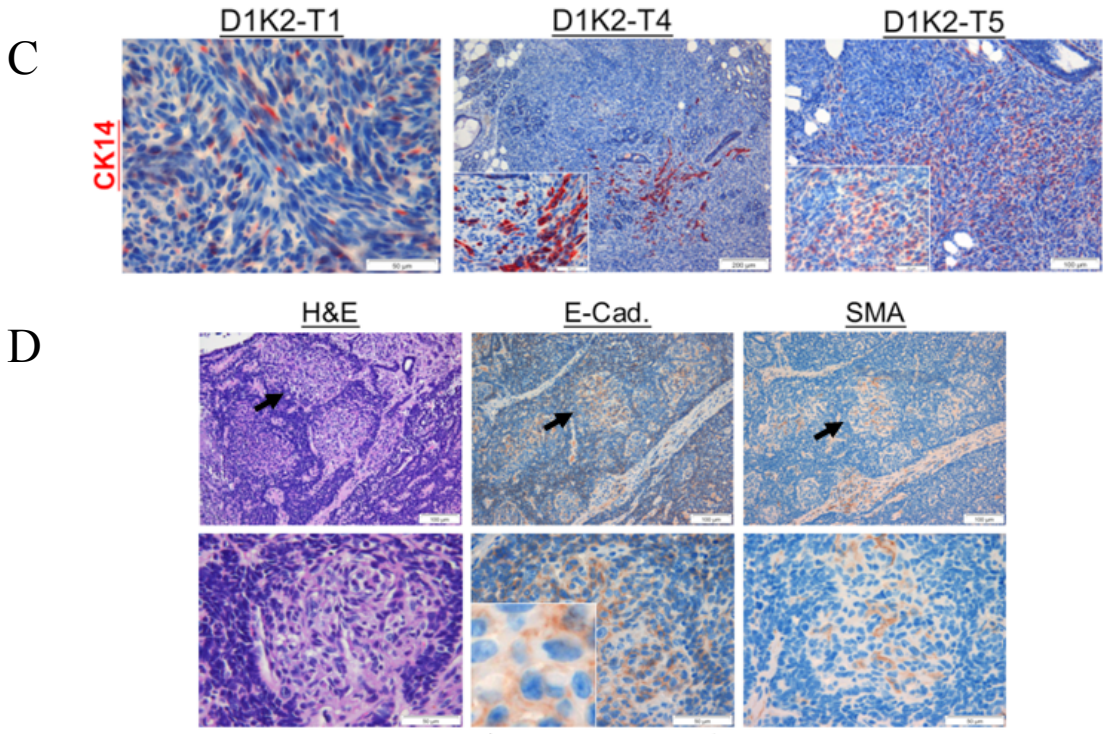

Figure 3-4.Continued.

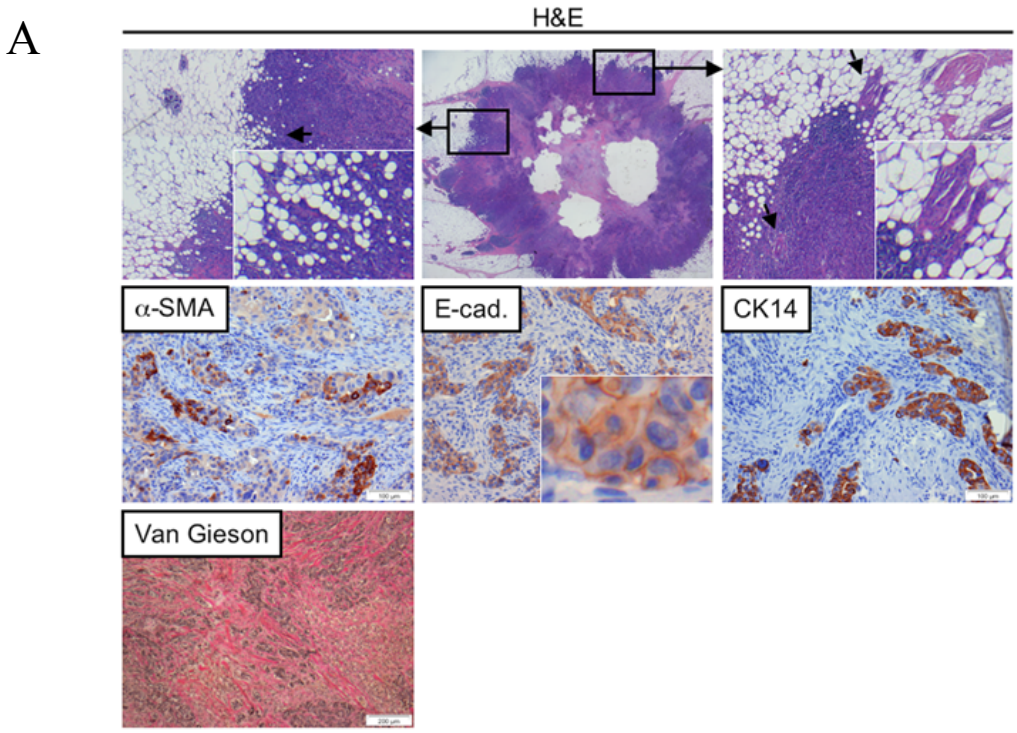

Figure 3-5.Basal-like breast cancers exhibit an invasive, mixed-lineage phenotype and tumor-associated fibrosis.
A) The top panel shows an H&E stained histological section (center) of a triple-negative human breast adenocarcinoma. The top-right and top-left panels show invasion of the tumor into the surrounding fat pad and inclusions of adipocytes in the tumor (inset). The second row of panels demonstrates immunohistochemical staining for the myoepithelial markers α-Smooth muscle actin (α-SMA) and Cytokeratin 14 (CK14), and the luminal marker E-cadherin (E-cad.). The bottom panel shows Van Gieson's staining of the tumor. The cancer cells stain brown. The intense red staining between the cancer cells shows extensive collagen deposition, indicative of tumor-associated fibrosis. B), MDA-MB-231 and MDA-MB-436 cell lines were grown as orthotopic xenograft tumors in athymic nude mice. Upper panels show H&E stained histological sections and lower panels show serial sections stained with Masson's Trichrome. Arrows in the MDA-MB-231 panels point out fibroblasts/fibrosis at the advancing tumor front, and the infiltration of cancer cells between stromal adipocytes. Arrows in the leftmost MDA-MB-436 panel point out numerous blood vessels at the advancing tumor boundary that colocalize with the extensive fibrosis at tumor/stroma interface. Arrows in the rightmost MDA-MB-436 panel show the necrotic, fibrotic center of a four millimeter tumor.

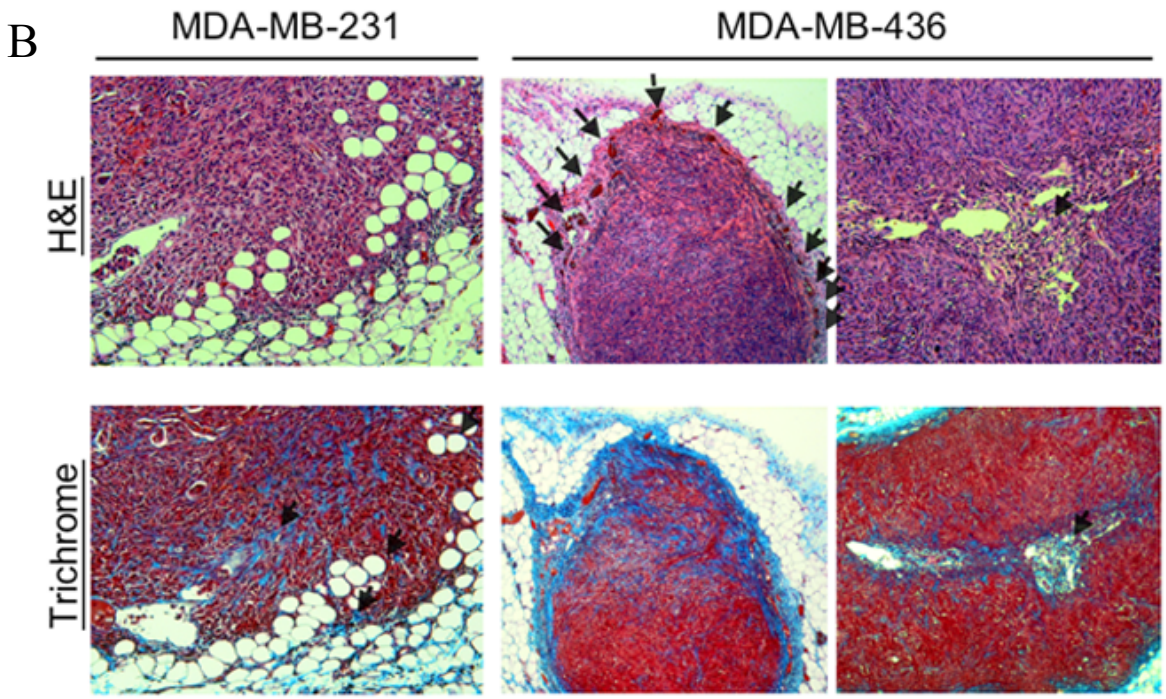

Figure 3-5.Continued.

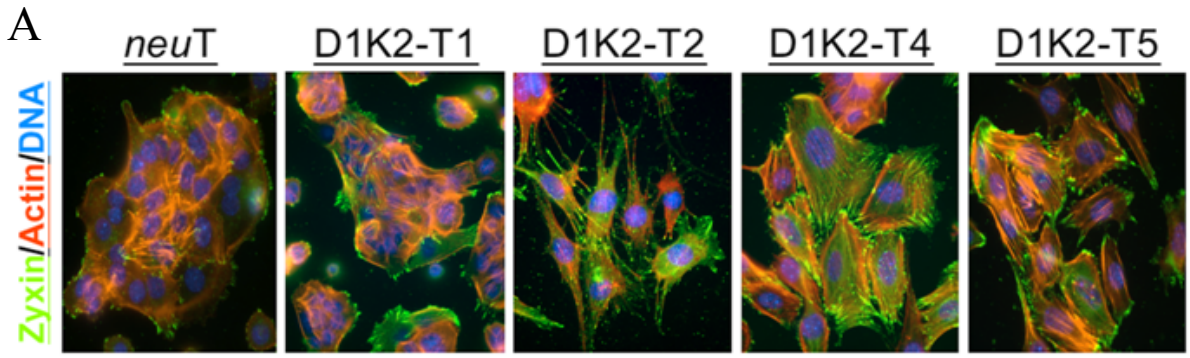

Figure 3-6. MMTV-D1K2 tumor-derived cell lines exhibit extensive stress fiber formation and E-cadherin, p120^{ctn}, and ß-catenin localization to the cytoplasm.
A) Immunofluorescence micrographs of the indicated cell lines stained for Zyxin (green), Actin (orange), and DNA (DAPI, blue). B) Immunofluorescent staining (yellow) for E-cadherin (upper panels), and p120^{ctn} (p120, lower panels). The cells were counterstained for DNA (DAPI, blue). E-cadherin and p120^{ctn} are localized to cell-cell junctions in the *neu*T cells, but are largely localized to the cytoplasm in the D1K2-T2,CL1, D1K2-T4,CL1, D1K2-T5,CL1, BT549, and MDA-MB-435s cell lines. C) Immunofluorescent staining for E-cadherin (orange) and β-Catenin (green) in the indicated cell lines showing that in the *neu*T cells E-cadherin and ß-Catenin localize to cell-cell contacts, while in the D1K2-T2,CL1, D1K2-T5,CL1 and BT549 cell lines E-cadherin and ß-Catenin do not co-localize. The cells were counterstained for DNA (DAPI, blue).

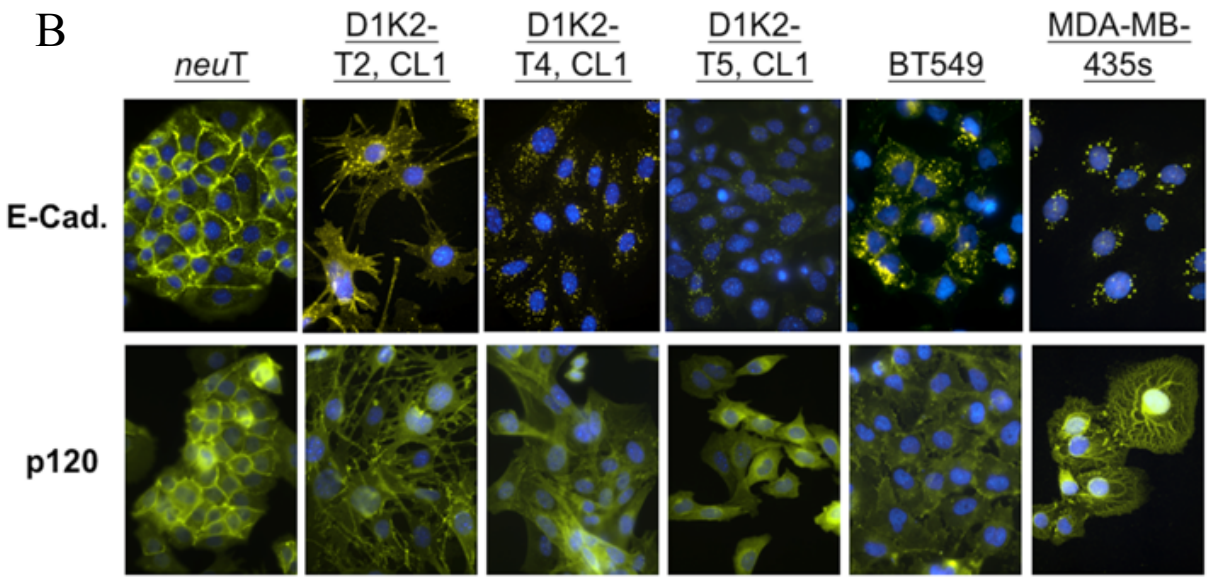

Figure 3-6.Continued.

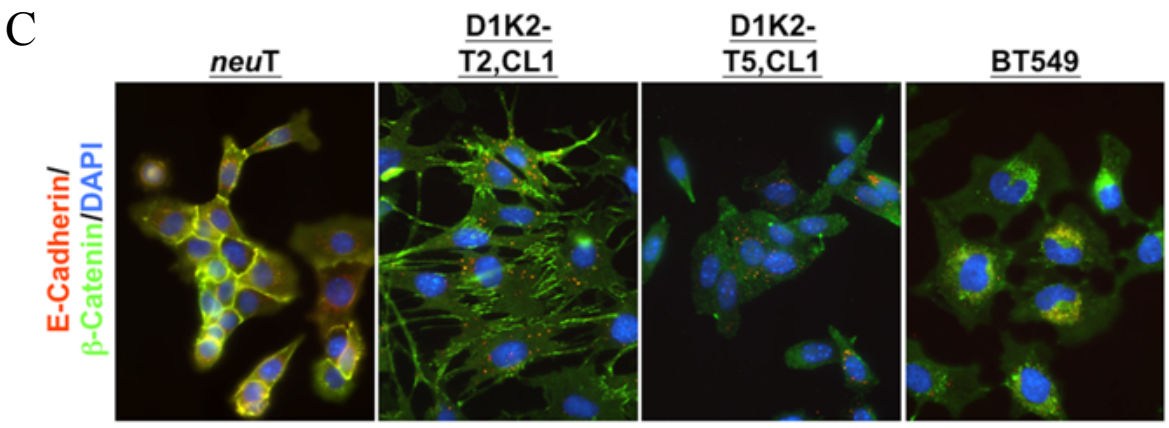

Figure 3-6.Continued.

CHAPTER 4
A NOVEL CLASS OF CYCLIN-DEPDENDENT KINASE INHIBITORS IDENTIFIED BY MOLECULAR DOCKING ACT THROUGH A UNIQUE MECHANISM

Introduction

Uncontrolled cell proliferation is one of the defining features of cancer. Cdks are serine/threonine protein kinases that play key roles in controlling cell cycle progression (1, 2). The concerted activities of cdks result in chromatin condensation, nuclear envelope breakdown, and the up-regulation of genes involved in nucleotide synthesis and DNA replication, among other events. Cdks have long been considered ideal targets for anti-cancer drugs, owing to their importance in the cell cycle. As a result, many cdk inhibitors have been developed, some of which have progressed to clinical trials. Roscovitine (Selicilib) and Flavopiridol (Alvocidib) are examples of cdk inhibitors that have passed Phase I clinical trials (61, 66) and have been approved for Phase II clinical trials (62, 63, 67). These drugs, as well as most other cdk inhibitors, are ATP-competitive. The disadvantage of using a therapeutic strategy involving ATP competition is that all kinases possess an ATP-binding site, leading to the potential for reduced target specificity. Recently, advances have been made in identifying cdk inhibitors that act through novel mechanisms. One example of this effort is the identification of a D-amino acid hexapeptide molecule, NBI1, that inhibits the kinase activity of cdk2 through its binding with cyclin A (80). A similar approach was taken in identifying a series of cyclic peptides that bind to the substrate recognition site of cdk complexes (81). Another example is the use of a small, 39 amino acid peptide that inhibits the kinase activity of cdk2 by mimicking the inhibitory effects of the pRb2/p130 spacer domain (173). These approaches are promising, but rely on peptide-based inhibitors that have inherent disadvantages for use as therapeutic agents.

The use of knockout mice has recently generated much information about the role of cdks with respect to cell cycle regulation. For instance, mice lacking cdk2, cdk4 and cdk6 are viable

(30, 174, 175). Furthermore, cells lacking both cdk4 and cdk6 proliferate almost normally (33). More recently it has been discovered that mouse embryonic fibroblast cells are able to cycle in the absence of cdk2, cdk4 and cdk6, needing only cdk1 to complete cell division (35). In light of the fact that cdks are able to functionally replace one another, highly selective cdk inhibitors that target only one type of cell cycle cdk may not be as effective anti-tumor agents as compounds that inhibit cdk1, cdk2, cdk4, and cdk6. An inhibitor that acts on multiple cell cycle cdks would therefore have a greater probability of inhibiting tumor cell growth by ensuring that the cell cycle is arrested. Here we report the identification of a novel structural pocket present on cdk2 that is likely conserved on cdks 1, 4, and 6. Using a high throughput *in silico* screening procedure we have identified compounds that decrease the function of cdks in cells through binding to this site.

Materials and Methods

Molecular Docking

The two protein crystal structures used for identification and *in silico* screening of the structural site in question were the cyclinA/cdk2 and $p27^{kip1}$/cyclin A/cdk2 complexes (RCSB Protein Data Bank codes: 1FIN (72) and 1JSU, respectively (74)). A molecular surface of 1JSU was prepared using the MSROLL program, which was then used as input for the sphere generating program SPHGEN. A cluster of spheres that was shown to be within the pocket of interest was then selected and edited manually to leave a cluster of 21 spheres. The SHOWBOX program was used to construct a 3-dimensional rectangle, 4 Angstroms in every direction from the sphere cluster. The program CHIMERA was used to convert the PDB file of 1JSU into the appropriate mol2 format. The box file that was generated was then used as input for the GRID program, which calculates and saves the information concerning the steric and electrostatic environment within the box of the 1JSU mol2 file. DOCK was used to screen the entire National Cancer Institute/Developmental Therapeutics Program (NCI/DTP) database of small molecules

(which consisted of approximately 140,000 small molecules at the time of docking) within the 1JSU grid, with the selected spheres as theoretical binding sites. CHIMERA was subsequently used to rank the small molecule output based on predicted energy scores composed of electrostatic interactions and van der Waals' forces. The top 40 compounds were obtained from the NCI/DTP for cell culture testing. All of the programs listed for this procedure were part of the DOCK5.0 suite developed at UCSF (176). Protein structure visualization and image generation were done using Pymol software (DeLano Scientific, Palo Alto, California).

Sequence Alignment

Human cdk1, cdk2, cdk4, and cdk6 were aligned using the program Geneious 3.8.5 (Biomatters, Auckland, New Zealand). Sequence similarity was calculated using the program MegAlign 3.07 (DNASTAR, Inc., Madison, WI).

Cell Culture

All experiments involving mammalian cell culture were performed using Dulbecco's Modified Eagle's Medium (DMEM) supplemented with 10% heat inactivated fetal bovine serum (Mediatech, Inc., Manassas VA – 35-011-CV). SF9 insect cells were cultured with SF-900 II SFM (Gibco, Invitrogen, Carlsbad, CA – 10902). BT549 and HCT116 cell lines were obtained from the American Type Culture Collection (ATCC, Manassas VA). QBI-293A kidney cells were obtained from Quantum (Montreal, Canada). The SF9 cells were generously provided by Dr. Sergei Zolotukhin (University of Florida, Gainesville, Florida).

Chemical Synthesis

Chemical reagents and solvents were purchased from Aldrich (St. Louis, MO) and Acros (Geel, Belgium). Both synthesized compounds displayed spectroscopic data consistent with the proposed structures.

NSC Compound 43067 (1-(5-Methyl-thiophen-2-yl)-3-phenyl-propenone): Solid NaOH (1.78 g, 44.5 mM) was dissolved in 50 mL of water/ethanol (2:1, v/v) with cooling in an ice bath. Sequential addition of 5-methyl-2-acetyl thiophene (5.00 g, 35.6 mM) and benzaldehyde (3.77 g, 35.6 mM) to the cooled solution of NaOH was followed by rapid stirring on ice for 2 hours. The mixture was stored overnight at 4 °C, resulting in formation of an oily solid. The solid was removed by vacuum filtration, and the filtrate was then concentrated *in vacuo*. The residue was dissolved in hot absolute ethanol and let cool to provide 4.04 g (50 % yield) of NSC 43067 as flaky yellow crystals, MP 93-95 °C.

NSC Compound 63002 (2-(4-methoxy-phenyl)-3-pyridin-2-yl-acrylonitrile): The compound was prepared in 26% yield as described in (177). MP 69-70 °C (lit 69.5-70.5).

Western Blot Analysis

Cells were lysed with extraction buffer (0.1% Triton X-100, 20 mM HEPES pH 7.6, 1 mM EDTA, 1 mM EGTA, 0.1% Triton X-100, 0.1% β-mercaptoethanol, 5% glycerol, 10 nM microcystin, 1 mM sodium orthovanadate, and 40 mM sodium pyrophosphate) followed by sonication. Extracts were cleared by centrifugation at 16,000 x g for 20 minutes. The cleared supernatant was then analyzed for total protein concentration with Bradford protein assay dye reagent (Biorad, Hercules, CA – 500-0006), and all extracts were normalized to the lowest protein concentration. The extracts were boiled with one-third volume of 4X SDS sample buffer (60 mM Tris pH 6.7, 24 mM EDTA, 200 mM SDS, 40% glycerol, 300 μM bromophenol blue, 0.4% β-mercaptoethanol) for 5 to 10 minutes. Samples were resolved on SDS-PAGE gels, and transferred to nitrocellulose membranes. Membranes were immunoblotted using antibodies specific for either Actin (α-rabbit, Santa Cruz, Santa Cruz, CA – sc-1616-R), cdk1 (α-mouse, Santa Cruz sc-54), cdk2 (α-rabbit, Santa Cruz sc-163), cdk4 (α-rabbit, Santa Cruz sc-601), Flag

(M2 antibody, Sigma, St. Louis, Mo – F-3165), E2F1 (α-rabbit, Santa Cruz sc-193), cyclin A (α-rabbit, Santa Cruz sc-596), B-myb (α-rabbit Santa Cruz sc-725), p-Rb (α-mouse, Cell Signaling, Danvers, MA - #9309), p-Rb-780 (α-mouse, Cell Signaling, #9307), p-Rb-807/811 (α-mouse, Cell Signaling #9308), or Erk1/2 (α-rabbit Santa Cruz sc-93).

Construction of Stable Cell Lines

Green Fluorescent Protein (GFP) fused to cdk4 was stably overexpressed in 293A cells. GFP cDNA was amplified from the pAcGFP-Tubulin plasmid (Clontech, Mountain View, CA) using the following PCR primers: 5' TTTTGGATCCGATATCCCACCATGGTGAGCAAGGGCGCCGAG 3' and 5' TTTTGGATCCCTTGTACAGCTCATCCATGCC 3'. Following amplification, the GFP PCR product was purified by chloroform/phenol extraction and ethanol precipitation. The PCR product was subsequently digested with BamHI. The previously described pcDNA3 plasmid encoding cdk4-His_6 contains a BamHI site 5' to cdk4-His_6 (57). This plasmid was also digested with Bam HI, followed by treatment with calf intestinal alkaline phosphatase for 1 h at 37 ^oC. Vector and insert DNA were ligated for 18 h at room temperature, creating a construct that contains cDNA encoding GFP in-frame with cDNA encoding cdk4-His_6. The orientation of the insert was confirmed with EcoRV digestion. Ten micrograms of the GFP-cdk4/pcDNA3 construct was transfected into 293A cells using lipofectamine (Invitrogen – 18324-020). Cells that stably retained the plasmid were first selected by treating the cells with medium containing 500 μg/ml G418 Sulfate (Cellgro 61-234-RG), followed by one round of cell sorting for GFP-positive cells using a FACSAria cell sorter (Becton Dickinson, Franklin Lakes, NJ) and the Diva program (version 6.1).

Mink lung epithelial cells (Mv1Lu) stably expressing a cyclin D1-cdk2 fusion protein or E2F1 were described previously (57, 93).

Ultracentrifugation Assay

Cell extracts were prepared as described in the previous section. Samples were centrifuged at either 16,000 x g for 20 minutes or 150,000 x g for 1 hour. In both cases, the supernatants were removed and normalized for protein concentration. The pellets were extracted with 300 µl extraction buffer containing 1.0% Triton X-100, 20 mM HEPES pH 7.6, 1 mM EDTA, 1 mM EGTA, 0.1% Triton X-100, 0.1% β-mercaptoethanol, 5% glycerol, 10 nM microcystin, 1 mM sodium orthovanadate, and 40 mM sodium pyrophosphate and 300 µl 2X SDS sample buffer. The extracted pellets were normalized using the same dilution factors as for the supernatant fraction, sonicated vigorously, and boiled for 5 to 10 minutes.

Fluorescence Microscopy

Cells for immunofluorescence studies were plated onto glass coverslips in 6-well plates. After a 24 hour incubation period, cells were treated with either vehicle control or the indicated NSC compounds. After a further 24 hour incubation, the cells were fixed with 1% paraformaldehyde in phosphate-buffered saline (PBS) for 20 minutes, followed by a 10 minute incubation with the quench solution (50 mM ammonium chloride + 0.5% Triton X-100 in PBS). The coverslips were subsequently incubated with antibody buffer (10% Goat Serum + 0.5% Triton X-100 in PBS) in a humidified chamber for 1 hour. Primary antibody staining was performed using an antibody for cdk4 (α-rabbit, Santa Cruz sc-601) at a 1:100 dilution in antibody buffer, or no primary antibody as a control for non-specific staining, for 2 hours. Following primary antibody incubation, the coverslips were washed four times with PBS, and incubated with a goat anti-Rabbit Fluor 488 secondary antibody (Invitrogen, Molecular Probes,

Carlsbad, CA - A11008) for 1 hour at a 1:200 dilution in antibody buffer. Following four more washes with PBS, coverslips were mounted onto slides with Vectashield + DAPI (Vector Laboratories, Orton Southgate, England – H-1200) to visualize nuclei. Slides were viewed on a Leica TCS SP2 AOBS spectral confocal microscope. Images were collected and processed using LCS (Leica Confocal Software, Leica Microsystems, Wetzlar, Germany) Version 2.61, Build 1537.

GFP tagged 293A cells were plated, treated, and processed the same as for immunofluorescence. However, instead of antibody incubation, the fixed and quenched cells were mounted directly onto slides with Vectashield + DAPI.

Cloning and Expression of a Cyclin D1- Cdk2 Fusion Protein (D1K2) Baculoviral Construct

cDNA encoding D1K2 was digested from the pcDNA3 expression vector (57) using the 5' EcoRI and 3'XhoI sites. DIK2 was subsequently subcloned into the 5'-EcoRI and 3'-SalI sites of pFBDM. Baculovirus generation in SF9 insect cells was performed as described (178, 179). The plaque isolated D1K2 virus, at a concentration of 2.5 x 10^9 plaque forming units (PFU) per ml was used to infect SF9 cells at a multiplicity of infection of five. Cells were allowed to grow for two days at 27 °C shaking at 100 RPM. Cells were pelleted by centrifugation and washed once with PBS, followed by extraction with 0.1% Triton X-100 extraction buffer (20 mM HEPES pH 7.6, 0.1% Triton X-100, 0.1% β-mercaptoethanol, 5% glycerol, 10 nM microcystin, 1 mM sodium orthovanadate, and 40 mM sodium pyrophosphate) and sonication. The supernatant was centrifuged at 100,000 x g for one hour and filtered through a 0.45 μm filter to remove remaining particulates. The lysate was then loaded onto a 1 ml Ni-NTA agarose column (Qiagen, Gaithersburg, MD) equilibrated with 25 mM Tris-HCl (pH 7.5) and 100 mM NaCl. The column was washed with 10 ml 10 mM imidazole in the same buffer at a flow rate of 1 ml

per minute. The D1K2 protein was then eluted with 200 mM imidazole-containing buffer. Peak fractions were pooled and exchanged into a buffer containing 40 mM HEPES (pH 7.0), 0.2 M NaCl and 5 mM dithiothreitol by alternating concentration and dilution using a 10,000 molecular weight cutoff Amicon Ultra centrifugal filter device (Millipore, Billerica, MA – UFC 901024) until a dilution factor of 1:10,000 of the original buffer had been reached. The protein was concentrated to approximately 200 μg/ml and centrifuged at 150,000 x g to remove particulates and aggregated protein.

In Vitro Aggregation Assay

Purified, concentrated, and ultracentrifuged protein was mixed with an equal volume of buffer containing either DMSO or NSC compound for a final reaction concentration of 100 μg/ml D1K2, 400 μM NSC compound or 0.8% DMSO vehicle in 40 mM HEPES (pH 7.0), 0.2 M NaCl, 5 mM dithiothreitol, and 0.1% Triton X-100. The reaction mixture was incubated at room temperature for 16 hours. Following incubation, the reactions were centrifuged at 16,000 x g for 20 minutes to pellet aggregated protein. Supernatants were removed and boiled with one third volume of 4X SDS sample buffer, while 2X SDS sample buffer was added to the pellets. These samples were resolved by SDS PAGE and stained with Coomassie blue.

Results

High Throughput Screening of a Novel Cdk Drug Binding Site

We examined the differences between several crystal structures of cdk2 in order to identify a novel inhibitor binding site on cdks. A side-by-side comparison of the structures of the catalytically active cyclinA/cdk2 complex and the catalytically inactive p27/cyclinA/cdk2 complex revealed the formation of a structural pocket, present only in the inhibited, p27-bound form of cyclinA/cdk2 (Fig. 4-1A). We hypothesized that a small molecule could bind to this pocket and stabilize the cyclinA/cdk2 complex in an “open” conformation which would mimic

the p27-bound form of cyclinA/cdk2, and would thereby inactivate the enzyme catalytically. A sequence alignment of cdks 1, 2, 4, and 6 revealed that the residues that comprise the pocket are conserved (between 48.3% and 86.2% sequence similarity) between these cdks, indicating that this pocket is likely to be present in the other cell cycle cdks (Fig. 4-1B). We performed a high-throughput *in silico* molecular docking screen on the p27-cyclinA/cdk2 crystal structure using the UCSF program suite DOCK5.0. Approximately 140,000 small molecules from the NCI/DTP database were docked into the pocket, designated by the appropriate spheres and scoring grid, and ranked according to their predicted binding energies. The top 40 compounds were ordered from the NCI/DTP and tested in cell culture. Figure 4-1C shows a selection of the most active compounds as determined by assays described in later sections, with predicted energy scores.

The NSC Compounds Inhibit the Proliferation of Cells in Culture

^{3}H-thymidine incorporation assays were performed to examine the influence of the compounds on cell proliferation. Initially, all 40 compounds ordered from the NCI/DTP were tested in cell culture at a concentration of 100 μM to determine if any cytostatic effect could be measured (data not shown). The most promising compounds were subsequently used in more detailed dose-response ^{3}H-thymdine incorporation assays, as well as in further mechanistic studies. The BT549 human breast cancer cell line and the HCT116 human colon cancer cell line exhibited decreased cell proliferation as measured by ^{3}H-thymidine incorporation after treatment with compounds NSC43067, NSC43042, and NSC63002 for 24 hours (Fig. 4-2A). Cell cycle analysis of each of these two cell lines was performed by flow cytometry of propidium iodide stained cells after treatment with the same compounds for 24 hours. In both cell lines, and for all three compounds, an arrest at the G0/G1 phase of the cell cycle is observed at lower concentrations, but an accumulation of cells in the G2/M cell cycle phase is apparent at higher

compound concentrations (Fig. 4-2B). This assay confirms that the decrease in DNA synthesis as determined by ^{3}H-thymdine incorporation is associated with cell cycle arrest.

Cytostatic Effects of the Compounds are a Result of an Apparent Reduction in Cellular Cdk Levels

We analyzed the total levels of several cdks by immunoblot to determine whether the compounds affect cdk abundance. BT549 cells were treated with compounds NSC43067, NSC269621 and NSC63002 at 100μM and 200μM concentrations for 24 or 48 hours. All three compounds significantly reduced the levels of soluble cdk1, cdk2 and cdk4, especially at the highest concentrations and longest time points. This effect was not due to a universal effect on all cellular proteins because the levels of the protein phosphatase PP2A and the structural protein Actin did not change appreciably (Fig. 4-3A).

E2F-1 is a transcription factor that plays a crucial role in mediating cdk-initiated cell cycle progression. Early cell cycle cdk activity (G1 to S phase) leads to the phosphorylation of the E2F inhibitor Rb, resulting in its release from E2F family proteins and increased E2F dependent transcription (14). Activation of E2F-dependent transcription is thought to be one of the primary cell cycle-related functions of the G1/S cdks. Therefore, E2F-1 overexpression would be expected to result in the partial reversion of the cdk reducing effects of the compounds. To examine this possibility, we used a mink lung epithelial cell line (Mv1Lu) engineered to overexpress E2F-1 (Mv1Lu-E2F1-11) (93). Treatment of the parental Mv1Lu cells with 200 μM NSC63002 resulted in an almost complete reduction of phosphorylation of Rb at Serine 780, as well as a decrease in the levels of several E2F-1 dependent transcription products including cyclin A, B-Myb, and E2F-1 itself (Fig. 4-3B). Levels of cdk1 and cdk4 also decreased, while the levels of the kinase Erk1/2 and Actin did not change. E2F1 overexpression resulted in a diminished response to compound NSC63002 compared to the effect observed in the parental

cells. A decrease in E2F dependent gene products, as well as serine 780 phosphorylation of Rb, was observed, albeit the response was much weaker than in parental cells. Similarly, an Mv1Lu cell line that overexpresses a constitutively active cyclinD1/cdk2 fusion protein (57) showed a dampened NSC63002-induced effect on Rb phosphorylation and E2F-dependent transcription, even though NSC63002 induced a partial decrease in the levels of the fusion protein.

Time course experiments were performed to ensure that cdk downregulation by the compounds occurred in parallel with cell cycle arrest. BT549 cells treated with 200 μM NSC43042 or NSC63002 were incubated for 4, 8, 12, or 24 hours before measuring cell proliferation by ^{3}H-Thymidine incorporation (Fig. 4-3D). The cytostatic effects of both compounds were observed as early as four hours after treatment. A decrease in cdks 1, 2, and 4 was observed as early as four hours as well (Fig. 4-3C), in accord with the cell proliferation assay. Taken together, these data suggest that the cytostatic effects of the compounds are mediated through a decrease in soluble cdk levels.

Decrease in Cdk Levels is a Result of Protein Aggregation

We initially examined the possibility that the compounds increase protein degradation of the cdks through proteolysis to determine the cause of the apparent decrease in cdk levels. Co-treatment of cells with proteasome inhibitors, such as lactacystin or NLVS, did not result in diminished cdk ablation, indicating that the effect was not induced by proteasomal degradation of the cdks (data not shown). Similarly, transfection of a degradation-resistant mutant of ubiquitin did not reduce the effect of the compounds, also suggesting that the effects of the compounds were not due to ubiquitin-dependent proteasomal degradation (data not shown). Overexposure of the higher molecular weight region of a cdk4 immunoblot of 293A cell lysates after treatment with 200 μM NSC63002 revealed the presence of cdk4 immunoreactive bands

exhibiting decreased electrophoretic mobility (Fig. 4-4A). Overexpression of cdk4 by transfection intensified this effect. This result is suggestive of an aggregation event involving cdk4, occurring in a compound-dependent manner.

We hypothesized that if aggregated cdks were being formed in cells treated with the NSC compounds, and that if they were of higher molecular weight than free, soluble cdks, this could be indicative of protein aggregation and that these aggregates could be pelleted by ultracentrifugation. To test this hypothesis, BT549 cells were treated with either DMSO or 200 μM NSC63002 for 24 hours. After harvesting and sonicating the cells, the cellular particulate was removed by centrifugation at either 16,000 x g or 150,000 x g for 20 minutes or 1 hour, respectively. The supernatants and the pellets from both centrifugations were collected and analyzed by immunoblot (Fig. 4-4B). While a dramatic decrease in the levels of cdks 1, 2, and 4 was observed in the supernatant, a corresponding increase in cdk levels was observed in the pellet, particularly after ultracentrifugation. Erk1/2 was also increased in the pellet. The relative ratio between the decrease in the supernatant levels of Erk1/2 and the increase in the pellet levels was, however, much less than that observed for the cdks.

We next performed immunofluorescence microscopy to visualize possible cdk aggregates in cells. BT549 cells were treated with DMSO or 200 μM NSC63002 for 24 hours. Cells were subsequently fixed and stained with an antibody for cdk4. Cells treated with DMSO exhibited a cdk4 staining pattern that was mostly uniform and homogenous, while compound NSC63002 treatment caused the formation of concentrated cdk4 staining at intense foci (Fig. 4-4C). The presence of these foci is consistent with cdk aggregation. In order to ensure that the apparent aggregation observed was not due to an artifact of the immunofluorescence staining procedure, we generated a cell line that stably expressed GFP fused to cdk4 (293A/GFP-cdk4). These cells

were treated in the same manner as in the previous experiment, except that after fixation the cells were mounted and viewed directly. A similar result was observed in the 293A/GFP-cdk4 cells as in the BT549 cells, where treatment with the NSC compounds induced the formation of aggregated foci of cdk4 (Fig. 4-4D). To confirm that the GFP fluorescence observed was from full length cdk4, we analyzed the 293A/GFP-cdk4 cell extract by immunoblot. We observed no significant bands of a lower molecular weight, indicating that the foci viewed by microscopy were not degradation products of full length cdk4-GFP (Fig. 4-4E). These results indicate that the apparent decrease in cdk levels in cells is due to the formation of insoluble protein aggregates that would presumably not have access to cellular substrates, and would be functionally inactive.

The NSC Compounds Bind Directly to Cdks

In order to determine whether the effect of the compounds on the cdks was direct or indirect, we tested the ability of the compounds to induce aggregation of a cyclin D1-cdk2 fusion protein (D1K2) *in vitro*. Purified D1K2 was ultracentrifuged for 2 hours at 150,000 x g to ensure that the starting material was free of aggregated material. The supernatant from this spin was incubated with DMSO (at a final concentration of 0.8%), the NSC compounds, or Roscovitine, an ATP-competitive cdk inhibitor (all at a final concentration of 400 μM) overnight at room temperature. Triton X-100 at a final concentration of 0.1% was used in the assay in order to inhibit non-specific colloidal aggregation of the small molecules. After the incubation period, the samples were centrifuged for 20 minutes at 16,000 x g to pellet the aggregated material. The soluble supernatant was removed from the pelleted material and both fractions were analyzed separately by SDS-PAGE. Figure 4-5A demonstrates that NSC compounds 43042, 269621, 63002, and 43067 decreased the amount of soluble D1K2 and increased the amount of insoluble pelleted material, in comparison with DMSO or Roscovitine.

In order to ensure that the effects of the NSC compounds were specific to D1K2, and not other proteins, the assay described above was repeated with purified bovine serum albumin (BSA). Figure 4-5B shows that none of the treatment conditions resulted in a decrease in BSA in the soluble fraction, and that no protein was visible in the pellet fraction. These results suggest that the compounds act directly on cdk proteins to induce their aggregation and that this is a protein-specific phenomenon.

Discussion

Cyclin D1 is overexpressed in approximately 50% of human primary breast cancers (180). Cdk4 is also up-regulated by gene amplification in several types of cancers (181, 182). The use of cdk inhibitors as anti-cancer agents has been considered a valuable approach for many years, owing to aberrant cdk activity in cancers combined with the fact that cdks are key controllers of the cell cycle. Furthermore, cdk inhibitors that do not act through ATP competition have the potential to be more selective drugs. We have identified a novel site on cdk2, distinct from the ATP binding site, which can be exploited for drug targeting. Moreover, this site is relatively well conserved among cell cycle cdks and is therefore ideal for decreasing overall cdk activity, as there is significant functional redundancy among cell cycle cdks. The compounds identified from a screen of this pocket potently inhibit cell proliferation. Flow cytometric analysis of cells treated with increasing doses of the compounds indicate that a G1 arrest occurred at lower concentrations, but a G2 arrest resulted after treatment with higher doses. This may be due to the fact that the compounds affect the activity of cdks 1, 2, and 4; most likely with different IC_{50}'s for each kinase. Possibly, the G1 arrest observed was due to the compounds displaying a higher affinity for the G1-S phase regulators, cdk2 and 4, and therefore affecting them at lower doses, while the G2 arrest observed at high doses was due to inhibition of cdk1 activity.

Our studies suggest that the NSC compounds bind directly to cdks 1, 2, and 4 and result in a decrease in the levels of soluble cdk protein in cell culture experiments. The mechanism through which these compounds act in a cell culture system is novel for a small molecular agent. A possible explanation for the ability of the compounds to reduce the solubility of the cdks to the point of aggregation could be the properties of the residues that line the structural pocket in question. The crystal structure of cdk2 used to screen for interacting molecules includes p27 in the structural complex, however we have no evidence to indicate that p27 is a necessary prerequisite for compound binding. Artificial removal of p27 from the crystal structure reveals that a series of hydrophobic residues are exposed to the solvent. If the compounds bind to this pocket in the absence of p27, it is possible that these residues would be exposed to the intracellular milieu resulting in aggregation. Another potential explanation for the induced aggregation is that the cdks may be inherently prone to aggregation themselves. Cdk1/cyclinB complexes localize as aggregates in *Xenopus* oocytes before resolubilizing and becoming active for the initiation of mitosis (183, 184). If cdks are inherently prone to aggregation, the stabilization by a small molecule of an alternate conformation in which hydrophobic residues become more exposed may be sufficient to trigger cdk precipitation.

There has been much research conducted on the practicality of high throughput molecular screens, including work on the prevalence of false positives in large molecular databases. With regards to the mechanism of action of the compounds presented in this paper, several studies have addressed the issue of promiscuous inhibitors that act through non-specific aggregation (185-187). Small molecules identified in high-throughput *in vitro* screens may exhibit apparent inhibition by decreasing enzymatic activity, but only due to the formation of small molecular colloidal aggregates which adsorb proteins, inhibiting enzymes non-specifically. The addition of

non-ionic detergents such as Triton X-100 at a concentration of 0.01-0.1% to the assay buffers inhibits the formation of these aggregates or even disrupts them after their formation (185-187). In all of our biochemical studies examining the aggregation of cdks, Triton X-100 was present at a concentration of either 0.1% or 1.0%. Furthermore, our screening procedure was based on *in silico* docking rather than high-throughput *in vitro* kinase assays, in which non-specific small molecular aggregates might have presented themselves as false-positives more frequently. The cdk aggregates observed in this study were formed in live cells in culture, indicating that the compounds had to be sufficiently soluble to pass through the cell membrane. All of this suggests that the cdk aggregates reported in this study are not due to non-specific small molecular colloidal aggregates, but rather due to specific small molecule-induced protein aggregation.

There is precedent for cdk ablative agents, although not for those that induce aggregation. The natural product Silibinin inhibits the progression of prostate cancer in mouse models concomitantly with the decrease of levels of cdk1, 2, 4, and 6 in prostate tissue (83, 84). These studies contribute to the idea that decreasing cdk levels can be effective in anti-cancer therapies.

The novel concept of a small molecule being able to decrease total protein levels in live cells can potentially open the door for other targets as well. Through *in silico* screening, we were able to take advantage of the fact that the RCSB protein structure database contains crystal structures of cdk2 in an active and an inactive conformation. By examining key differences between two conformations of the same protein, it may be possible in other circumstances to stabilize proteins in inactive conformations, or to encourage protein aggregation.

A

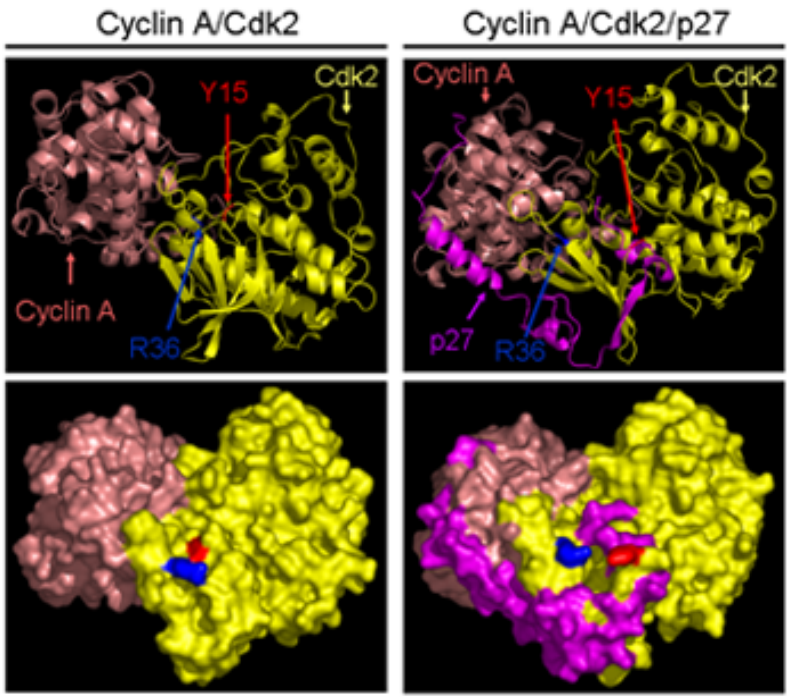

Figure 4-1. Identification of a novel cdk2 binding pocket and interacting molecules by high-throughput *in silico* screening
A) Visualization of the cyclinA/cdk2 and cyclinA/cdk2/p27 crystal structure with Pymol (Yellow-cdk2, Salmon-cyclin A, Purple-p27, Tyrosine 15 and Arginine36 are colored red and blue respectively as a point of reference). B) Sequence alignments of human cdk1, cdk2, cdk4, and cdk6. Shaded regions represent amino acid residues lining the pocket targeted by molecular docking. C) A selection of the most effective compounds identified by molecular docking as determined by ^{3}H-thymidine incorporation.

B

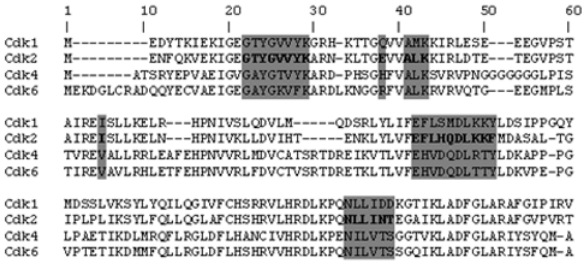

C

Rank	NSC Number	Mol Formula	Molecular Weight	Energy Score	Vdw Score	ES Score	2D Image
1	43067	$C_{14}H_{12}OS$	228	-16.679359	-16.419577	-0.259783	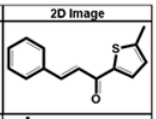
3	43042	$C_{10}H_{14}N_2O_2$	194	-16.355101	-16.278448	-0.076652	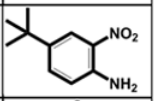
4	269621	$C_{10}H_{10}N_2S_2$	222	-15.208357	-13.682803	-1.525554	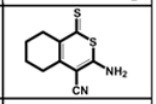
7	63002	$C_{15}H_{12}N_2O$	236	-14.166451	-15.107031	0.94058	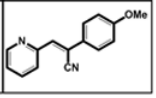

Figure 4-1.Continued.

A

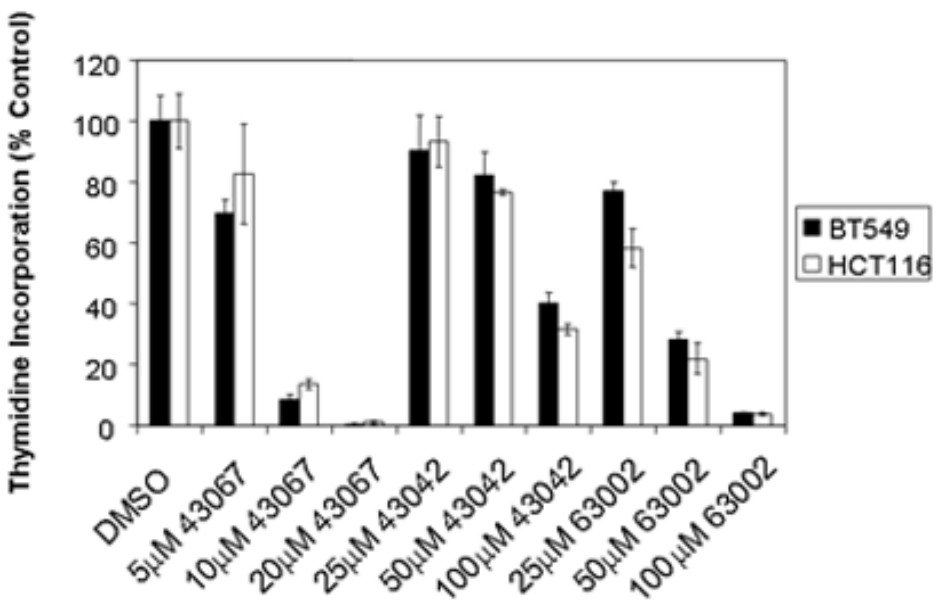

Figure 4-2.Compounds inhibit cell proliferation

A) BT549 breast cancer, and HCT116 colon cancer cells were treated with increasing doses of NSC43067, NSC43042, and NSC63002. After a 24 hour incubation, the cells were pulsed with ^{3}H-thymidine for 2 hours to measure DNA synthesis. All compounds displayed a dose-dependent decrease in cell proliferation in both cell lines. B) BT549 cells were treated with increasing doses of NSC43067, NSC43042, and NSC63002. After 24 hours, the nuclei of the cells were stained with propidium iodide and subjected to flow cytometric analysis. Cells arrested in the G1, S, and G2 phases of the cell cycle were observed depending on the compound and the concentration. C) HCT116 cells were treated with increasing doses of NSC43067, NSC43042, and NSC63002. After 24 hours, the nuclei of the cells were stained with propidium iodide and subjected to flow cytometric analysis. Cells arrested in the G1, S, and G2 phases of the cell cycle were observed depending on the compound and the concentration.

B

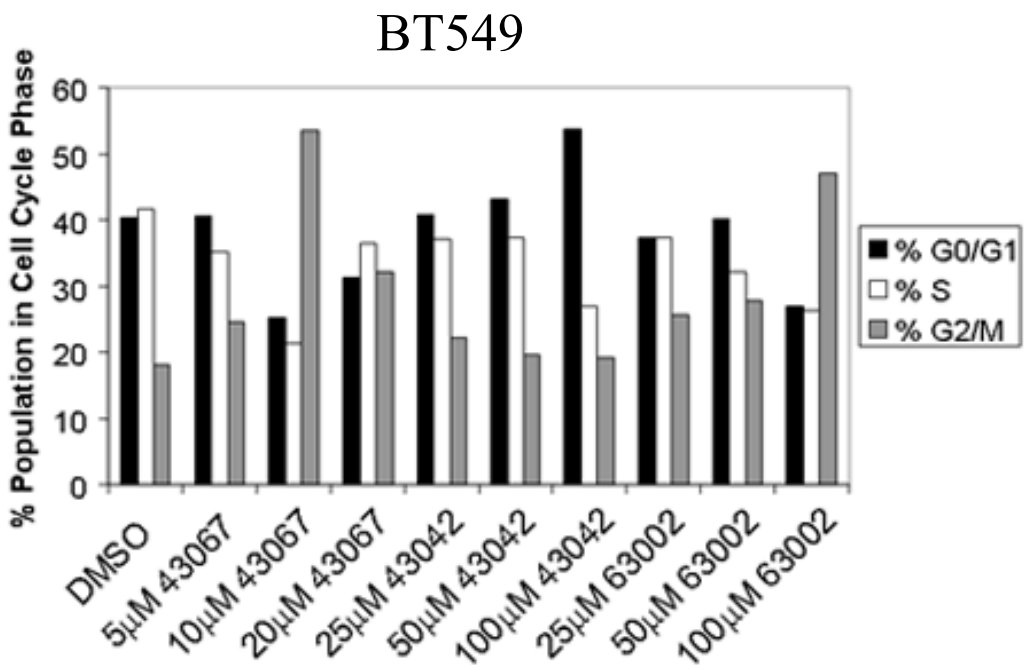

Figure 4-2.Continued.

C

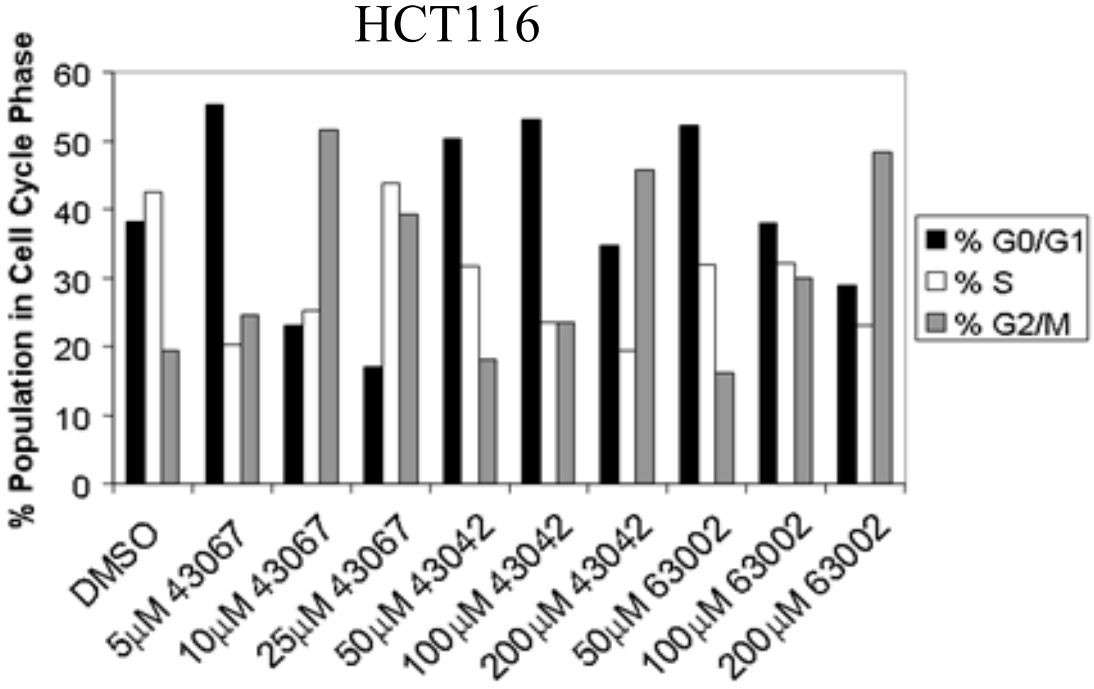

Figure 4-2.Continued.

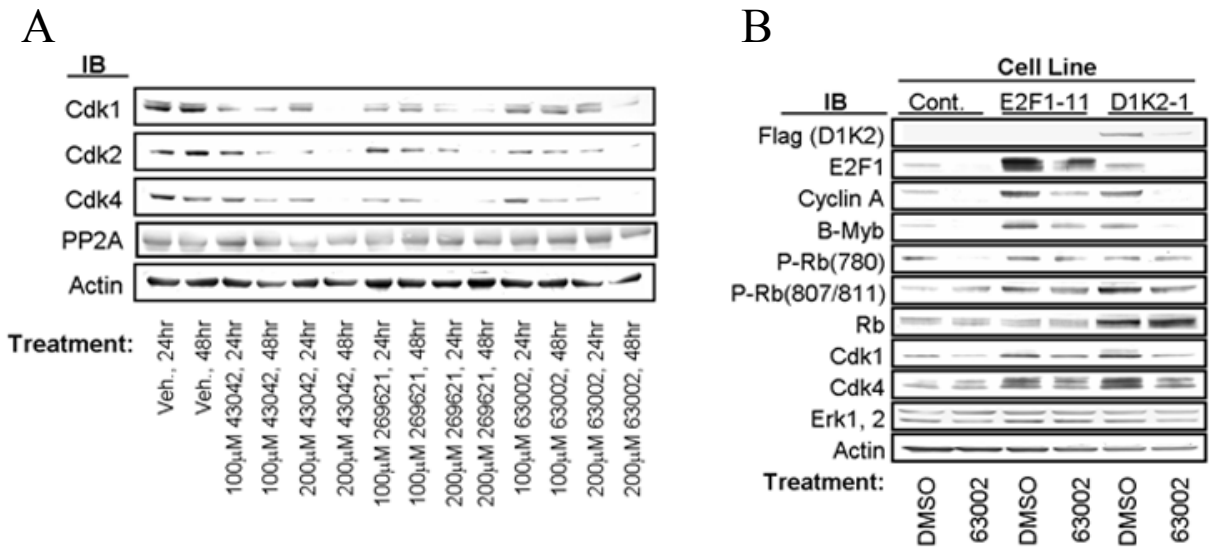

Figure 4-3.Compounds affect cell cycle cdks

A) BT549 cells were treated with 100 μM or 200 μM NSC43067, NSC269621 or NSC63002 for 24 or 48 hours. Protein from the cells was extracted with 0.1% Triton X-100 extraction buffer, normalized, and subjected to immunoblot analysis. The levels of cdk1, cdk2, and cdk4, but not Actin or Protein Phosphatase 2A (PP2A), decrease sharply after treatment with the NSC compounds. B) Mv1Lu mink lung epithelial cells overexpressing D1K2, E2F1, or empty vector were treated with either 0.2% DMSO or 200 μM NSC63002 for 24 hours. The presence of higher levels of E2F1 or a constitutively active form of cdk2 (D1K2) partially reverses the effects of the compounds on levels of E2F dependent gene products. C) BT549 cells were treated with 0.2% DMSO or 200 μM NSC43042 or NSC63002 for 1, 2, 4, and 24 hours. Immunoblot analysis reveals a decrease in levels of cdk1 as early as 4 hours, with cdk2 and cdk4 decreasing by 24 hours. D) BT549 cells were treated with 0.2% DMSO or 200 μM NSC43042 or NSC63002 for 4, 8, 12, and 24 hours. ^{3}H-Thymidine incorporation analysis reveals that the decrease in cdk levels occurs on the same time scale as the inhibition of cell proliferation.

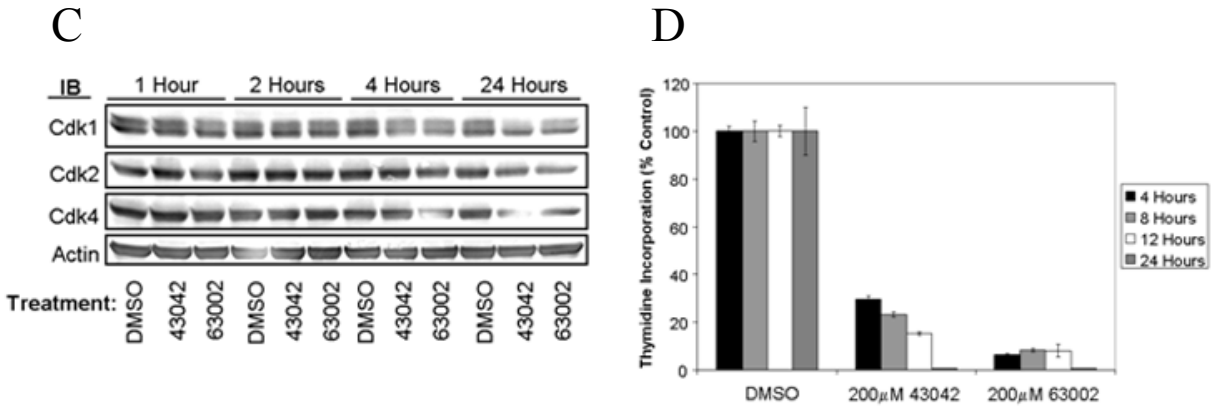

Figure 4-3.Continued.

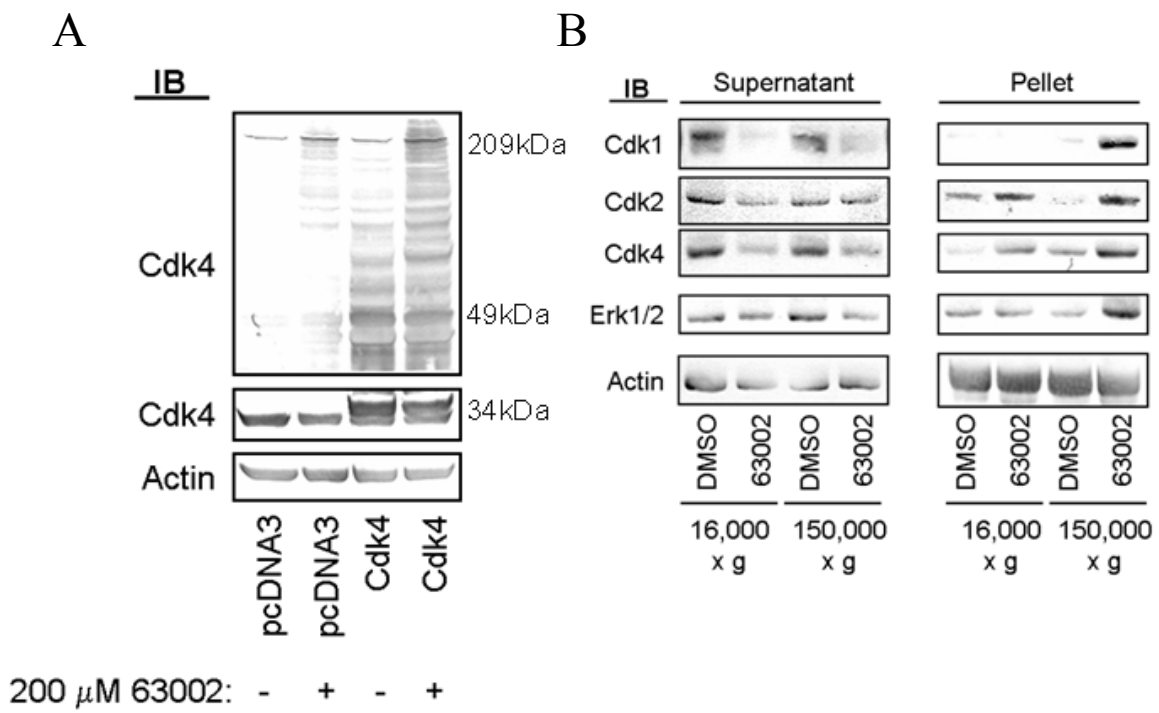

Figure 4-4.Decrease in cdk levels is a result of protein aggregation

A) 293A cells were transiently transfected with either pcDNA3 vector or cdk4/pcDNA3 and treated with 0.2% DMSO or 200 μM NSC63002 for 24 hours. Immunoblot analysis reveals a marked increase in high molecular mass bands in samples treated with NSC63002. B) BT549 cells were treated with 0.2% DMSO or 200 μM NSC63002 for 24 hours. Cell extracts were centrifuged at either 16,000 x g for 20 minutes or 150,000 x g for one hour. Immunoblot analysis reveals that more cdk 1, 2, and 4 pelleted by high speed centrifugation from samples treated with 200 μM NSC63002 than the DMSO treated samples or the lower speed centrifugation. C) BT549 cells were treated with 0.2% DMSO or 200 μM NSC 63002 for 24 hours. Immunofluorescence analysis reveals the formation of cdk4 aggregates in samples treated with NSC 63002. D) 293A cells stably expressing a GFP-cdk4 fusion protein were treated with 0.2% DMSO or 200 μM NSC 63002 for 24 hours. Fluorescence microscopy reveals the formation of cdk4 aggregates in NSC compound treated cells. E) Immunoblot analysis of the 293A cells overexpressing GFP-cdk4 confirms the presence of full-length GFP-cdk4 and no significant degradation products.

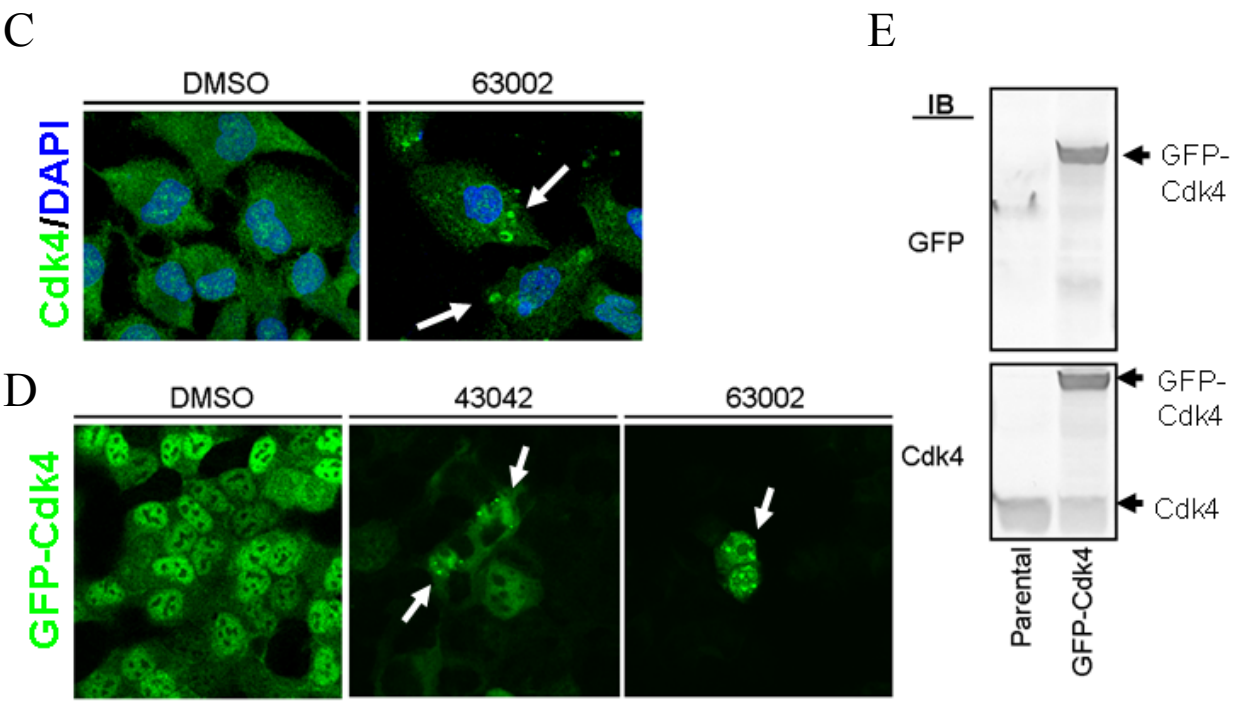

Figure 4-4.Continued.

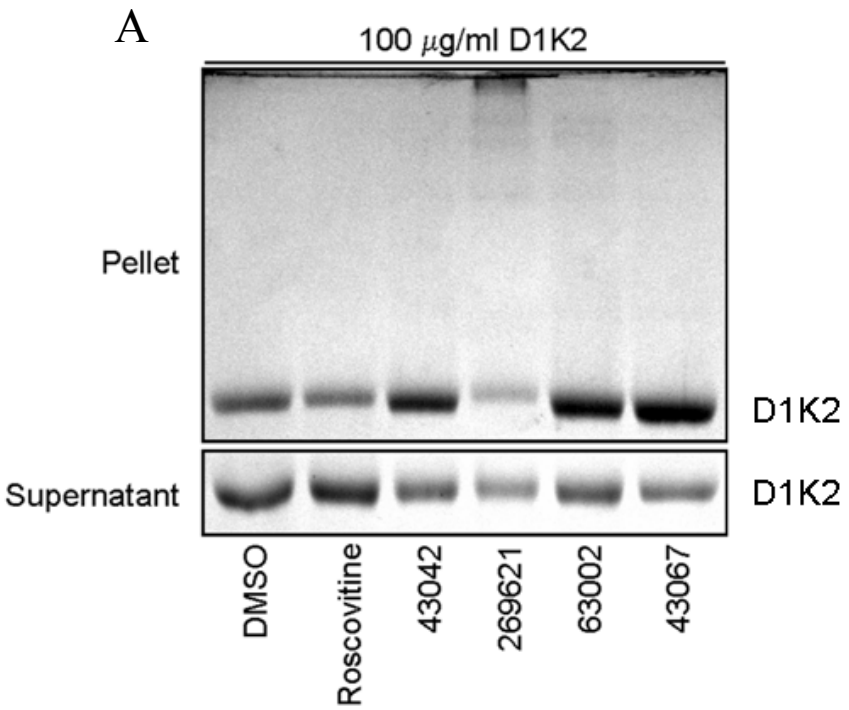

Figure 4-5.Compounds act directly on cdks

A) A purified cyclin D1-cdk2 fusion protein was incubated with 400 μM of Roscovitine, NSC 43042, NSC269621, NSC63002, or NSC43067, or 0.8% DMSO in a buffer containing 40 mM HEPES (pH 7.0), 200 mM NaCl, 5 mM DTT and 0.1% Triton X-100 overnight at room temperature. The incubated samples were centrifuged and the supernatant and pellet fractions were processed separately for SDS-PAGE analysis. The NSC compounds, but not DMSO or Roscovitine, caused a decrease in D1K2 in the soluble fraction, and an increase in the pellet fraction. B) The assay in part A) was repeated with bovine serum albumin (BSA). No differences in the supernatant fractions are observed, and no pelleted protein is detected by Coomassie staining.

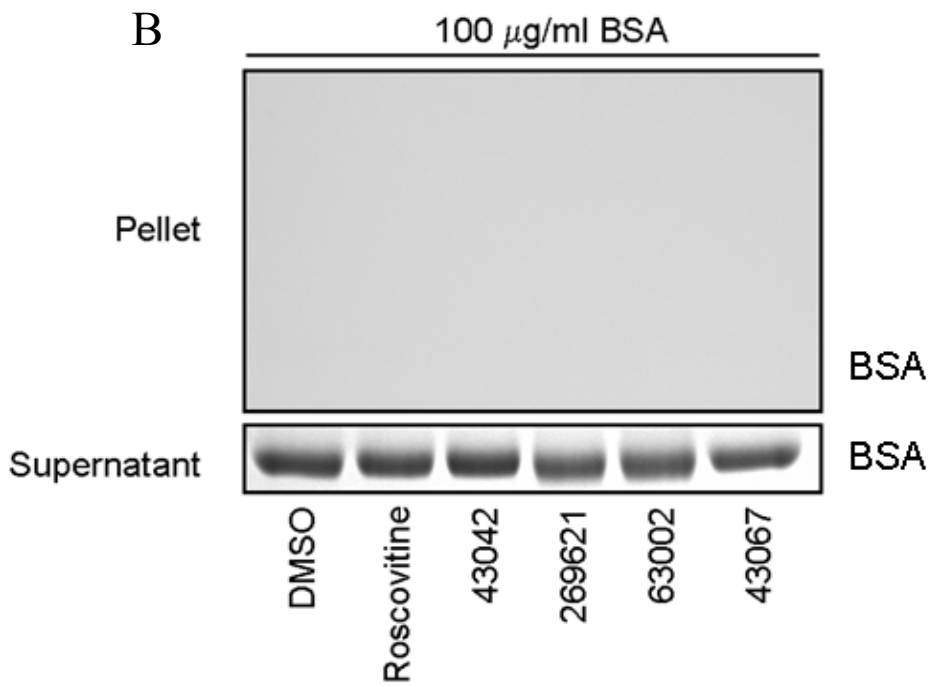

Figure 4-5.Continued.

CHAPTER 5
CONCLUSION

Discussion

Summary

Chapters 2 and 3 described the generation and characterization of a novel transgenic mouse tumor model system with which to study basal-like breast cancer etiology. The results from these two sections have provided new evidence for the role of cdk2 and cyclin D1 in breast tumorigenesis. The mouse tumor model described in this study will be a useful tool in examining invasiveness and differentiation of cancer cells in mammary tissue. It will also provide a means with which to test the ability of potential novel therapeutics to inhibit tumor growth. Furthermore, it presents an opportunity to examine the effects of potential chemopreventive drugs as prophylactic agents.

Chapter 4 described the characterization of a novel class of cdk inhibitors identified by high throughput *in silico* molecular screening. The screen was designed to target a site on cdk2 that was distinct from the ATP-binding site. Through an apparent direct interaction with cdks, the compounds identified by this screening method decrease total soluble levels of cdks in cells through a mechanism of aggregation. This decrease in cdk levels correlates with a potent inhibition of cell proliferation. This is a unique mechanism of action for cdk inhibition.

Taken together, these studies describe the role of cdk2 in breast tumorigenesis, followed by a novel means by which to inhibit cdks and halt the progression of cancer. It examines the entire process of cancer from initiation to potential cure.

The Nature of Cdk Aggregation

At this point, there is insufficient data to identify the precise mechanism for the observed cdk aggregation induced by treatment with the compounds. As mentioned in the discussion

section of chapter 4, one possible explanation for the aggregation is that a structural change in the cdks occurs, exposing hydrophobic side chains of residues in the pocket. Originally, the crystal structure used for the high throughput *in silico* screen contained p27. However, immunoprecipitation studies indicate that there is no increase in p27 binding to cdk2 upon compound treatment. This suggests that the compounds bind to cdk2 regardless of p27 presence. If this is the case, then the compounds may be able to induce a similar conformational change in cdk2 to that induced by p27. By artificially removing p27 from the original crystal structure using the protein structure viewer PYMOL, we can visualize what the pocket may look like in the presence of one of the compounds, and in the absence of p27. In the absence of p27, the side chains of a tyrosine, lysine, and two valine residues are exposed to the surrounding solvent. If this is any indication of what the structure of cdk2 bound to a compound in the absence of p27 would be, then these residues could serve as the basis of aggregation by interacting with the surrounding intracellular milieu.

Several studies have been published that describe the aggregation of cyclinB1/cdk1 complexes in starfish oocytes (183, 184). These studies discuss the dynamic aggregation and resolublization of these cyclin/cdk complexes with relation to their activation and regulation. These aggregates, which exist in the cytoplasm, disperse after treatment with maturation hormone, thereby responding to cell cycle stimulation. As of yet, such aggregates have not been described in other cellular systems. Although it is unclear whether or not these complexes cycle between states of solubility and insolubility in mammalian cells, these papers set a precedent for the aggregation of cdks in cells.

Cdk2 is a client of the chaperone proteins hsp90 and cdc37 (188). Furthermore, when cells are treated with an inhibitor of hsp90, cdk2 levels decrease dramatically (188), indicating a

requirement for chaperone assistance in protein stability. Taken together, these studies indicate that the cdks are relativity unstable. In the context of treatment with the compounds described in this study, these proteins may be sensitive to slight changes in conformations that could lead to the aggregation observed.

Implications for Aggregate-Inducing Molecules in Cancer Therapy

As discussed in the introduction, compounds that reversibly inhibit the enzymatic activity of cdks have proven to be somewhat successful as anti-cancer therapeutics. However, as with all drugs, there is a finite half-life within cells, and once the drug is metabolized or excreted, cdk activity will recover. In this respect, the compounds identified in this study have an added advantage, affecting total levels of cdks. The outcome is that when the drug is metabolized, the cell will need to replenish the levels of the cdks by protein synthesis, resulting in a lag period, in which cell cycle activity will be low. This could allow the compounds to have effects that extend beyond their natural half-life, a potential advantage with respect to dosage intervals in the clinical setting.

Future Research

In Vivo Compound Studies

As the *in vitro* data collected on the NSC compounds indicate that they induce cell cycle arrests, the next logical step in the course of drug development would be to test the compounds on mice *in vivo*. Mice will be injected into the mammary fat pad with tumor cells to initiate tumorigenesis. After the tumors grow to a palpable size, intraperitoneal injections of several of the NSC compounds will be administered, and tumor growth will be monitored. As mentioned above, the transgenic mouse tumor model described in chapters 2 and 3 will be a useful tool for examining the effect of novel cancer therapeutics on tumor growth. As this model is driven by a

constitutively active form of cdk2, and the compounds are directed towards cdks, the two projects will overlap well.

Protein Crystallization

Although chapter 4 describes multiple lines of evidence that the identified compounds directly affecting cdks, it is as of yet still undetermined whether or not these compounds bind to the exact pocket to which they were directed. In order to address this issue, it will be necessary to solve the crystal structures of a cdk protein either alone or in complex with a cyclin, with one of the compounds in the crystallization solution. A crystal structure of a cdk with an NSC compound will be definitive evidence that the compounds interact directly with cdks, and will validate the study. Furthermore, it will be interesting to see whether or not the solved crystal structures reveal a conformational change in the cdk induced by one or more of the NSC compounds. Any changes observed will be informative in understanding the regulation of cdks.

Alternative Structural Pocket for Screening

As mentioned above, p27 can be artificially removed from the cylinA/cdk2/p27 crystal structure, revealing a possible conformation of cdk2 in the absence of p27. In an attempt to develop another class of small molecular inhibitors of cdk2, we have used this structure as a basis for a second round of high throughput *in silico* molecular screening. The second pocket chosen (pocket 2) partially contains the ATP binding site of cdk2, which interacts with p27 in the original structure. In this sense, compounds directed to this site could act as p27 mimetics, by stabilizing the conformation of cdk2 in an inhibited form. The ATP binding site is altered in this structure, which would mean that compounds designed to bind to this site would have different characteristics to other compounds targeted to this site, giving them an advantage in terms of kinase specificity.

Lead Compound Optimization

Several of the compounds identified by the high-throughput molecular docking screen described in this study have IC_{50} values for inhibiting cell proliferation in the low micromolar range. While these are promising results for lead compounds, to become marketable as potential cancer therapeutics, a dramatic increase in potency would be desirable. Of course not all drugs must have IC_{50} values in the low nanomolar range to be effective therapeutics; salicylate for example, has an IC_{50} value of greater than 1.5 mM for inhibiting cyclooxgenase-1 (189). Nevertheless, to improve the chances of having successful clinical trials with any of the compounds described in this study, some degree of optimization will most likely be necessary. There are several means through which this can be pursued. Firstly, rational modifications can be made to the original compounds based on their modeled orientation in the structural pocket of the protein. Software tools similar to the DOCK program used to screen the cdk2 pocket can be used to make logical structural modifications to the lead compounds. The program RACHEL, for example, will add molecular groups one at a time to selected attachment sites on the compound. This process of iterative refinement is designed to increase the affinity of the compounds for the protein.

A second means of lead compound optimization could involve bridging two compounds that occupy two separate protein pockets that are in close proximity to one another. Some compounds directed to the original pocket (pocket 1) are only 3.5 angstroms away from some pocket 2 compounds. As these two pockets are within such close proximity, this approach is entirely feasible. Once again there is computer software available that is designed to build scaffolds to link separate compounds together. The program CHARLIE (a module within the RACHEL program) iteratively adds small molecular groups between two compounds, outputting the highest scoring linker groups based on predicted molecular interactions. By combining two

compounds, the IC_{50} values could be decreased by orders of magnitude. For either of these two approaches, the ideal situation would involve obtaining the crystal structures of the compounds bound to the pocket of cdk2. By determining the precise orientation of the compounds in the pocket, the process of optimization will be much more likely to yield effective drugs.

Alternative Mouse Model Systems

The cyclin D1/cdk2 fusion protein is a useful tool in understanding the precise function of this complex in cells. The transgenic mouse model based on this protein has further allowed us to examine the contribution of cyclin D1/cdk2 complexes in tumor development. An extension of this project will involve the generation of alternative cyclin/cdk complexes including cyclin E/cdk2 and cyclin D1/cdk4 by fusing them together. A thorough characterization of these complexes to determine their phosphorylation state and kinase activity will be conducted *in vitro*. Upon establishing that these fusion proteins function in a manner comparable to their endogenous counterparts, they will be used to generate transgenic mouse lines for tumor studies. It will be informative to determine how the tumors generated by these alternative fusion proteins compare to the cancer etiology of the original D1K2 mouse model, or if they generate tumors at all. This approach is a unique way with which to understand the contribution of specific cyclin/cdk complexes in breast tumorigenesis *in vivo*. It will help to better understand whether the characteristics of the D1K2 tumors are brought about by cdk2, or cyclin D1, or whether both are necessary for the specific etiology observed.

Conclusion

This study was an effort in further determining the role of cdks, and in particular cdk2, in cancer. It examines the effects of overactive cdk2 in tumorigenesis, and the effect of cdk inhibition on cell cycle dynamics. Together, the work here provides new tools in understanding

the pathways involved in tumor development, as well as identifying promising new compounds that may eventually be used as anti-cancer agents in the clinical setting.

LIST OF REFERENCES

1. Deshpande, A, Sicinski, P, and Hinds, PW Cyclins and cdks in development and cancer: a perspective. Oncogene, 2005; 24(17): 2909-2915.

2. Sanchez, I and Dynlacht, BD New insights into cyclins, CDKs, and cell cycle control. Semin Cell Dev Biol, 2005; 16(3): 311-321.

3. Desai, D, Gu, Y, and Morgan, DO Activation of human cyclin-dependent kinases in vitro. Mol Biol Cell, 1992; 3(5): 571-582.

4. Desai, D, Wessling, HC, Fisher, RP, and Morgan, DO Effects of phosphorylation by CAK on cyclin binding by CDC2 and CDK2. Mol Cell Biol, 1995; 15(1): 345-350.

5. Parker, LL and Piwnica-Worms, H Inactivation of the p34cdc2-cyclin B complex by the human WEE1 tyrosine kinase. Science, 1992; 257(5078): 1955-1957.

6. Toyoshima, H and Hunter, T p27, a novel inhibitor of G1 cyclin-Cdk protein kinase activity, is related to p21. Cell, 1994; 78(1): 67-74.

7. Xiong, Y, Hannon, GJ, Zhang, H, Casso, D, Kobayashi, R, and Beach, D p21 is a universal inhibitor of cyclin kinases. Nature, 1993; 366(6456): 701-704.

8. Lee, MH, Reynisdottir, I, and Massague, J Cloning of p57KIP2, a cyclin-dependent kinase inhibitor with unique domain structure and tissue distribution. Genes Dev, 1995; 9(6): 639-649.

9. Canepa, ET, Scassa, ME, Ceruti, JM, et al. INK4 proteins, a family of mammalian CDK inhibitors with novel biological functions. IUBMB Life, 2007; 59(7): 419-426.

10. Aktas, H, Cai, H, and Cooper, GM Ras links growth factor signaling to the cell cycle machinery via regulation of cyclin D1 and the Cdk inhibitor p27KIP1. Mol Cell Biol, 1997; 17(7): 3850-3857.

11. Sherr, CJ Mammalian G1 cyclins. Cell, 1993; 73(6): 1059-1065.

12. Harbour, JW, Luo, RX, Dei Santi, A, Postigo, AA, and Dean, DC Cdk phosphorylation triggers sequential intramolecular interactions that progressively block Rb functions as cells move through G1. Cell, 1999; 98(6): 859-869.

13. Hatakeyama, M, Brill, JA, Fink, GR, and Weinberg, RA Collaboration of G1 cyclins in the functional inactivation of the retinoblastoma protein. Genes Dev, 1994; 8(15): 1759-1771.

14. Dyson, N The regulation of E2F by pRB-family proteins. Genes Dev, 1998; 12(15): 2245-2262.

15. Flemington, EK, Speck, SH, and Kaelin, WG, Jr. E2F-1-mediated transactivation is inhibited by complex formation with the retinoblastoma susceptibility gene product. Proc Natl Acad Sci U S A, 1993; 90(15): 6914-6918.

16. Lees, JA, Saito, M, Vidal, M, et al. The retinoblastoma protein binds to a family of E2F transcription factors. Mol Cell Biol, 1993; 13(12): 7813-7825.

17. Wu, L, Timmers, C, Maiti, B, et al. The E2F1-3 transcription factors are essential for cellular proliferation. Nature, 2001; 414(6862): 457-462.

18. Magnaghi-Jaulin, L, Groisman, R, Naguibneva, I, et al. Retinoblastoma protein represses transcription by recruiting a histone deacetylase. Nature, 1998; 391(6667): 601-605.

19. Classon, M and Harlow, E The retinoblastoma tumour suppressor in development and cancer. Nat Rev Cancer, 2002; 2(12): 910-917.

20. DeGregori, J, Kowalik, T, and Nevins, JR Cellular targets for activation by the E2F1 transcription factor include DNA synthesis- and G1/S-regulatory genes. Mol Cell Biol, 1995; 15(8): 4215-4224.

21. Nevins, JR E2F: a link between the Rb tumor suppressor protein and viral oncoproteins. Science, 1992; 258(5081): 424-429.

22. Lee, HH, Chiang, WH, Chiang, SH, Liu, YC, Hwang, J, and Ng, SY Regulation of cyclin D1, DNA topoisomerase I, and proliferating cell nuclear antigen promoters during the cell cycle. Gene Expr, 1995; 4(3): 95-109.

23. Ohtani, K, DeGregori, J, and Nevins, JR Regulation of the cyclin E gene by transcription factor E2F1. Proc Natl Acad Sci U S A, 1995; 92(26): 12146-12150.

24. Schulze, A, Zerfass, K, Spitkovsky, D, et al. Cell cycle regulation of the cyclin A gene promoter is mediated by a variant E2F site. Proc Natl Acad Sci U S A, 1995; 92(24): 11264-11268.

25. Akiyama, T, Ohuchi, T, Sumida, S, Matsumoto, K, and Toyoshima, K Phosphorylation of the retinoblastoma protein by cdk2. Proc Natl Acad Sci U S A, 1992; 89(17): 7900-7904.

26. Doree, M and Hunt, T From Cdc2 to Cdk1: when did the cell cycle kinase join its cyclin partner? J Cell Sci, 2002; 115(Pt 12): 2461-2464.

27. Fang, F and Newport, JW Evidence that the G1-S and G2-M transitions are controlled by different cdc2 proteins in higher eukaryotes. Cell, 1991; 66(4): 731-742.

28. Santamaria, D and Ortega, S Cyclins and CDKS in development and cancer: lessons from genetically modified mice. Front Biosci, 2006; 11(1164-1188.

29. van den Heuvel, S and Harlow, E Distinct roles for cyclin-dependent kinases in cell cycle control. Science, 1993; 262(5142): 2050-2054.

30. Berthet, C, Aleem, E, Coppola, V, Tessarollo, L, and Kaldis, P Cdk2 knockout mice are viable. Curr Biol, 2003; 13(20): 1775-1785.

31. Aleem, E, Kiyokawa, H, and Kaldis, P Cdc2-cyclin E complexes regulate the G1/S phase transition. Nat Cell Biol, 2005; 7(8): 831-836.

32. Rodriguez-Puebla, ML, Miliani de Marval, PL, LaCava, M, Moons, DS, Kiyokawa, H, and Conti, CJ Cdk4 deficiency inhibits skin tumor development but does not affect normal keratinocyte proliferation. Am J Pathol, 2002; 161(2): 405-411.

33. Malumbres, M, Sotillo, R, Santamaria, D, et al. Mammalian cells cycle without the D-type cyclin-dependent kinases Cdk4 and Cdk6. Cell, 2004; 118(4): 493-504.

34. Barrière, C, Santamaría, D, Cerqueira, A, et al. Mice thrive without Cdk4 and Cdk2. Molecular Oncology, 2007; 1(1): 72-83.

35. Santamaria, D, Barriere, C, Cerqueira, A, et al. Cdk1 is sufficient to drive the mammalian cell cycle. Nature, 2007; 448(7155): 811-815.

36. Salon, C, Merdzhanova, G, Brambilla, C, Brambilla, E, Gazzeri, S, and Eymin, B E2F-1, Skp2 and cyclin E oncoproteins are upregulated and directly correlated in high-grade neuroendocrine lung tumors. Oncogene, 2007; 26(48): 6927-6936.

37. Foulkes, WD, Brunet, JS, Stefansson, IM, et al. The prognostic implication of the basal-like (cyclin E high/p27 low/p53+/glomeruloid-microvascular-proliferation+) phenotype of BRCA1-related breast cancer. Cancer Res, 2004; 64(3): 830-835.

38. Keyomarsi, K, Tucker, SL, Buchholz, TA, et al. Cyclin E and survival in patients with breast cancer. N Engl J Med, 2002; 347(20): 1566-1575.

39. Akli, S and Keyomarsi, K Cyclin E and its low molecular weight forms in human cancer and as targets for cancer therapy. Cancer Biol Ther, 2003; 2(4 Suppl 1): S38-47.

40. Harwell, RM, Mull, BB, Porter, DC, and Keyomarsi, K Activation of cyclin-dependent kinase 2 by full length and low molecular weight forms of cyclin E in breast cancer cells. J Biol Chem, 2004; 279(13): 12695-12705.

41. Buckley, MF, Sweeney, KJ, Hamilton, JA, et al. Expression and amplification of cyclin genes in human breast cancer. Oncogene, 1993; 8(8): 2127-2133.

42. Sutherland, RL and Musgrove, EA Cyclin D1 and mammary carcinoma: new insights from transgenic mouse models. Breast Cancer Res, 2002; 4(1): 14-17.

43. Parker, MA, Deane, NG, Thompson, EA, et al. Over-expression of cyclin D1 regulates Cdk4 protein synthesis. Cell Prolif, 2003; 36(6): 347-360.

44. Bosch, F, Jares, P, Campo, E, et al. PRAD-1/cyclin D1 gene overexpression in chronic lymphoproliferative disorders: a highly specific marker of mantle cell lymphoma. Blood, 1994; 84(8): 2726-2732.

45. Knudsen, KE, Diehl, JA, Haiman, CA, and Knudsen, ES Cyclin D1: polymorphism, aberrant splicing and cancer risk. Oncogene, 2006; 25(11): 1620-1628.

46. Zheng, Y, Shen, H, Sturgis, EM, et al. Cyclin D1 polymorphism and risk for squamous cell carcinoma of the head and neck: a case-control study. Carcinogenesis, 2001; 22(8): 1195-1199.

47. Satinder, K, Chander, SR, Pushpinder, K, Indu, G, and Veena, J Cyclin D1 (G870A) polymorphism and risk of cervix cancer: a case control study in north Indian population. Mol Cell Biochem, 2008; 315(1-2): 151-157.

48. Alkarain, A, Jordan, R, and Slingerland, J p27 deregulation in breast cancer: prognostic significance and implications for therapy. J Mammary Gland Biol Neoplasia, 2004; 9(1): 67-80.

49. Blain, SW and Massague, J Breast cancer banishes p27 from nucleus. Nat Med, 2002; 8(10): 1076-1078.

50. Winters, ZE, Hunt, NC, Bradburn, MJ, et al. Subcellular localisation of cyclin B, Cdc2 and p21(WAF1/CIP1) in breast cancer. association with prognosis. Eur J Cancer, 2001; 37(18): 2405-2412.

51. Xia, W, Chen, JS, Zhou, X, et al. Phosphorylation/cytoplasmic localization of p21Cip1/WAF1 is associated with HER2/neu overexpression and provides a novel combination predictor for poor prognosis in breast cancer patients. Clin Cancer Res, 2004; 10(11): 3815-3824.

52. Liggett, WH, Jr. and Sidransky, D Role of the p16 tumor suppressor gene in cancer. J Clin Oncol, 1998; 16(3): 1197-1206.

53. Rane, SG, Cosenza, SC, Mettus, RV, and Reddy, EP Germ line transmission of the Cdk4(R24C) mutation facilitates tumorigenesis and escape from cellular senescence. Mol Cell Biol, 2002; 22(2): 644-656.

54. Dou, QP, Molnar, G, and Pardee, AB Cyclin D1/cdk2 kinase is present in a G1 phase-specific protein complex Yi1 that binds to the mouse thymidine kinase gene promoter. Biochem Biophys Res Commun, 1994; 205(3): 1859-1868.

55. Dulic, V, Drullinger, LF, Lees, E, Reed, SI, and Stein, GH Altered regulation of G1 cyclins in senescent human diploid fibroblasts: accumulation of inactive cyclin E-Cdk2 and cyclin D1-Cdk2 complexes. Proc Natl Acad Sci U S A, 1993; 90(23): 11034-11038.

56. Sweeney, KJ, Swarbrick, A, Sutherland, RL, and Musgrove, EA Lack of relationship between CDK activity and G1 cyclin expression in breast cancer cells. Oncogene, 1998; 16(22): 2865-2878.

57. Chytil, A, Waltner-Law, M, West, R, et al. Construction of a cyclin D1-Cdk2 fusion protein to model the biological functions of cyclin D1-Cdk2 complexes. J Biol Chem, 2004; 279(46): 47688-47698.

58. Canduri, F and de Azevedo, F Structural basis for interaction of inhibitors with Cyclin-dependent kinase 2. Curr Comp-Aid Drug Design, 2005; 1(53-64.

59. Noble, ME, Endicott, JA, and Johnson, LN Protein kinase inhibitors: insights into drug design from structure. Science, 2004; 303(5665): 1800-1805.

60. Shapiro, GI Preclinical and clinical development of the cyclin-dependent kinase inhibitor flavopiridol. Clin Cancer Res, 2004; 10(12 Pt 2): 4270s-4275s.

61. Christian, BA, Grever, MR, Byrd, JC, and Lin, TS Flavopiridol in the treatment of chronic lymphocytic leukemia. Curr Opin Oncol, 2007; 19(6): 573-578.

62. Schwartz, GK, Ilson, D, Saltz, L, et al. Phase II study of the cyclin-dependent kinase inhibitor flavopiridol administered to patients with advanced gastric carcinoma. J Clin Oncol, 2001; 19(7): 1985-1992.

63. Shapiro, GI, Supko, JG, Patterson, A, et al. A phase II trial of the cyclin-dependent kinase inhibitor flavopiridol in patients with previously untreated stage IV non-small cell lung cancer. Clin Cancer Res, 2001; 7(6): 1590-1599.

64. Kahn, ME, Senderowicz, A, Sausville, EA, and Barrett, KE Possible mechanisms of diarrheal side effects associated with the use of a novel chemotherapeutic agent, flavopiridol. Clin Cancer Res, 2001; 7(2): 343-349.

65. Senderowicz, AM Small-molecule cyclin-dependent kinase modulators. Oncogene, 2003; 22(42): 6609-6620.

66. Benson, C, White, J, De Bono, J, et al. A phase I trial of the selective oral cyclin-dependent kinase inhibitor seliciclib (CYC202; R-Roscovitine), administered twice daily for 7 days every 21 days. Br J Cancer, 2007; 96(1): 29-37.

67. Belani, C Efficacy study of oral Seliciclib to treat Non-Small Cell Lung Cancer. ClinicalTrials.gov identifier: NCT00372073; 2006.

68. Hahntow, IN, Schneller, F, Oelsner, M, et al. Cyclin-dependent kinase inhibitor Roscovitine induces apoptosis in chronic lymphocytic leukemia cells. Leukemia, 2004; 18(4): 747-755.

69. Jimeno, A, Rudek, MA, Purcell, T, et al. Phase I and pharmacokinetic study of UCN-01 in combination with irinotecan in patients with solid tumors. Cancer Chemother Pharmacol, 2008; 61(3): 423-433.

70. Hotte, SJ, Oza, A, Winquist, EW, et al. Phase I trial of UCN-01 in combination with topotecan in patients with advanced solid cancers: a Princess Margaret Hospital Phase II Consortium study. Ann Oncol, 2006; 17(2): 334-340.

71. Lara, PN, Jr., Mack, PC, Synold, T, et al. The cyclin-dependent kinase inhibitor UCN-01 plus cisplatin in advanced solid tumors: a California cancer consortium phase I pharmacokinetic and molecular correlative trial. Clin Cancer Res, 2005; 11(12): 4444-4450.

72. Jeffrey, PD, Russo, AA, Polyak, K, et al. Mechanism of CDK activation revealed by the structure of a cyclinA-CDK2 complex. Nature, 1995; 376(6538): 313-320.

73. Honda, R, Lowe, ED, Dubinina, E, et al. The structure of cyclin E1/CDK2: implications for CDK2 activation and CDK2-independent roles. Embo J, 2005; 24(3): 452-463.

74. Russo, AA, Jeffrey, PD, Patten, AK, Massague, J, and Pavletich, NP Crystal structure of the p27Kip1 cyclin-dependent-kinase inhibitor bound to the cyclin A-Cdk2 complex. Nature, 1996; 382(6589): 325-331.

75. De Azevedo, WF, Leclerc, S, Meijer, L, Havlicek, L, Strnad, M, and Kim, SH Inhibition of cyclin-dependent kinases by purine analogues: crystal structure of human cdk2 complexed with roscovitine. Eur J Biochem, 1997; 243(1-2): 518-526.

76. Wang, NP, To, H, Lee, WH, and Lee, EY Tumor suppressor activity of RB and p53 genes in human breast carcinoma cells. Oncogene, 1993; 8(2): 279-288.

77. Wu, SY, McNae, I, Kontopidis, G, et al. Discovery of a novel family of CDK inhibitors with the program LIDAEUS: structural basis for ligand-induced disordering of the activation loop. Structure, 2003; 11(4): 399-410.

78. Schulze-Gahmen, U and Kim, SH Structural basis for CDK6 activation by a virus-encoded cyclin. Nat Struct Biol, 2002; 9(3): 177-181.

79. Jeffrey, PD, Tong, L, and Pavletich, NP Structural basis of inhibition of CDK-cyclin complexes by INK4 inhibitors. Genes Dev, 2000; 14(24): 3115-3125.

80. Canela, N, Orzaez, M, Fucho, R, et al. Identification of an hexapeptide that binds to a surface pocket in cyclin A and inhibits the catalytic activity of the complex cyclin-dependent kinase 2-cyclin A. J Biol Chem, 2006; 281(47): 35942-35953.

81. Andrews, MJ, McInnes, C, Kontopidis, G, et al. Design, synthesis, biological activity and structural analysis of cyclic peptide inhibitors targeting the substrate recruitment site of cyclin-dependent kinase complexes. Org Biomol Chem, 2004; 2(19): 2735-2741.

82. De Luca, A, MacLachlan, TK, Bagella, L, et al. A unique domain of pRb2/p130 acts as an inhibitor of Cdk2 kinase activity. J Biol Chem, 1997; 272(34): 20971-20974.

83. Raina, K, Blouin, MJ, Singh, RP, et al. Dietary feeding of silibinin inhibits prostate tumor growth and progression in transgenic adenocarcinoma of the mouse prostate model. Cancer Res, 2007; 67(22): 11083-11091.

84. Singh, RP, Deep, G, Blouin, MJ, Pollak, MN, and Agarwal, R Silibinin suppresses in vivo growth of human prostate carcinoma PC-3 tumor xenograft. Carcinogenesis, 2007; 28(12): 2567-2574.

85. Catzavelos, C, Bhattacharya, N, Ung, YC, et al. Decreased levels of the cell-cycle inhibitor p27Kip1 protein: prognostic implications in primary breast cancer. Nat Med, 1997; 3(2): 227-230.

86. Han, S, Park, K, Kim, HY, Lee, MS, Kim, HJ, and Kim, YD Reduced expression of p27Kip1 protein is associated with poor clinical outcome of breast cancer patients treated with systemic chemotherapy and is linked to cell proliferation and differentiation. Breast Cancer Res Treat, 1999; 55(2): 161-167.

87. Viglietto, G, Motti, ML, Bruni, P, et al. Cytoplasmic relocalization and inhibition of the cyclin-dependent kinase inhibitor p27(Kip1) by PKB/Akt-mediated phosphorylation in breast cancer. Nat Med, 2002; 8(10): 1136-1144.

88. Coletta, RD, Christensen, K, Reichenberger, KJ, et al. The Six1 homeoprotein stimulates tumorigenesis by reactivation of cyclin A1. Proc Natl Acad Sci U S A, 2004; 101(17): 6478-6483.

89. Deans, AJ, Khanna, KK, McNees, CJ, Mercurio, C, Heierhorst, J, and McArthur, GA Cyclin-dependent kinase 2 functions in normal DNA repair and is a therapeutic target in BRCA1-deficient cancers. Cancer Res, 2006; 66(16): 8219-8226.

90. Wesierska-Gadek, J and Schmid, G Dual action of the inhibitors of cyclin-dependent kinases: targeting of the cell-cycle progression and activation of wild-type p53 protein. Expert Opin Investig Drugs, 2006; 15(1): 23-38.

91. Matsui, Y, Halter, SA, Holt, JT, Hogan, BL, and Coffey, RJ Development of mammary hyperplasia and neoplasia in MMTV-TGF alpha transgenic mice. Cell, 1990; 61(6): 1147-1155.

92. Methods in Mammary Gland Biology and Breast Cancer Research. In. New York, New York 10013: Kluwer Academic/Plenum Publishers; 2000. p.317.

93. Law, BK, Chytil, A, Dumont, N, et al. Rapamycin potentiates transforming growth factor beta-induced growth arrest in nontransformed, oncogene-transformed, and human cancer cells. Mol Cell Biol, 2002; 22(23): 8184-8198.

94. Hall, C, Nelson, DM, Ye, X, et al. HIRA, the human homologue of yeast Hir1p and Hir2p, is a novel cyclin-cdk2 substrate whose expression blocks S-phase progression. Mol Cell Biol, 2001; 21(5): 1854-1865.

95. Brown, KA, Roberts, RL, Arteaga, CL, and Law, BK Transforming growth factor-beta induces Cdk2 relocalization to the cytoplasm coincident with dephosphorylation of retinoblastoma tumor suppressor protein. Breast Cancer Res, 2004; 6(2): R130-139.

96. Law, M, Forrester, E, Chytil, A, et al. Rapamycin disrupts cyclin/cyclin-dependent kinase/p21/proliferating cell nuclear antigen complexes and cyclin D1 reverses rapamycin action by stabilizing these complexes. Cancer Res, 2006; 66(2): 1070-1080.

97. Abe, M, Harpel, JG, Metz, CN, Nunes, I, Loskutoff, DJ, and Rifkin, DB An assay for transforming growth factor-beta using cells transfected with a plasminogen activator inhibitor-1 promoter-luciferase construct. Anal Biochem, 1994; 216(2): 276-284.

98. Bacus, SS, Gudkov, AV, Esteva, FJ, and Yarden, Y Expression of erbB receptors and their ligands in breast cancer: implications to biological behavior and therapeutic response. Breast Dis, 2000; 11(63-75.

99. Hulit, J, Lee, RJ, Russell, RG, and Pestell, RG ErbB-2-induced mammary tumor growth: the role of cyclin D1 and p27Kip1. Biochem Pharmacol, 2002; 64(5-6): 827-836.

100. Bowe, DB, Kenney, NJ, Adereth, Y, and Maroulakou, IG Suppression of Neu-induced mammary tumor growth in cyclin D1 deficient mice is compensated for by cyclin E. Oncogene, 2002; 21(2): 291-298.

101. Lee, RJ, Albanese, C, Fu, M, et al. Cyclin D1 is required for transformation by activated Neu and is induced through an E2F-dependent signaling pathway. Mol Cell Biol, 2000; 20(2): 672-683.

102. Nelsen, CJ, Kuriyama, R, Hirsch, B, et al. Short term cyclin D1 overexpression induces centrosome amplification, mitotic spindle abnormalities, and aneuploidy. J Biol Chem, 2005; 280(1): 768-776.

103. Duensing, A, Liu, Y, Tseng, M, Malumbres, M, Barbacid, M, and Duensing, S Cyclin-dependent kinase 2 is dispensable for normal centrosome duplication but required for oncogene-induced centrosome overduplication. Oncogene, 2006; 25(20): 2943-2949.

104. Desmouliere, A, Guyot, C, and Gabbiani, G The stroma reaction myofibroblast: a key player in the control of tumor cell behavior. Int J Dev Biol, 2004; 48(5-6): 509-517.

105. Ohtani, H, Kuroiwa, A, Obinata, M, Ooshima, A, and Nagura, H Identification of type I collagen-producing cells in human gastrointestinal carcinomas by non-radioactive in situ hybridization and immunoelectron microscopy. J Histochem Cytochem, 1992; 40(8): 1139-1146.

106. Walker, RA The complexities of breast cancer desmoplasia. Breast Cancer Res, 2001; 3(3): 143-145.

107. Ronnov-Jessen, L and Petersen, OW Induction of alpha-smooth muscle actin by transforming growth factor-beta 1 in quiescent human breast gland fibroblasts. Implications for myofibroblast generation in breast neoplasia. Lab Invest, 1993; 68(6): 696-707.

108. Ronnov-Jessen, L, Van Deurs, B, Nielsen, M, and Petersen, OW Identification, paracrine generation, and possible function of human breast carcinoma myofibroblasts in culture. In Vitro Cell Dev Biol, 1992; 28A(4): 273-283.

109. Ronnov-Jessen, L, Petersen, OW, Koteliansky, VE, and Bissell, MJ The origin of the myofibroblasts in breast cancer. Recapitulation of tumor environment in culture unravels diversity and implicates converted fibroblasts and recruited smooth muscle cells. J Clin Invest, 1995; 95(2): 859-873.

110. Beauchamp, RD, Coffey, RJ, Jr., Lyons, RM, Perkett, EA, Townsend, CM, Jr., and Moses, HL Human carcinoid cell production of paracrine growth factors that can stimulate fibroblast and endothelial cell growth. Cancer Res, 1991; 51(19): 5253-5260.

111. Christensen, JG, Burrows, J, and Salgia, R c-Met as a target for human cancer and characterization of inhibitors for therapeutic intervention. Cancer Lett, 2005; 225(1): 1-26.

112. Christensen, JG, Schreck, R, Burrows, J, et al. A selective small molecule inhibitor of c-Met kinase inhibits c-Met-dependent phenotypes in vitro and exhibits cytoreductive antitumor activity in vivo. Cancer Res, 2003; 63(21): 7345-7355.

113. Ge, R, Rajeev, V, Ray, P, et al. Inhibition of growth and metastasis of mouse mammary carcinoma by selective inhibitor of transforming growth factor-beta type I receptor kinase in vivo. Clin Cancer Res, 2006; 12(14 Pt 1): 4315-4330.

114. Halder, SK, Beauchamp, RD, and Datta, PK A specific inhibitor of TGF-beta receptor kinase, SB-431542, as a potent antitumor agent for human cancers. Neoplasia, 2005; 7(5): 509-521.

115. Matsuyama, S, Iwadate, M, Kondo, M, et al. SB-431542 and Gleevec inhibit transforming growth factor-beta-induced proliferation of human osteosarcoma cells. Cancer Res, 2003; 63(22): 7791-7798.

116. Sorlie, T, Perou, CM, Tibshirani, R, et al. Gene expression patterns of breast carcinomas distinguish tumor subclasses with clinical implications. Proc Natl Acad Sci U S A, 2001; 98(19): 10869-10874.

117. Rakha, EA, El-Rehim, DA, Paish, C, et al. Basal phenotype identifies a poor prognostic subgroup of breast cancer of clinical importance. Eur J Cancer, 2006; 42(18): 3149-3156.

118. Carey, LA, Perou, CM, Livasy, CA, et al. Race, breast cancer subtypes, and survival in the Carolina Breast Cancer Study. Jama, 2006; 295(21): 2492-2502.

119. Li, H, Cherukuri, P, Li, N, et al. Nestin is expressed in the basal/myoepithelial layer of the mammary gland and is a selective marker of basal epithelial breast tumors. Cancer Res, 2007; 67(2): 501-510.

120. Abd El-Rehim, DM, Pinder, SE, Paish, CE, et al. Expression of luminal and basal cytokeratins in human breast carcinoma. J Pathol, 2004; 203(2): 661-671.

121. Dabbs, DJ, Chivukula, M, Carter, G, and Bhargava, R Basal phenotype of ductal carcinoma in situ: recognition and immunohistologic profile. Mod Pathol, 2006; 19(11): 1506-1511.

122. McCarthy, A, Savage, K, Gabriel, A, Naceur, C, Reis-Filho, JS, and Ashworth, A A mouse model of basal-like breast carcinoma with metaplastic elements. J Pathol, 2007; 211(4): 389-398.

123. Weaver, Z, Montagna, C, Xu, X, et al. Mammary tumors in mice conditionally mutant for Brca1 exhibit gross genomic instability and centrosome amplification yet display a recurring distribution of genomic imbalances that is similar to human breast cancer. Oncogene, 2002; 21(33): 5097-5107.

124. Poole, AJ, Li, Y, Kim, Y, Lin, SC, Lee, WH, and Lee, EY Prevention of Brca1-mediated mammary tumorigenesis in mice by a progesterone antagonist. Science, 2006; 314(5804): 1467-1470.

125. Brodie, SG, Xu, X, Qiao, W, Li, WM, Cao, L, and Deng, CX Multiple genetic changes are associated with mammary tumorigenesis in Brca1 conditional knockout mice. Oncogene, 2001; 20(51): 7514-7523.

126. Gauthier, ML, Berman, HK, Miller, C, et al. Abrogated response to cellular stress identifies DCIS associated with subsequent tumor events and defines basal-like breast tumors. Cancer Cell, 2007; 12(5): 479-491.

127. Corsino, P, Davis, B, Law, M, et al. Tumors initiated by constitutive Cdk2 activation exhibit transforming growth factor beta resistance and acquire paracrine mitogenic stimulation during progression. Cancer Res, 2007; 67(7): 3135-3144.

128. Sarrio, D, Perez-Mies, B, Hardisson, D, et al. Cytoplasmic localization of p120ctn and E-cadherin loss characterize lobular breast carcinoma from preinvasive to metastatic lesions. Oncogene, 2004; 23(19): 3272-3283.

129. Livasy, CA, Karaca, G, Nanda, R, et al. Phenotypic evaluation of the basal-like subtype of invasive breast carcinoma. Mod Pathol, 2006; 19(2): 264-271.

130. Kim, MJ, Ro, JY, Ahn, SH, Kim, HH, Kim, SB, and Gong, G Clinicopathologic significance of the basal-like subtype of breast cancer: a comparison with hormone receptor and Her2/neu-overexpressing phenotypes. Hum Pathol, 2006; 37(9): 1217-1226.

131. Laakso, M, Tanner, M, Nilsson, J, et al. Basoluminal carcinoma: a new biologically and prognostically distinct entity between basal and luminal breast cancer. Clin Cancer Res, 2006; 12(14 Pt 1): 4185-4191.

132. Maeda, M, Johnson, KR, and Wheelock, MJ Cadherin switching: essential for behavioral but not morphological changes during an epithelium-to-mesenchyme transition. J Cell Sci, 2005; 118(Pt 5): 873-887.

133. Sarrio, D, Rodriguez-Pinilla, SM, Hardisson, D, Cano, A, Moreno-Bueno, G, and Palacios, J Epithelial-mesenchymal transition in breast cancer relates to the basal-like phenotype. Cancer Res, 2008; 68(4): 989-997.

134. Warburton, MJ, Ormerod, EJ, Monaghan, P, Ferns, S, and Rudland, PS Characterization of a myoepithelial cell line derived from a neonatal rat mammary gland. J Cell Biol, 1981; 91(3 Pt 1): 827-836.

135. Zavizion, B, Politis, I, and Gorewit, RC Bovine mammary myoepithelial cells. 2. Interactions with epithelial cells in vitro. J Dairy Sci, 1992; 75(12): 3381-3393.

136. Zavizion, B, Politis, I, and Gorewit, RC Bovine mammary myoepithelial cells. 1. Isolation, culture, and characterization. J Dairy Sci, 1992; 75(12): 3367-3380.

137. Zavizion, B, van Duffelen, M, Schaeffer, W, and Politis, I Establishment and characterization of a bovine mammary myoepithelial cell line. In Vitro Cell Dev Biol Anim, 1996; 32(3): 149-158.

138. Neve, RM, Chin, K, Fridlyand, J, et al. A collection of breast cancer cell lines for the study of functionally distinct cancer subtypes. Cancer Cell, 2006; 10(6): 515-527.

139. Casey, G, Lo-Hsueh, M, Lopez, ME, Vogelstein, B, and Stanbridge, EJ Growth suppression of human breast cancer cells by the introduction of a wild-type p53 gene. Oncogene, 1991; 6(10): 1791-1797.

140. Katayose, D, Gudas, J, Nguyen, H, Srivastava, S, Cowan, KH, and Seth, P Cytotoxic effects of adenovirus-mediated wild-type p53 protein expression in normal and tumor mammary epithelial cells. Clin Cancer Res, 1995; 1(8): 889-897.

141. Schafer, JM, Lee, ES, O'Regan, RM, Yao, K, and Jordan, VC Rapid development of tamoxifen-stimulated mutant p53 breast tumors (T47D) in athymic mice. Clin Cancer Res, 2000; 6(11): 4373-4380.

142. Crawford, AW, Michelsen, JW, and Beckerle, MC An interaction between zyxin and alpha-actinin. J Cell Biol, 1992; 116(6): 1381-1393.

143. Maruyama, K, Ochiai, A, Nakamura, S, Baba, S, and Hirohashi, S [Dysfunction of E-cadherin-catenin system in invasion and metastasis of colorectal cancer]. Nippon Geka Gakkai Zasshi, 1998; 99(7): 402-408.

144. Nollet, F, Berx, G, and van Roy, F The role of the E-cadherin/catenin adhesion complex in the development and progression of cancer. Mol Cell Biol Res Commun, 1999; 2(2): 77-85.

145. Wong, AS and Gumbiner, BM Adhesion-independent mechanism for suppression of tumor cell invasion by E-cadherin. J Cell Biol, 2003; 161(6): 1191-1203.

146. Bellovin, DI, Bates, RC, Muzikansky, A, Rimm, DL, and Mercurio, AM Altered localization of p120 catenin during epithelial to mesenchymal transition of colon carcinoma is prognostic for aggressive disease. Cancer Res, 2005; 65(23): 10938-10945.

147. Shibata, T, Kokubu, A, Sekine, S, Kanai, Y, and Hirohashi, S Cytoplasmic p120ctn regulates the invasive phenotypes of E-cadherin-deficient breast cancer. Am J Pathol, 2004; 164(6): 2269-2278.

148. Loden, M, Stighall, M, Nielsen, NH, et al. The cyclin D1 high and cyclin E high subgroups of breast cancer: separate pathways in tumorogenesis based on pattern of genetic aberrations and inactivation of the pRb node. Oncogene, 2002; 21(30): 4680-4690.

149. Brodie, SG and Deng, CX BRCA1-associated tumorigenesis: what have we learned from knockout mice? Trends Genet, 2001; 17(10): S18-22.

150. Hayami, R, Sato, K, Wu, W, et al. Down-regulation of BRCA1-BARD1 ubiquitin ligase by CDK2. Cancer Res, 2005; 65(1): 6-10.

151. Shakya, R, Szabolcs, M, McCarthy, E, et al. The basal-like mammary carcinomas induced by Brca1 or Bard1 inactivation implicate the BRCA1/BARD1 heterodimer in tumor suppression. Proc Natl Acad Sci U S A, 2008; 105(19): 7040-7045.

152. Junk, DJ, Vrba, L, Watts, GS, Oshiro, MM, Martinez, JD, and Futscher, BW Different mutant/wild-type p53 combinations cause a spectrum of increased invasive potential in nonmalignant immortalized human mammary epithelial cells. Neoplasia, 2008; 10(5): 450-461.

153. Willenbring, H, Sharma, AD, Vogel, A, et al. Loss of p21 permits carcinogenesis from chronically damaged liver and kidney epithelial cells despite unchecked apoptosis. Cancer Cell, 2008; 14(1): 59-67.

154. Sutherland, RL and Musgrove, EA Cyclins and breast cancer. J Mammary Gland Biol Neoplasia, 2004; 9(1): 95-104.

155. Wang, TC, Cardiff, RD, Zukerberg, L, Lees, E, Arnold, A, and Schmidt, EV Mammary hyperplasia and carcinoma in MMTV-cyclin D1 transgenic mice. Nature, 1994; 369(6482): 669-671.

156. Kong, G, Chua, SS, Yijun, Y, et al. Functional analysis of cyclin D2 and p27(Kip1) in cyclin D2 transgenic mouse mammary gland during development. Oncogene, 2002; 21(47): 7214-7225.

157. Pirkmaier, A, Dow, R, Ganiatsas, S, et al. Alternative mammary oncogenic pathways are induced by D-type cyclins; MMTV-cyclin D3 transgenic mice develop squamous cell carcinoma. Oncogene, 2003; 22(28): 4425-4433.

158. Asano-Miyoshi, M, Hamamichi, R, and Emori, Y Cytokeratin 14 is expressed in immature cells in rat taste buds. J Mol Histol, 2008; 39(2): 193-199.

159. Carriere, C, Seeley, ES, Goetze, T, Longnecker, DS, and Korc, M The Nestin progenitor lineage is the compartment of origin for pancreatic intraepithelial neoplasia. Proc Natl Acad Sci U S A, 2007; 104(11): 4437-4442.

160. Laakso, M, Loman, N, Borg, A, and Isola, J Cytokeratin 5/14-positive breast cancer: true basal phenotype confined to BRCA1 tumors. Mod Pathol, 2005; 18(10): 1321-1328.

161. Li, L, Mignone, J, Yang, M, et al. Nestin expression in hair follicle sheath progenitor cells. Proc Natl Acad Sci U S A, 2003; 100(17): 9958-9961.

162. Wiese, C, Rolletschek, A, Kania, G, et al. Nestin expression--a property of multi-lineage progenitor cells? Cell Mol Life Sci, 2004; 61(19-20): 2510-2522.

163. Wu, PC, Lai, VC, Fang, JW, Gerber, MA, Lai, CL, and Lau, JY Hepatocellular carcinoma expressing both hepatocellular and biliary markers also expresses cytokeratin 14, a marker of bipotential progenitor cells. J Hepatol, 1999; 31(5): 965-966.

164. Kleeberger, W, Bova, GS, Nielsen, ME, et al. Roles for the stem cell associated intermediate filament Nestin in prostate cancer migration and metastasis. Cancer Res, 2007; 67(19): 9199-9206.

165. Sy, SM, Lai, PB, Pang, E, et al. Novel identification of zyxin upregulations in the motile phenotype of hepatocellular carcinoma. Mod Pathol, 2006; 19(8): 1108-1116.

166. Arima, Y, Inoue, Y, Shibata, T, et al. Rb depletion results in deregulation of E-cadherin and induction of cellular phenotypic changes that are characteristic of the epithelial-to-mesenchymal transition. Cancer Res, 2008; 68(13): 5104-5112.

167. Xie, L, Law, BK, Chytil, AM, Brown, KA, Aakre, ME, and Moses, HL Activation of the Erk pathway is required for TGF-beta1-induced EMT in vitro. Neoplasia, 2004; 6(5): 603-610.

168. Honeth, G, Bendahl, PO, Ringner, M, et al. The CD44+/CD24- phenotype is enriched in basal-like breast tumors. Breast Cancer Res, 2008; 10(3): R53.

169. Sheridan, C, Kishimoto, H, Fuchs, RK, et al. CD44+/CD24- breast cancer cells exhibit enhanced invasive properties: an early step necessary for metastasis. Breast Cancer Res, 2006; 8(5): R59.

170. Shipitsin, M, Campbell, LL, Argani, P, et al. Molecular definition of breast tumor heterogeneity. Cancer Cell, 2007; 11(3): 259-273.

171. Lohr, M, Schmidt, C, Ringel, J, et al. Transforming growth factor-beta1 induces desmoplasia in an experimental model of human pancreatic carcinoma. Cancer Res, 2001; 61(2): 550-555.

172. Roberts, AB, Sporn, MB, Assoian, RK, et al. Transforming growth factor type beta: rapid induction of fibrosis and angiogenesis in vivo and stimulation of collagen formation in vitro. Proc Natl Acad Sci U S A, 1986; 83(12): 4167-4171.

173. Bagella, L, Sun, A, Tonini, T, et al. A small molecule based on the pRb2/p130 spacer domain leads to inhibition of cdk2 activity, cell cycle arrest and tumor growth reduction in vivo. Oncogene, 2007; 26(13): 1829-1839.

174. Rane, SG, Dubus, P, Mettus, RV, et al. Loss of Cdk4 expression causes insulin-deficient diabetes and Cdk4 activation results in beta-islet cell hyperplasia. Nat Genet, 1999; 22(1): 44-52.

175. Malumbres, M, Hunt, SL, Sotillo, R, et al. Driving the cell cycle to cancer. Adv Exp Med Biol, 2003; 532(1-11.

176. Moustakas, DT, Lang, PT, Pegg, S, et al. Development and validation of a modular, extensible docking program: DOCK 5. J Comput Aided Mol Des, 2006; 20(10-11): 601-619.

177. Magarian, EO and Nobles, WL New compounds: acrylonitrile derivatives as potential antineoplastic agents. J Pharm Sci, 1969; 58(9): 1166-1167.

178. Berger, I, Fitzgerald, DJ, and Richmond, TJ Baculovirus expression system for heterologous multiprotein complexes. Nat Biotechnol, 2004; 22(12): 1583-1587.

179. Fitzgerald, DJ, Berger, P, Schaffitzel, C, Yamada, K, Richmond, TJ, and Berger, I Protein complex expression by using multigene baculoviral vectors. Nat Methods, 2006; 3(12): 1021-1032.

180. Bartkova, J, Lukas, J, Muller, H, Lutzhoft, D, Strauss, M, and Bartek, J Cyclin D1 protein expression and function in human breast cancer. Int J Cancer, 1994; 57(3): 353-361.

181. An, HX, Beckmann, MW, Reifenberger, G, Bender, HG, and Niederacher, D Gene amplification and overexpression of CDK4 in sporadic breast carcinomas is associated with high tumor cell proliferation. Am J Pathol, 1999; 154(1): 113-118.

182. Kanoe, H, Nakayama, T, Murakami, H, et al. Amplification of the CDK4 gene in sarcomas: tumor specificity and relationship with the RB gene mutation. Anticancer Res, 1998; 18(4A): 2317-2321.

183. Slepchenko, BM and Terasaki, M Cyclin aggregation and robustness of bio-switching. Mol Biol Cell, 2003; 14(11): 4695-4706.

184. Terasaki, M, Okumura, E, Hinkle, B, and Kishimoto, T Localization and dynamics of Cdc2-cyclin B during meiotic reinitiation in starfish oocytes. Mol Biol Cell, 2003; 14(11): 4685-4694.

185. McGovern, SL, Caselli, E, Grigorieff, N, and Shoichet, BK A common mechanism underlying promiscuous inhibitors from virtual and high-throughput screening. J Med Chem, 2002; 45(8): 1712-1722.

186. McGovern, SL, Helfand, BT, Feng, B, and Shoichet, BK A specific mechanism of nonspecific inhibition. J Med Chem, 2003; 46(20): 4265-4272.

187. Feng, BY, Simeonov, A, Jadhav, A, et al. A high-throughput screen for aggregation-based inhibition in a large compound library. J Med Chem, 2007; 50(10): 2385-2390.

188. Prince, T, Sun, L, and Matts, RL Cdk2: a genuine protein kinase client of Hsp90 and Cdc37. Biochemistry, 2005; 44(46): 15287-15295.

189. Amann, R and Peskar, BA Anti-inflammatory effects of aspirin and sodium salicylate. Eur J Pharmacol, 2002; 447(1): 1-9.

BIOGRAPHICAL SKETCH

Patrick Corsino was born in Port of Spain, Trinidad and Tobago on October 30th 1982. He received his high school education at St. George's British International School in Rome, Italy. He graduated with a B.Sc. in medical biochemistry from the University of Birmingham, UK, in 2004. After graduation he immediately began the Interdisciplinary Program in the College of Medicine at the University of Florida and received his doctoral training in the lab of Brian Law.